BEAM SHAPING OF SECTORAL ELECTROMAGNETIC HORN ANTENNAS USING CORNER REFLECTOR TECHNIQUE

K. T. MATHEW

A thesis submitted for the Degree of
DOCTOR OF PHILOSOPHY
To
THE UNIVERSITY OF COCHIN

MICROWAVE LABORATORY, DEPARTMENT OF PHYSICS,
UNIVERSITY OF COCHIN, COCHIN,
KERALA, INDIA.

1978

DECLARATION

This is to certify that this thesis is an original authentic record of original work carried out by Mr.K.T. Mathew, M.Sc. under my supervision and guidance, in the Department of Physics, University of Cochin, Cochin 682 022 and that no part thereof has been presented by him for any other degree.

Mr.K.T.Mathew has passed the M.Sc. Degree Examination of the University of Kerala in the First Class. He has also passed the Ph.D. Qualifying Examination of the Cochin University in February 1977.

Cochin - 22
10 May 1978

Supervising Teacher
Dr.K.Gopalakrishnan Nair
Reader in Industrial Physics
Cochin University.

ACKNOWLEDGEMENTS

It is with great pleasure I express my sincere gratitude to Dr.K.Gopalakrishnan Nair, Reader in Industrial Physics, for his able guidance and competent advice throughout my research work. His considerate and inspiring attitude encouraged me much for completing this work in time.

I am extremely grateful to Prof.K.Sathyanandan and Prof. Joy George for providing Laboratory and Library facilities.

All the members of the faculty and technical personnel in the Department of Physics were very cooperative and helpful and I wish to place on record my sincere gratitude to all of them.

I acknowledge with pleasure the cooperation and encouragement I received from the Principal, Prof.(Sr.) Marita and my colleagues of St.Teresa's College, Ernakulam.

I am sincerely thankful to all my friends in particular Mr.G.Mohanachandran, Mr.E.J.Zachariah and Mr.K. Vasudevan for their cooperative attitude.

My thanks are also due to Mr. M.S. Mukundan for carefully typewriting the manuscript.

K.T. MATHEW

CONTENTS

LIST OF SYMBOLS

L	:	Axial length of a horn
Φ_o	:	Flare angle of a horn
δ_o	:	Difference of Path length for a wave reaching the side of the horn
T_E	:	Transverse Electric
T_M	:	Transverse Magnetic
λ	:	The free space wavelength of radiation
A_E	:	Aperture of the horn in the E-plane expressed in free space wavelength
A_H	:	Aperture of the horn in the H-plane expressed in free space wavelength
θ	:	Bearing angle of the antenna or the angular displacement of the distant point where power or intensity is measured.
2α	:	Included angle of the flange or corner reflector elements.
r	:	Distance of the point in the far field.
u	:	$\frac{A_E \sin\theta}{\lambda}$
P_θ	:	Power or square of amplitude of the field at a distant point corresponding to the bearing angle θ .
P_o	:	On-axis power.
n	:	Any integer including zero.

Ω	:	Net phase change of the field at a point due to the secondary source relative to the primary.
Σ	:	Phase difference of radiation from the secondary due to the difference in path affected at a point M.
W	:	Width of flange or corner reflector element.
W_1, W_2	:	Width of individual elements when not equal.
Z	:	Distance of flange from the aperture of horn measured along horn axis.
Z_o, Z_m	:	Optimum and Minimum values of Z giving maximum and minimum values of P_o respectively.
Δ	:	Angle between the horn axis and flange axis.
D_1, D_2	:	Longer aperture dimension of the transmitting and receiving antennas.
G	:	Gain of an antenna.
VSWR	:	Voltage Standing Wave Ratio.
HPBW	:	Half Power Beam Width
β	:	$\frac{2\pi}{\lambda}$
K	:	Amplitude of excitation of the secondary radiators.
R	:	The resultant amplitude of excitation of the secondary radiators.

S	:	Distance of feed dipole from the apex of the corner reflector.
j	:	Complex quantity $\sqrt{-1}$
J	:	Bessel function of the order indicated by the suffix and arguement shown in brackets.

LIST OF FIGURES

LIST OF TABLES

BEAM SHAPING OF

SECTORAL ELECTROMAGNETIC

HORN ANTENNAS

USING CORNER REFLECTOR

TECHNIQUE

CHAPTER I

INTRODUCTION

1.1 Antenna in General

An antenna may be defined as a device for transmitting or receiving electromagnetic waves. The word "antenna" is actually borrowed from zoology, where it means sensory organ on heads of insects and crustacea. The structure, in any form, associated with the region of transmission between a guided wave and a free-space wave or vice versa is termed as an antenna.

In 1873 James Clark Maxwell formulated the electromagnetic theory which gave a comprehensive outlook for the propagation of electromagnetic energy in the form of waves. Hertz, in 1885, constructed the first antenna and demonstrated the existence of electromagnetic waves. Further developments and progress were in very rapid speed and antennas of different varieties came into existence to suit many requirements.

Different types of antennas will have different current and charge distribution and different geometries. So the radiation characteristics of each will be different. An imaginary antenna with no aperture is a point source antenna. It provides a convenient isotropic reference with which other antennas can be compared. The simplest antenna is a one dimensional wire antenna. This includes short and long wire monopole, dipole and loops. The main drawback of the wire antennas is their low gain and directivity. At microwave frequencies, they have other drawbacks also. For example the beam width may be undesirably high and the matching may not be perfect. To obtain higher gain and more directive radiation patterns, antennas with larger effective areas are used.

1.2 Electromagnetic horn antenna

For many years, horns have been used as an ac~~c~~oustical instrument to amplify or direct sound waves. As an electromagnetic device the horn cannot have any such longevity. In fact, both microwaves and horn antennas were in use in the late nineteenth century only.

The forerunner of the horn, namely the hollow pipe radiator, seems first have been used by Sir Oliver Lodge. In 1897, Indian Physicist Prof. J.C. Bose visited London and lectured at the Royal Institution. His lecture included a demonstration of a millimeter wave spectrometer operating at a frequency of 60GHz. Among the components constituting the spectrometer were a few dielectric prisms and a true pyramidal horn which Bose referred to as a "collecting funnel"[1(a)].

Electromagnetic horn radiator is a convenient form of directional antenna used in high frequency circuits. Its simple structure, high directivity and bandwidth are all attractive features desirable to such short wave antennas. In practice, the electromagnetic horn antennas are the primary feeds of secondary antennas like paraboloidal or cylindrical reflectors and cheese mirrors which are widely used in radar systems. For getting radar beams of desired directional properties, electromagnetic waves from the primary horn feed must be properly shaped. Even if the horn is used as a primary antenna, the radiation pattern must be shaped properly to get optimum directivity. Thus the shaping of beams from electromagnetic horns has got special significance and practical applications.

The horn has much greater utility than merely that of a feed for reflectors and lenses. It is a common element in phased array antennas. It is a reliable and accurate gain standard and finally, it is a useful radiator, easy to excite and simple to build. These qualities make the horn invaluable to engineers and scientists in a number of fields.

1.3(a) Action of an Electromagnetic horn antenna

The experiments on the use of open ended wave guides as radiators indicated that an increase in the dimensions of the waveguide cross section reduces the beam angle. But this will cause secondary sidelobes. The higher order waves present in the mouth of the waveguide cause these sidelobes. These higher order waves can be prevented by having proper dimensions of the waveguide which will sustain only the dominant mode and flaring the waveguide in the vicinity of the open end to obtain a large aperture that is necessary to achieve a small beam angle. Such a flared section of a waveguide is called an "electromagnetic horn". A sectoral horn is one of the rectangular cross section flared only in one plane. Thus, we have the E-plane and the H-plane sectoral horns. Horns flared in both planes are called "pyramidal horns". For circular waveguides, conical horns of circular cross section are used. Figure 1.1 shows different types of horns.

A horn attached to the end of a waveguide provides large aperture. It also serves as a means of better impedence matching between the waveguide and the medium beyond it. Hence it will reduce the backward reflection at the mouth of the guide system. The extent

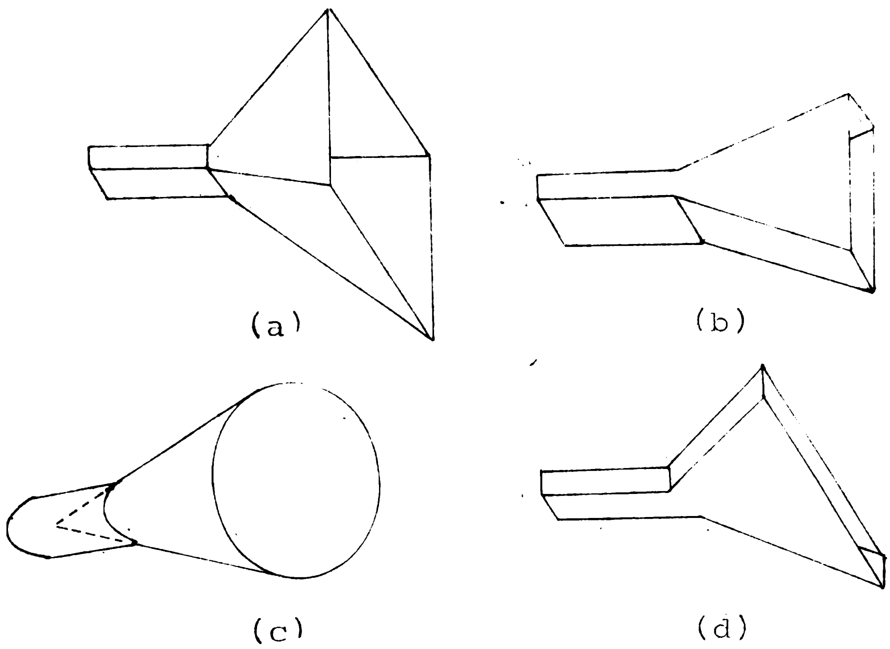

FIGURE 1-1.

DIFFERENT TYPES OF HORN ANTENNNAS

(a) Pyramidal Horn (b)E-Plane Sectoral Horn

(b) Conical Horn (d)H-Plane Sectoral Horn of directivity and power-gain depends on the horn-length and the flare angle.

A horn antenna may be considered as a taper transformer between guided waves and waves in free space. The horn itself may be assumed to be a waveguide with variable characteristic impedence. If the rate of taper is not too great, the reflection from the aperture will be small. The beam shape is controlled only in the plane where the horn is flared, while in the other principal plane, the beam shape is that of an open ended waveguide with the same dimensions. A sectoral horn provides a fan shaped beam. Such fan shaped beams are used for surface based and navigational radar system.

A horn may be excited by attaching it to the end of a section of a waveguide of appreciable length which is connected to a microwave resonance chamber through a probe. If the edge effects are neglected the radiation patterns of horn antennas can be determined from the aperture dimension and the aperture distribution. To obtain a uniform aperture distribution a long horn with small flare angle is required. But for practical convenience the horn should be as small as possible. An optimum horn will be in between these extremities and has the minimum beamwidth without excessive sidelobes for a given length.

A longitudinal section of a horn antenna is shown in Fig.1.2. L is the axial length of the horn, A_E is its aperture and φ the flare angle. δ represents the difference in path length for a wave reaching the aperture at the side of the horn. If δ is sufficiently small, compared to the wavelength, of radiation used, the field is nearly uniform over the entire aperture. For a constant length L, the directivity of the horn increases as the aperture and flare angle φ_0 are increased. However, when A_E and φ_0 become so large that δ is 180 degrees, the field at the edge of the aperture is in phase opposition to the field at the axis. This will increase the sidelobes and hence decrease the directivity. It follows that the directivity occurs at the largest flare angle for which δ does not exceed a certain value δ_0. Thus the optimum horn dimensions can be related by

$$\delta_0 = \frac{L}{\cos(\varphi_0/2)} - L$$

$$L = \frac{\delta_0 \cos(\varphi_0/2)}{1 - \cos(\varphi_0/2)}$$

$$\text{i.e.} \quad \varphi_0 = 2 \cos^{-1} \frac{L}{(L+\delta_0)}$$

The inherent limitation of all horn antennas is the end effect. For better directivity this endeffect is to be minimised by some techniques such as lens compen-

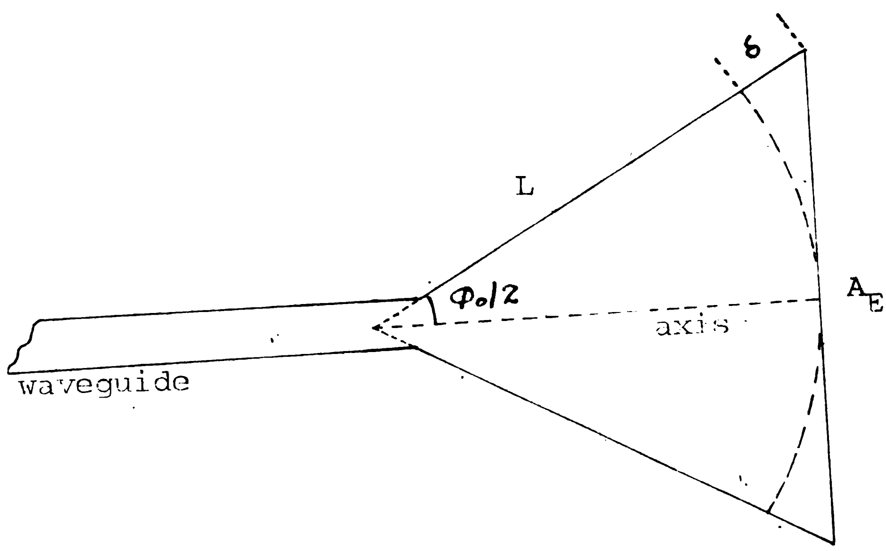

FIGURE 1-2

LONGITUDNAL SECTION OF A HORN

sated antennas. Another limitation of horn antenna is excitation of higher modes. For uniform aperture illuminations, these higher modes must be suppressed.

1.3(b) Corner Reflector Antennas

Kraus[40] suggested a beam antenna, called the corner, V or sphenoidal reflector type antenna which consists of a driven linear radiator kept along the bisector of two metallic reflectors which are joined along a line by hinges. A corner reflector system is shown in Figure 1.3. From the assumption that the reflecting planes are perfectly conducting and infinite extent and by using the method of images, he obtained analytical expressions for the antenna characteristics such as gain and directional radiation pattern. One of the important theoretical conclusions drawn by Kraus is that too small a spacing for the driven radiator from the apex of the corner reflector will adversely affect the gain of the system. Again, the spacing will have an upper limit also, above which the beam splits up to sidelobes. When reflectors of larger dimensions are taken, their widths or lengths are found to have negligible effect on the radiation patterns. Thus the gain and directional patterns of the system can be conveniently adjusted by varying the spacing 's' or the corner angle 2α or both.

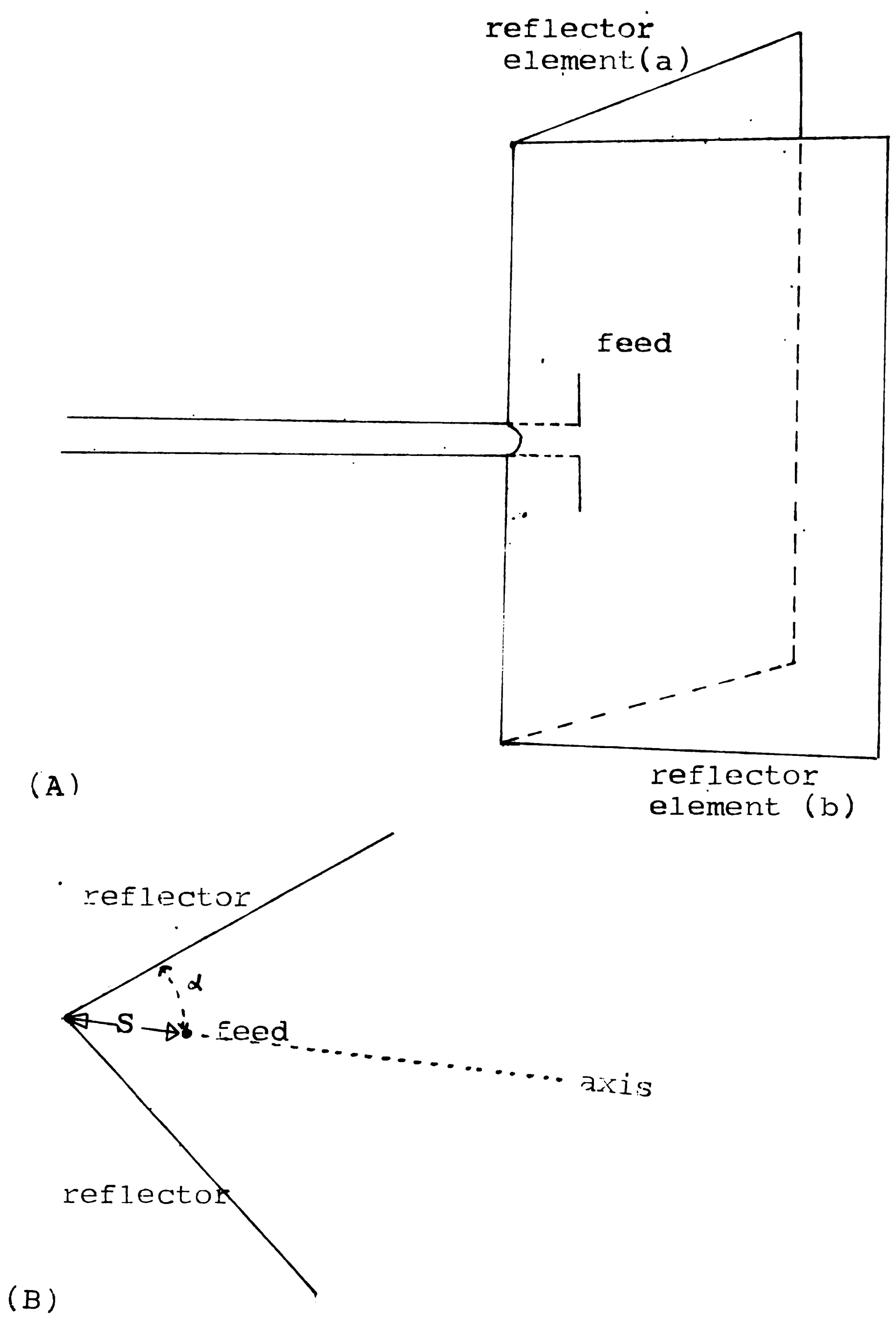

FIGURE 1-3

CORNER REFLECTOR SYSTEM

A characteristic of the corner reflector antenna is that, it will return a signal in the same direction exactly along which it was received. Because of this characteristic, the corner reflector antennas find applications in radar and microwave system. In military vehicles and ships, sharp corners of metal plates are avoided in the design to eliminate the possibility of forming "corner reflectors" which will increase the possibility of "seeing" them by the enemy radars. One of the greatest uses of a corner reflector antenna is in home television reception.

1.4 Scheme of Present Work

In the present investigation, possibility of beam shaping of sectoral horns and corner reflector systems has been studied in detail. The experimental results obtained in the above two cases are compared. As far as the flanged sectoral horns are concerned, the special advantage is that the gain is increased without impairing impedance conditions. An intense study on corner reflector antennas shows that the beam broadening or focussing will be possible by adjusting parameters involved. Beam tilting by imposing asymmetries is another interesting property of both the systems. A comprehensive study of the past work in these fields has been presented in Chapter II.

Chapter III is exclusively for describing the experimental techniques used in the present investigation.

In Chapter IV, experimental results on flanged sectoral horns and corner reflector systems are presented.

A comparative analysis of the experimental results obtained with flanged sectoral horns and corner reflector systems is presented in the Chapter V. The similarity and close resemblance in each aspects are shown by presenting typical results from these two systems.

Theoretical aspects of both types of antennas are considered in Chapter VI. Attempts are made for co-ordinating the theoretical aspects and drawing a final conclusion.

In Chapter VII, the final conclusion that the flanged sectoral horn may be considered as a corner reflector system has been drawn. The importance of the conclusions and usefulness are pointed out. The scope for further work in these lines has been indicated.

The work done by the author in related fields is given as two appendices A_1 and A_2. References are given at the end. Most of these references are directly scrutinised by the author. In a few cases, the author had to satisfy himself by seeing only the abstracts as the papers were not available to him in their original form inspite of his best efforts.

CHAPTER II

PAST WORK IN THE FIELD

2.1 Introduction

A great deal of work on both flanged sectoral horns and corner reflectors has been reported in literature. In this chapter, the past work done in the field of electromagnetic horns and corner reflector antennas in general has been summarised. Different attempts made for the beam shaping of sectoral horns and corner reflector systems are presented.

2.2 Electromagnetic Horn Radiators

Along with the development of horn antennas, several attempts were made by scientists for effectively shaping the beam by artificial means. The following i′ a brief description of these efforts.

With the revival of interest in microwave and waveguide transmission lines by 1930, many papers appeared in the arena. The first analysis of radiation by an active horn antenna was given by Barrow and Chu[1b]. A clear description of the radially propagating modes in a sectoral radial waveguide is given in their paper. In their terminology, H modes have no component of electric field in the radial direction, ($E_\rho = 0$). In their second paper[2] they applied Huyghens' principle to the waveguide field that would occur in the hornmouth when the sides were of infinite extent. On this assumption they calculated the H-plane radiation pattern of H-plane sectoral horns. They observed that the radiation patterns of a sectoral and rectangular guide behave similarly when the flare angle is small and the radial length not too long. But for fixed radial length and increasing flare angle, the beam first begins to sharpen, reaches a minimum width and then broadens again.

Southworth and King[3] described some experiments made to determine the directive properties of metal pipes and horns when used as receivers of electromagnetic waves. The experiments include the measurement of received power with and without the horn in place and the determination of the directional patterns of the horn in two orthogonal planes. Their study indicates that the horns are simple and effective means of obtaining power ratios of a hundred or more. The effect of varying different horn parameters shows that there is an optimum angle of flare, for maximum directivity.

The principles of designing electromagnetic horn antennas to obtain beams of specified angular spread, smoothness of contour and power gain are described in a later paper by Chu and Barrow[2].

Chu[4] in his paper, described the method of calculating the radiation properties of hollow pipes and horns. For the TE_{11} wave in circular pipe and the TE_{01} wave in rectangular pipe the directivities are analytically expressed in terms of beam angle and power gain. It is found that the two waves have substantially equal power gains on the basis of equal areas of openings.

In a lecture delivered at the Radio location Convention 1946, Rust[5] introduced ths phase correction to the horn radiators. It will be noticed that the maximum phase difference between the wavelets proceeding through the centre and through the sides depends upon the length of horn. He suggested that this length must be at least 50 wavelengths to reduce this phase difference. He pointed out that the metal partitions acting as sections of waveguide could be used to obtain this correction.

Horton[6] explained a method based on Schelkunoff's theory for the computation of radiation patterns of electromagnetic horns of moderate flare angles. For the case of transverse electric field in a wave guide or horn of moderate flare angle, the problem of calculating the radiation pattern is reduced to that of evaluating two definite integrals. Experimental data is presented to illustrate the agreement between theory and experiment.

Electromagnetic fields from conical horns were subject of intense study by M.G. Schorr, E.J. Beck[7] and A.P. King[8]. They solved Maxwell's equations for perfectly conducting conical waveguides for their analysis.

The edge diffraction theory applied by Russo[9] et.al. describes a new method for computing E-plane patterns including backlobe region. The diffraction fields are obtained by applying the relations developed by Pauli in conjunction with reciprocity theorem. It has been shown that the radiation of the horn is due to diffraction by the E-plane edges and by direct radiation from the source at the apex of the horn.

Using the edge diffraction theory Yu, Rudduck and Peters[10] studied the radiation characteristics of horn antennas. The far-side-lobes and backlobe radiation have been solved without employing field equivalence principle. A corner reflector with a magnetic line source located at the vertex is proposed as a model for the principal E-plane radiation of horn antennas. A complete pattern including multiple interactions and images of induced line sources is obtained in the form of an infinite series.

Hamid[11] used the geometrical diffraction theory to investigate the gain and radiation pattern of a conical horn excited by a circular waveguide operating in the TE_{11}

mode. Narasimhan and Rao[12] presented a simple, accurate and self consistent solution for modes in a conical horn. The eigen functions and eigen values derived from the simple solution for the TE and TM modes of different orders were found to be very close to the exact solution.

James J. Epis[13] suggested a modification to the electromagnetic horn to get identical radiation patterns in the E and H-planes. The radiation polar diagrams of typical conical and square pyramidal horns have E-plane patterns which are generally narrower than their respective H-plane patterns, due to several reasons. The modification is effected by simply fastening metallic pins of small diameters or mechanical screws on the exterior periphery of the horn aperture. The most important advantage of this compensated horn is that equalisation of the E and H-plane patterns was possible for all polarisations. The input VSWR is not affected adversely by this aperture modification.

Walton and Sundberg[14] used dielectric composite lenses to correct the phase error present across the aperture.

John L Kerr[15] described a horn model with broad band width and a substantial reduction in axial length. This horn could be operated in the 0.2 - 2.0 GHz range. He fabricated the H-plane walls in the form of grids.

E.H. Braun[16] described methods of evaluating the parameters of horn and he suggested a simple procedure for designing such a horn.

A.W. Love[17] suggested a diagonal horn. The waves which are propogated in such a horn are composed of a TE_{01} mode and TE_{10} mode orthogonally. This type of horn antenna can easily be used to radiate circular polarisation. The diagonal horn can be used as a feed horn for illuminating parabolic reflectors.

A new technique is described by Seymour[18] for controlling E-plane aperture distribution and radiation pattern of a pyramidal or conical horn. Small variations of flare angle at one or more points along the horn are used to produce a tapered aperture field in the E-plane. Equal E and H-plane beam-widths with low side lobes are obtained. The structure is simple and economical to fabricate and offers low VSWR and minimum dissipation loss.

Ching C. Han and Adam Wickert[19] fabricated a multi-mode rectangular horn antenna generating a circulary polarised elliptical beam. This antenna operated in two orthogonal modes set and used in conjunction with a spacecraft to illuminate an elliptical zone on the earth surface offered a high edge coverage gain, low side lobes, low edge of coverage axial ratio and low cost.

Corrugated horn feed is a fairly new model. Kay and Simmons[20] in United States observed that grooved walls in a horn would present the same boundary conditions to all polarisations and would therefore create a tapered aperture field distributions in all planes. This would eliminate the spurious effects at the E-plane edges caused by diffraction and would result in equal E and H-plane beam widths. Lawers and Peters[21] did some work independently on this field in the same period. They studied the effect of corrugation depth, separation and corrugation thickness. They also found that the back lobes and side lobes could be minimised by introducing a series of quarter wave length deep choke slots in to the walls of the horn near the aperture.

Important contributions in the field of corrugated feed-horn are made by Clarricoats[22, 23, 24] and his group. Comprehensive theoretical explanations for radiation patterns of corrugated conical and rectangular horns were presented by them. They also studied the radiation patterns of lens corrected conical scalar horn. Jauken and Lambrechtse[25] studied small corrugated conical horn antennas with wide flare angles.

Narasimhan and Rao[26] studied different hybrid modes in corrugated horn and they have shown a deviation to the rigorous solution obtained by Clarricoats for corrugated horns. Narasimhan[27] investigated the form of field in a conical horn with uniform circumferential corrugations with arbitrary corrugation depth.

Dielectric rod and tube antennas are relatively old but the first combination of a dielectric cone and a horn seems to have occurred in the mid 1960's. The aperture efficiency in dielectrically loaded horn antennas was investigated by Tsandoulas and Fitzgerald[28]. It is shown that aperture efficiencies of the order of 92-96 per cent may be obtained easily and inexpensively. This method has application in limited scan arrays. By lining all four sides of a square horn with a dielectric a circularly polarised feed was obtained. Several authors[29,30,31] conducted studies on this subject. Clarricoats et.al[32] demonstrated that the radiation pattern of a dielectric cone excited by a horn can be predicted with sufficient accuracy. The results also show that the radiation pattern of the dominant HE_{11} mode of the dielectric cone is similar to that of the same mode of the corrugated horn.

Horn reflector antenna[33,34] is another type of horn radiator. It is a combination of a square electromagnetic horn and a reflector that is a sector of a paraboloid of revolution. The apex of the horn coincides with the focus of the paraboloid. It is an extremely broad band antenna. Since it is not polarisation-sensitive, it can be used in any linear or circular polarisation. As it is an offset paraboloidal antenna, impedance mismatch due to reflected signal on the feed is very little. This type is commonly used in satellite communication systems.

From the elaborate study of horn antennas, Pao[35] suggested the possibility of shaping the primary pattern of horn feeds. He put small pins and other such obstacles at the mouth of the horn radiators. The radiation patterns were shaped considerably but with terrible mismatch. He also suggested metal flanges and strips.

Owen and Reynolds[36] conducted a series of experiments to establish the effect of metal flanges on radiation patterns of small horns. They studied the effect of length and included angle of the flange on radiation characteristics. An approximate theory was suggested by them. Butson and Thompson[37] performed experiments on the same line. They proved the validity of the assumption made by Owen and Reynold that two secondary radiators may be assumed to be situated at the edges of the flanges.

A bulk of work has been reported on theoretical and experimental field on the radiation pattern and characteristics of horn sadiators. An exhaustive study on the beam shaping of sectoral horn antennas by metallic flanges is made by Nair and Keshy[38,39].

2.3 Corner Reflector Antenna

Although a parabolic surface can produce greatest directivity, it has been found that a highly effective directional system results from the use of two flat conducting sheets arranged to intersect at an angle forming a corner. A 90° corner reflector is forming a square reflector. A 180° corner is equivalent to a single flat sheet reflector, a limiting case of the corner reflector. The first significant contribution in this field was made by J.D. Kraus[40]. In his own words, "A corner reflector consisting of two flat conducting sheets or their aquivalent constitutes a distinct type of reflector system capable of substantial gains and possessing many unique characteristics". The theoretical explanation for the various results obtained is given on the basis of the theory of images in electrostatics. Kraus could develop expressions for both gain and directional patterns. In his experiment, he used a half wave dipole as the driven element. He constructed grid type corner reflector having spaced parallel wires or conductors. He also discussed the bidirectional corner reflectors.

Edward E. Harris[41] made an extensive experimental investigation of the corner reflector antennas taking into consideration the different parameters involved. He studied the radiation patterns for various corner angles and for different spacing of the dipole. Heplane and E-plane patterns were studied separately. Radiation resistances of a driven half wave dipole for various positions of the dipole were determined.

A theory developed by James R. Wait[42] provided a straight forward solution for the resultant fields any-where within the angle subtended by the corner reflector. Comments on Moullin's[47] theoretical treatment are also made in this paper.

Cottonny and Wilson[43] studied the effect of aperture angle on the optimum position of the dipole. They used corner reflector of variable widths. The effect of dimensions of reflecting surfaces on the gain was also investigated.

In another paper, A.C. Wilson and H.V. Cottonny[44] measured radiation patterns for corner reflector antennas having various combinations of widths and lengths of the reflecting surface. The aperture angle was set at a value required to minimise gain. They also constructed and tested corner reflectors with a collinear array of dipoles.

M.A.K. Hamid[45] described a modified radiation pattern of sectoral horns and corner reflector antennas loaded with shaped dielectric slabs along the walls. This can improve the directivity in all cases.

David Proctor[46] presents a series of computer-derived design charts for maximising the radiated field from a corner reflector. Optimum feed positions are shown for various corner reflector angles. The performance of corner reflector is analysed by the method of images. He obtained the position of the driven element from the apex of the corner reflector for various corner angles.

A close follow up of the past work done in this field indicates that no attempt has been made to co-relate the flanged sectoral horn with a corner reflector system. This point has been taken up in the present investigation.

CHAPTER III

METHODOLOGY: EXPERIMENTAL TECHNIQUES AND MEASUREMENTS

3.1 Introduction

This chapter deals with experimental set up and measurement techniques used in this investigation. The description of the equipment used and their arrangement is followed by a discussion of the methods of measurements employed.

Measurements have been carried out in X and S bands. Most of the work is done in the X-band, with a mean frequency of 9.4 GHz. But the results obtained have been verified with S-band which has a frequency range of 5.6 GHz to 8.2 GHz.

3.2 Equipment : General Description

The principal components in this investigation comprise of the microwave sources, waveguide assembly pyramidal and sectoral horns, metallic flanges, corner reflectors, field detecting system and so on. A reflex klystron oscillator operating with a stabilised power supply and modulation circuit, couples microwave power through a probe assembly to a waveguide bench. The waveguide test bench includes a circulator or an isolator, frequency meter (cavity wavemeter) calibrated variable attenuator, monitor to detect power, standing wave detector and a transmitting antenna which is usually a pyramidal horn. The receiving system consists of the horn under test, and a crystal detector, which is mounted on the waveguide. The waveguide is furnished with a variable short circuiting plunger. This system is mounted on a stand capable of rotation about a vertical axis to record radiation patterns. The output across the crystal is given to a very sensitive spot type microgalvanometer.

3.3 Microwave Sources and Waveguide System

The X-band microwave unit of mean frequency 9.4 GHz consists of a stabilised power supply and a klystron oscillator 723 A/B. The microwave radiations are coupled to the waveguide through a probe. Small variation in the frequency can be accomplished by tuning the cavity of the oscillator. The frequency can be read with the help of the frequency meter. The voltage standing wave ratio is measured with a slotted section, tunable probe with crystal detector and a VSWR meter. Schematic diagram of experimental arrangement is shown in Fig.3.1.

The reciprocity theorem in antennas enables us to use test horn as a receiver. A pyramidal horn with

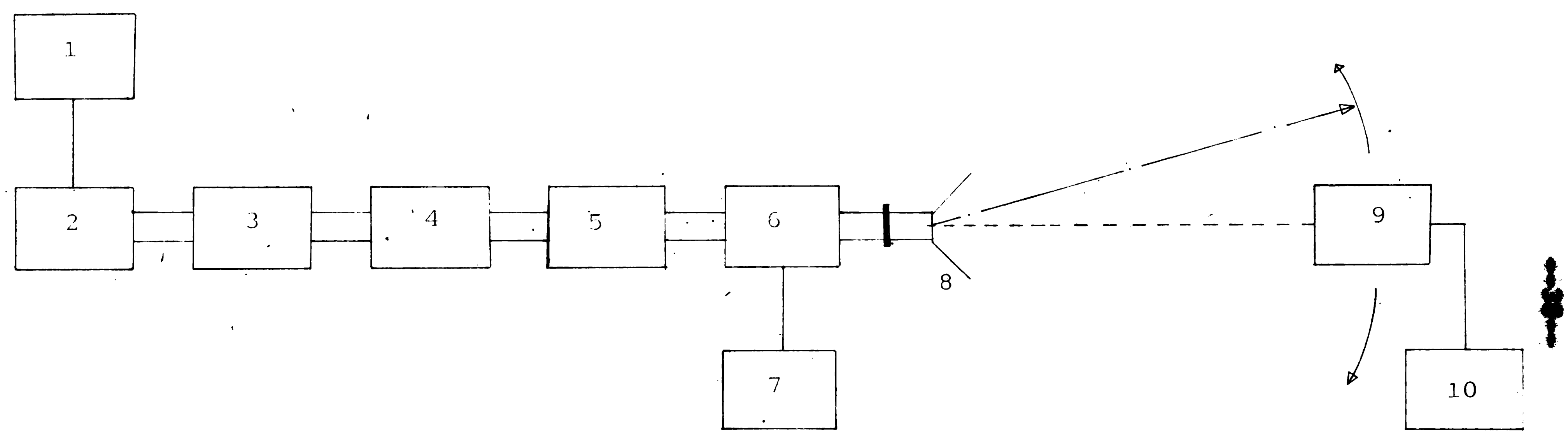

FIGURE 3-1.

SCHEMATIC DIAGRAM OF EXPERIMENTAL ARRANGEMENT USED

1.Power supply; 2. Klystron oscillator; (3)calibrated attenuator;
4.Frequency meter; 5. Tuner; 6. Slotted section and tunable probe;
7.V.S.W.R.meter; 8.Horn antenna; 9.Receiver, 10.Scalamp galvanometer.

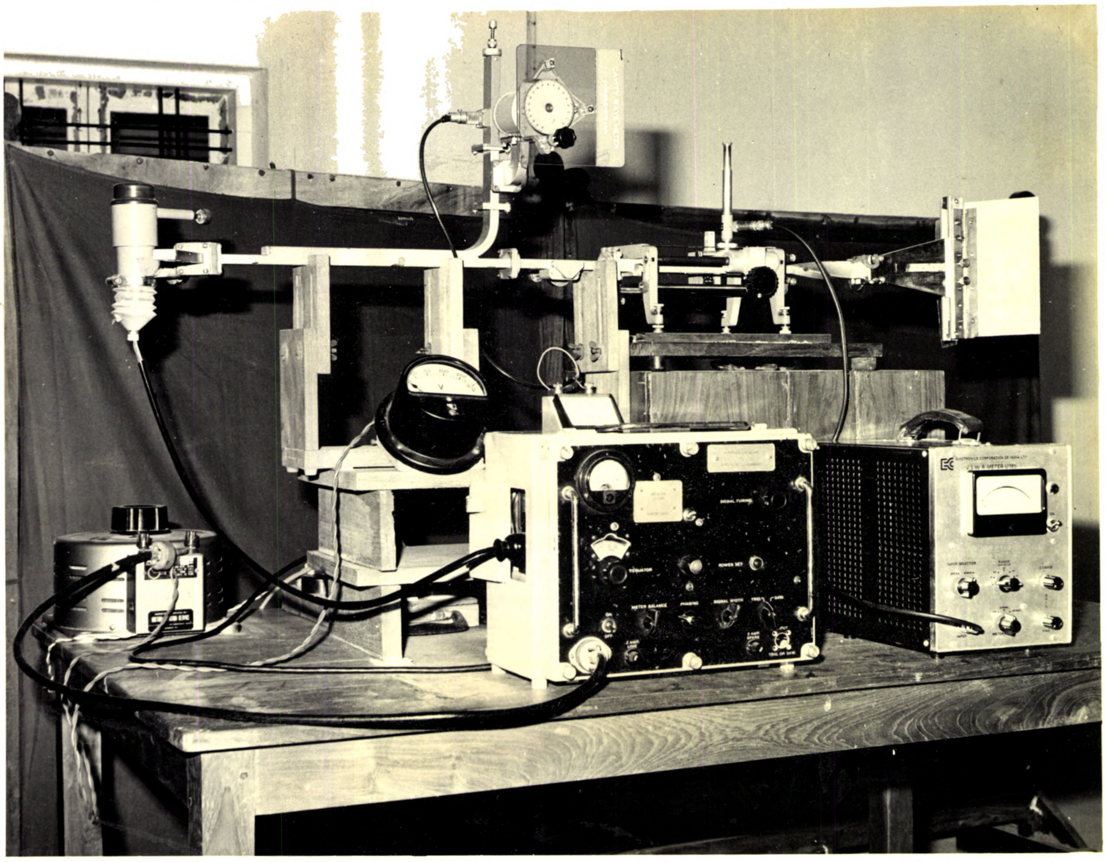

FIGURE 3.2

X-band Microwave source and Waveguide system.

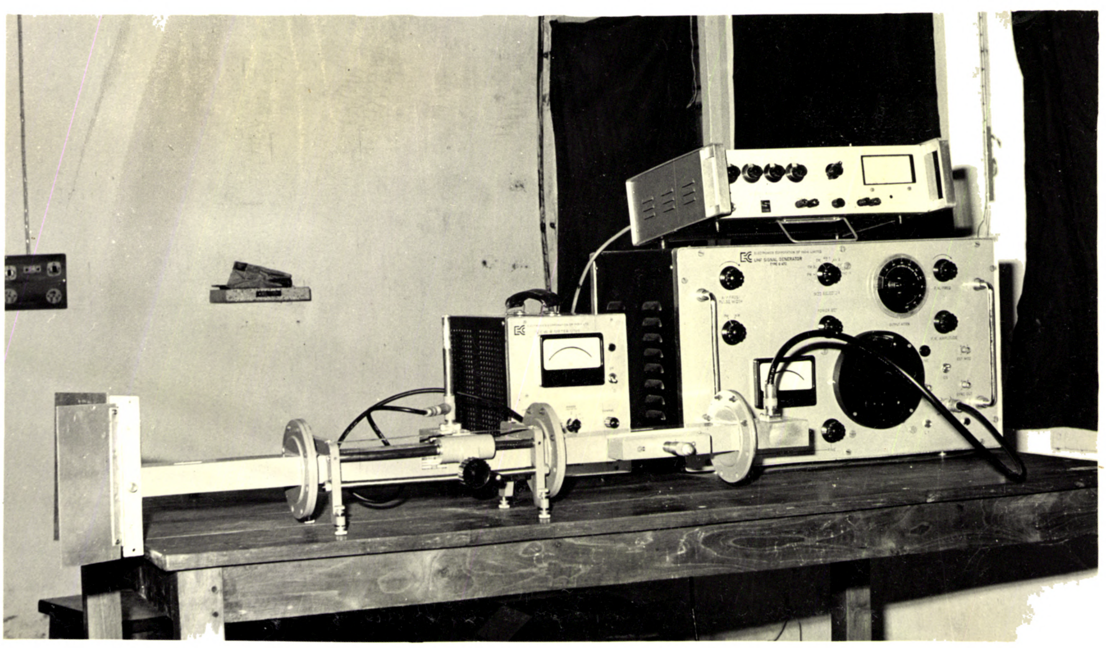

FIGURE 3.3

S-Band Test Assembly

20cm x 10cm aperture dimensions is used as a standard transmitter. The whole system can be set up on an adjustable stand at any desired height. E-plane or H-plane radiation pattern can be studied by connecting appropriate waveguide twist to the waveguide preceeding the transmitting horn. Figure 3.2 shows the photograph of X-band microwave source and waveguide system.

S-band microwave bench is a compact variable frequency unit consisting of a regulated power supply modulation unit and the klystron. It is a variable frequency source with range 5.6 GHz to 8.2 GHz. The power output can be adjusted and power level is indicated by an internal d.c. meter. The output can be made continuous or modulated wave. The power from the klystron (RK 5727) is coupled to the waveguide through a co-axial cable RG 58/U and a probe assembly. The S-band test bench resembles the X-band set up described above. The S-band test assembly is shown in Fig. 3.3.

3.4 Sectoral Horns

Both E-plane and H-plane sectoral horns are used, in this investigation. Since X-band and S-band have different frequencies and hence waveguide dimensions are different. E-plane and H-plane sectoral horns are made of moderately thin copper or brass sheets. To obtain good conductivity the inner surfaces of horns are silvered. Different parameters of horns used are given in the Table 3.1. Figure 3.4 gives a view of these horns.

FIGURE 3.4

View of some of the E-plane and H-Plane Sectoral Horns used in this investigation

3.5 Flange System

Aluminium and brass flanges are used to study their effect on the radiation patterns of the horn radiators. The flanges are designed to enable easy adjustment of angle, width, orientation and other related parameters. The flanges are nothing but two metal sheets joined with screws on a hinge on either side of a rectangular frame. Fig. 3.5 shows a view of the flange system. The rectangular frame with flange elements can be inserted on the sectoral horn so that the flange elements are situated on either sides of the flared region of the horn. Fig. 3.6 gives the lay out of a flanged sectoral horn. Thus, the edges of the flange elements are parallel to the aperture of the horn. The flange can be slided over the horn and fixed at any desired position. A calibrated scale fixed on the outer surface parallel to the axis of the horn enables to find the position of the flange with respect to the aperture.

3.6 Corner Reflectors

A corner reflector is formed by the intersection of two plane reflectors. It is fed by a dipole. Though there are striking resemblances in the characteristic patterns of flanged sectoral horns and corner reflectors the setting of both is entirely different. The driving element in a corner reflector is not a directional feed. A half-wave dipole is used in this investi-

TABLE 3.1 Parameters of Sectoral Horns

	Horn No.	Mean Frequency of operation GHz.	Radial length cm.	Flare angle (deg)	Aperture Dimensions in cm. In H-plane A_H	Aperture Dimensions in cm. In E-plane A_E
H-plane Sectoral Horns	H_1	9.40	10.8	60	11.90	1.016
	H_2	9.40	14.3	30	7.50	1.016
	H_3	9.40	23.1	25	10.20	1.016
	H_4	7.50 6.66 6.00	18.8	35	12.30	1.50
	H_5	7.50 6.66 6.00	18.8	40	14.00	1.50
	H_6	7.50 6.66 6.00	15.7	60	18.00	1.50
E-plane Sectoral Horns	E_1	9.40	15.0	60	2.54	17.40
	E_2	9.40	9.9	60	2.54	11.40
	E_3	9.40	8.95	45	2.54	10.70
	E_4	7.50 6.66 6.00	28.0	40	3.5	19.50
	E_5	7.50 6.66 6.00	25.0	45	3.5	20.00
	E_6	7.50 6.66 6.00	20.5	45	3.5	15.50

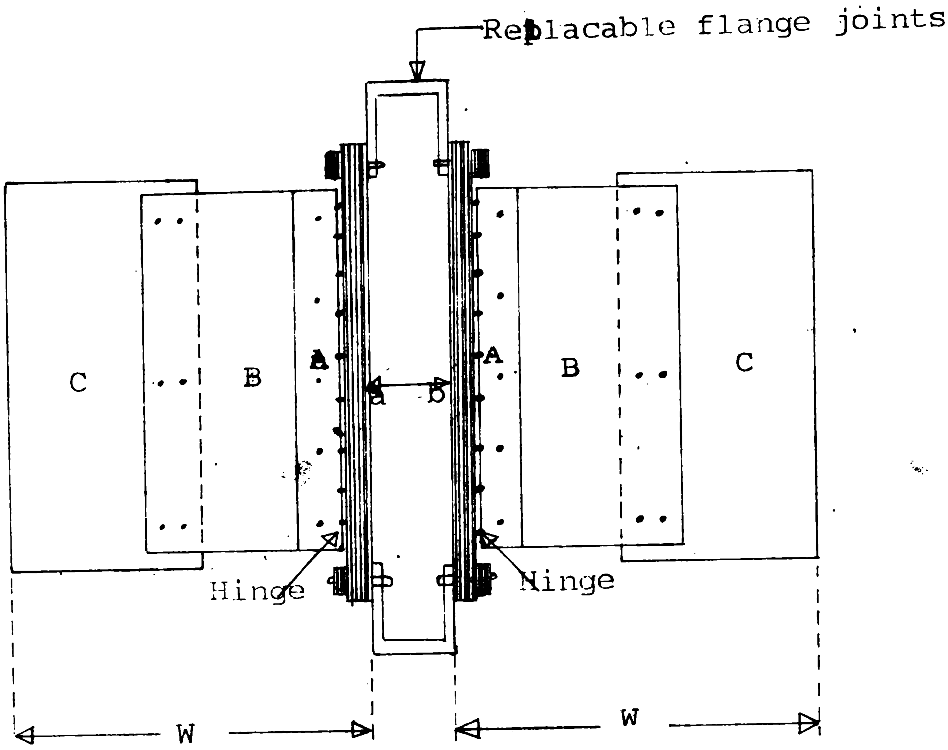

ab:widthe of the sectoral horn

FIGURE 3-5

METALLIC FLANGE SYSTEM

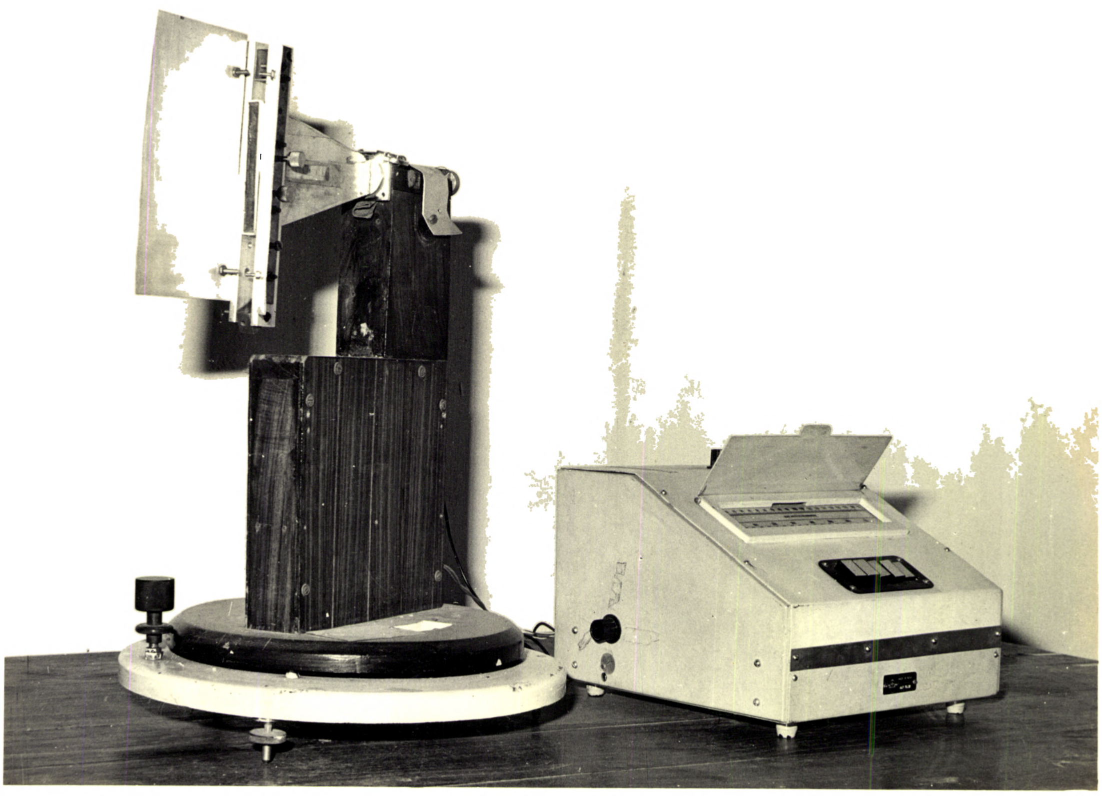

FIGURE 3.6

Flanged Sectoral Horn Receiver of Microwaves.

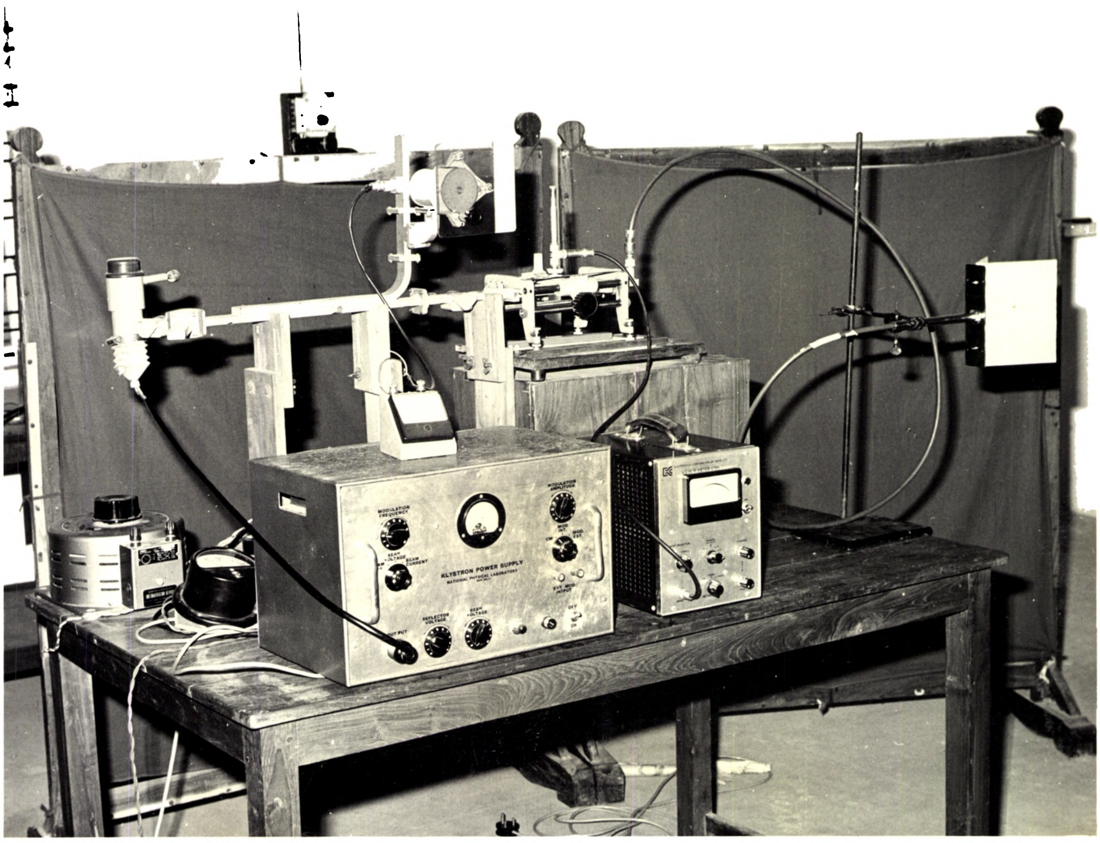

FIGURE 3.7

Microwave Source and Corner Reflector Antenna.

gation as the feed for the corner reflector. The arrangement of the corner reflector system is shown in Fig. 3.7. The pyramidal horn used in the previous investigation as transmitter is replaced by the corner reflector system. The waveguide is coupled through a co-axial cable, the other end of which feeds the dipole. The cable passes through the groove cut at the centre of the wedge of the corner reflector. The system is mounted on a convenient stand. For plotting the radiation patterns of corner reflector system the classical method of using the test antenna as a transmitter is employed. The receiver is a pyramidal horn with a crystal detector IN23. The receiver is moved along the circumference of a circle of constant radius $> \frac{2D^2}{\lambda}$ with the apex of the corner reflector as centre. The output of the crystal is given to a highly sensitive microgalvanometer. Fig. 3.8 shows the corner reflector antenna with pyramidal horn as the receiver.

3.7 <u>Measurements : Methods and Techniques</u>

1. <u>On-axis Power</u>. The power of the electromagnetic energy radiated along the axis of the antenna system has to be measured in the case of both flanged sectoral horns and corner reflector systems. This is measured by placing a small horn fitted with a detector crystal in a crystal mount. The crystal used is IN21 or IN23. The axis of the receiver horn is arranged to be

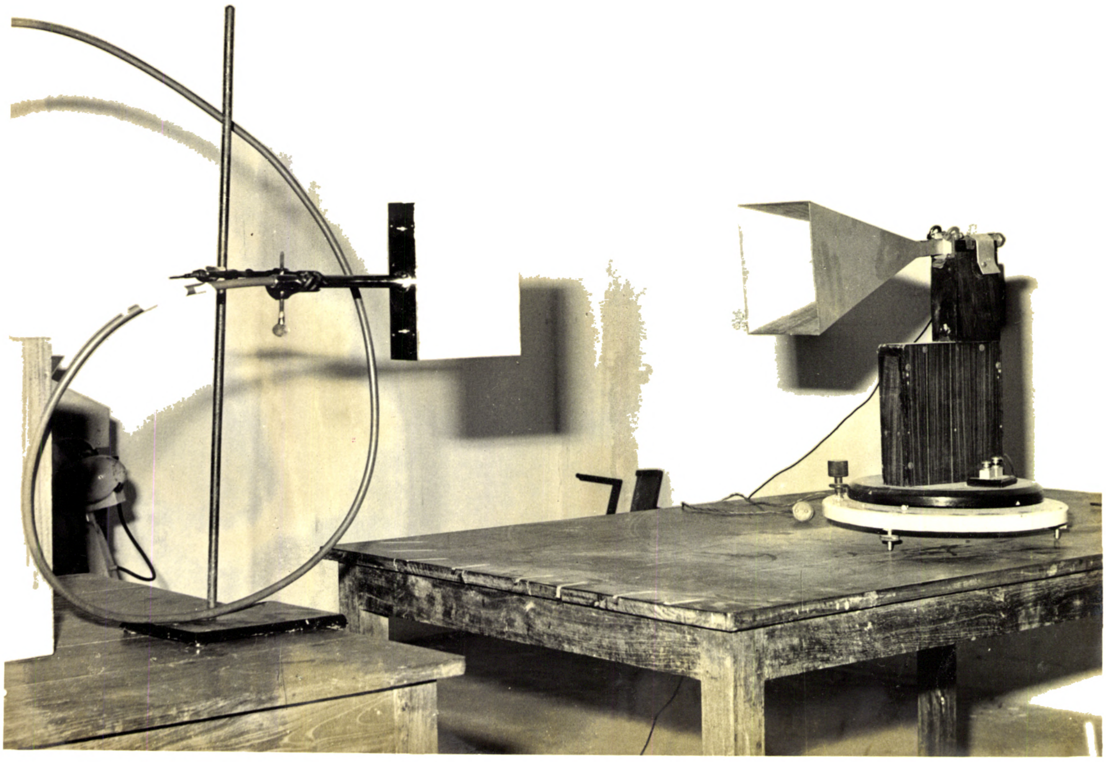

FIGURE 3.8

A View of Corner Reflector and Pyramidal Horn Receiver.

collinear with the axis of the transmitter antenna, so that the receiver will be at a point along the axis of the transmitter. The distance between the two antennas is adjusted to be greater than $\frac{2(D_1^2 + D_2^2)}{\lambda}$ where D_1 and D_2 are the larger aperture dimensions of the transmitter and receiver antennas respectively. This restriction is for taking the observations only in the far-field region. In the actual set up, the receiver horn is attached to a stand which is capable of moving along a long wooden bench, so that the distance can be convaniently adjusted. The output from the crystal detector is given to a very sensitive microgalvanometer (scalamp type) whose deflections are proportional to the crystal current and hence to the power of the radiated energy at the point where the crystal is kept. The galvanometer deflections can thus be taken as a measure of the on-axis power at the point. The intensity of the field at the point will be proportional to the square root of the galvanometer deflection.

2. Radiation Patterns: Power and Intensity Patterns. For plotting the radiation patterns of antennas, there are two methods. (a) By using the antenna under test as a transmitter of electromagnetic waves while the power or intensity distribution at different points along the circumference of a circle with the antenna as the centre is studied by another receiving antenna. (b) By using

the antenna under test as a receiver of electromagnetic waves transmitted by a standard antenna. From the well known reciprocity theorem in antennas, it can be seen that the characteristics of an antenna will be the same in both cases. For the major part of the work described in this thesis, the second technique is used, as it is more convenient and simple. For plotting the radiation patterns of corner reflector antennas, the first method is employed since it is difficult to fabricate a movable frame holding the corner reflector elements and the feed dipole togehher. However, for experimental confirmation, both the techniques are employed in many cases and average patterns are developed.

When the horn under test is used as a transmitter of C.W. signal, the radiation patterns are plotted in the following way. The long arm on which the small receiving horn with crystal mount is arranged, is capable of rotating about an axis passing through the centre of the aperture of the transmitting antenna under test. (Flanged sectoral horn or corner reflector system). Thus the receiver can be kept at different points on the circumference of a circle of constant radius $R > \frac{2D^2}{\lambda}$ around the test antenna. As mentioned earlier, this lmit of distance is chosen for taking the observations only in the far field region of the antenna. The power at these points are readily obtained from the galvanometer deflections. By plotting these on polar co-ordinate paper, the power pattern of the transmitting antenna can be obtained. If the square root of the galvanometer deflections are plotted, we will get the intensity pattern from which the antenna gain in the plane can be easily claculated by numerical integration of the pattern[52].

Particular care is taken in avoiding all possible interactions of external objects in the region of the radiated field. The walls of the big room used for the investigations are coated with a paint or graphite which is a good absorbing material for microwaves. Metallic surfaces are avoided in the radiation field of the antenna.

In the second method of plotting the radiation patterns, a standard pyramidal horn is used as a transmitter of C.W. signal[53]. The antenna under test is used as a receiver. The crystal output current from this receiver is fed to a sensitive microgalvanometer, the deflection of which may be taken as of the power received by the receiver. The receiving system is mounted on a turn-table which is capable of rotating about a vertical axis passing through the centre of the antenna. The standard transmitting antenna and the horn under test used as the receiver are properly designed so that their axes are in the same line. The bearing angle of the receiver can be noted from a circular scale attached to the frame. The separation between the two antennas is adjusted to be $R > \frac{2(D_1^2 + D_2^2)}{\lambda}$, so that the patterns will be those in the far field region of the antenna. Here D_1 and D_2 are the larger dimensions of the two horns. In all cases the patterns are normalised. (Fig.3.9)

3. Beam Width. Beam width determines the quality of an antenna. The angular width of the main lobe of the pattern at the half-power point is called the beam width or the half power beam width of an antenna[54]. As the E and H-planes have different patterns, they will have different beam widths also. The half power points are the three decibel points on the decible plot, the 0.5 points on the power plot or the 0.707 points on the voltage plot. The chart is always normalised so that the maximum point is unity, or zero decibels.

4. Gain of the Horns. The gain of an antenna is an important measure of its performance in a system. Antenna gain[55] is the ratio of the maximum radiation intensity at the peak of the main beam to the radiation intensity in the same direction which would be produced by an isotopic radiator having the same input power. The gain function describes the variation in the radiated power with angle and is given by

$$G(\theta,\varphi) = \frac{P(\theta,\varphi)}{W_T / 4\pi}$$

Where $P(\theta,\varphi)$ is the power radiated per unit solid angle in the direction θ,φ and W_T is the total radiated power.

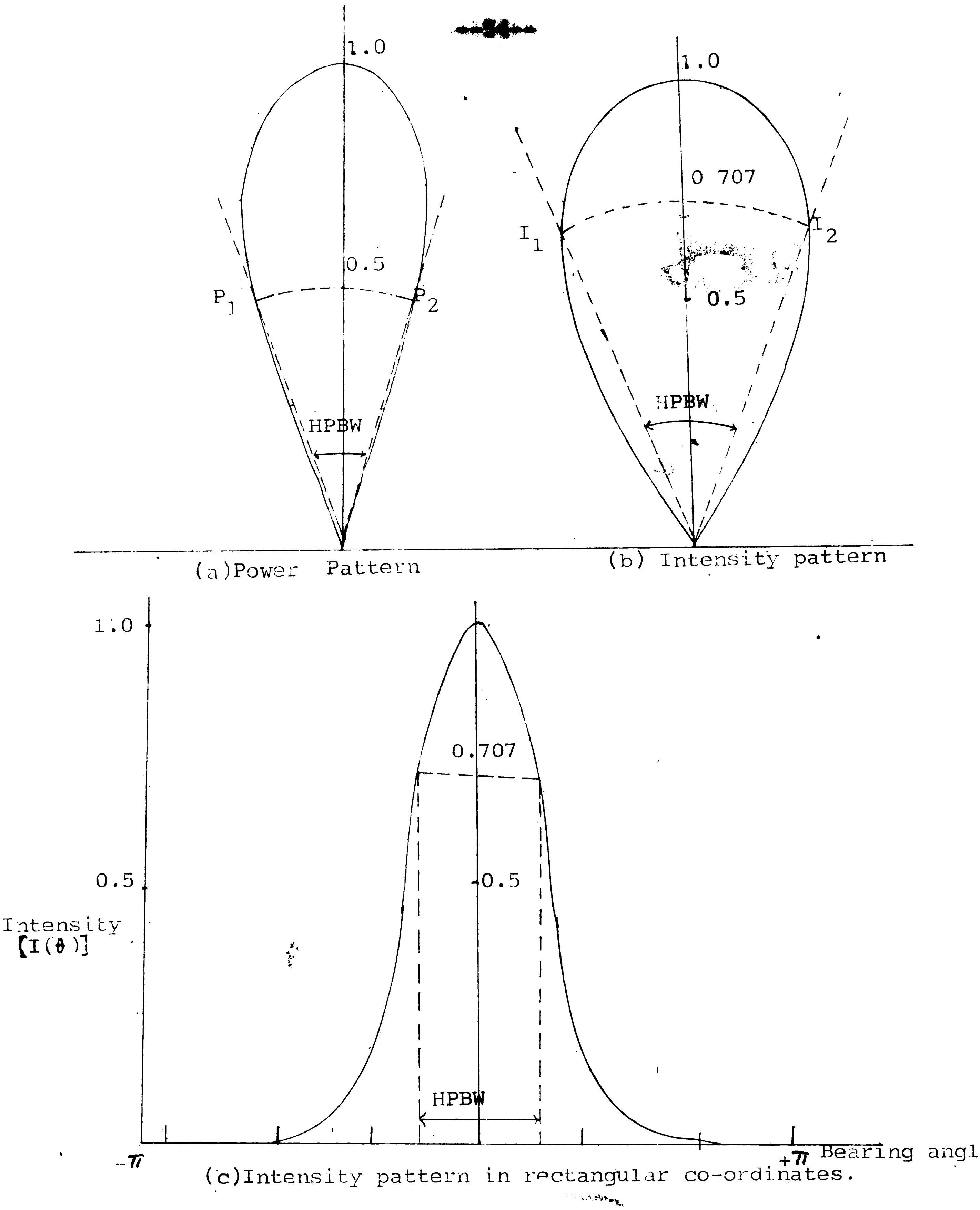

FIGURE 3-8

Determination of Half-Power Beam Width(HPBW) from power and intensity patterns.

Thus a high gain antenna has a main beam with a large amplitude and narrow beam width and side-lobes of relatively small amplitude.

The numerical integration of ~~the~~ intensity pattern in a plane represented in the rectangular co-ordinate gives the gain in that plane (Montgomery)[51].

$$G_\theta = \frac{2\pi I_{max}}{\int_0^{2\pi} I_\theta \, d\theta}$$

I_θ is the intensity corresponding to any bearing angle θ. $\int_0^{2\pi} I_\theta \, d\theta$ is numerically given by the area enclosed between the intensity curve and the axis on which θ is represented with limits 0 to 2π. In decibels, gain is given by

$$G_{dB} = 20 \log_{10} \left[\frac{2\pi I_{max}}{\int_0^{2\pi} I_\theta \, d\theta} \right]$$

5. Voltage Standing Wave Ratio (VSWR).

Standing waves are an indication of the quality of transmission. When there is a reflection from a discontinuity or from the end of a transmission line, part or all of the incident wave is made to travel back towards the input end. Thus, there will be two waves travelling in opposite directions. The places, where the two waves add, will be point of maximum voltage while position of cancellation will have minimum voltage. A well matched line has no reflections. The ratio of the maximum voltage on the line to the voltage at the minimum is called the voltage standing wave ratio.

$$\mathrm{VSWR} = \frac{E_{max}}{E_{mini}}$$

Since the reflected voltage is proportional to the absolute magnitude of the reflection coefficient the standing wave ratio becomes

$$\mathrm{VSWR} = \frac{E_{max}}{E_{mini}} = \frac{1 + |\Gamma|}{1 - |\Gamma|}$$

ie $$|\Gamma| = \frac{\mathrm{VSWR} - 1}{\mathrm{VSWR} + 1}$$

The standing wave ratio may be measured by simply testing the voltage along a transmission line or wave guide. The set up is as shown in Figure 3.2. A longitudinal slot is provided in the wall of a waveguide. A small probe is inserted to sample the voltage and is slided along the waveguide to find the maximum and minimum. The piece of the waveguide with the slot and the probe is called a slotted section or a slotted line. The inserted probe acts as an antenna to receive a small portion of the signal at each point. A crystal is mounted to detect the output voltage which is given to the VSWR meter. VSWR is measured under various flange conditions especially at the optimum and minimum positions of the flange. This is achieved by measuring on axis power and VSWR simultaneously for various flange positions.

6. Parameters - Flange and Corner Reflector. An exhaustive study of the effects of various flange parameters on the beam shape of flanged sectoral horns is carried out in this study. The flange parameters are, the width of the flange elements included angle, position of flange with respect to horn aperture, angle between flange axis and horn axis and different flange elements. The above said parameters are applicable to corner reflectors also. These parameters are obtained by direct measurement made on the flange or corner reflector system.

For theoretical calculations, electronic calculators are widely used. A few radiation patterns are calculated using an ECIL computer facility elsewhere.

CHAPTER IV

EXPERIMENTAL RESULTS

4.1 Introduction

In this chapter experimental results obtained from various investigation with flanged sectoral horns and corner reflector systems are presented. In order to compare the action of flanges with that of corner reflector system, the observations are confined to the main effects produced by the systems. The main aspects thus investigated are:

a) Variation of on-axis power of the systems when the distance of the primary feed from the apex of the flange or corner reflector system is varied.

b) The existence of O and M positions. (Optimum and Minimum positions).

c) Variations of the radiation patterns of the systems at the O and M positions.

d) Changes in the beam width of the systems for various positions of the primary with respect to the apex.

e) Possibility of the beam tilt by imposing asymmetry on the systems.

A. Results Obtained with Metallic Flanges Fitted on Sectoral Electromagnetic Horn Antennas

4.2 Variation of On-axis Power with Relative Position of the Flange with respect to the Aperture

It has been observed that the on-axis power of a flanged sectoral horn depends on the position of the flanges with respect to the aperture of the horn. The nature of this variation is established by the set up shown in Figures 4.1(A) and 4.1(B). The detector is kept at a point in the far zone, ($R > \frac{2D^2}{\lambda}$) along the axis of the system. The flange system is gradually moved backwards.

The distance Z and the corresponding on-axis power are measured. Observations representing on-axis power, P_e versus flange position Z are taken for a number of horns with flanges of varying length and included angle. Few such observations are given in Tables 4.1 to 4.3. Figures 4.2 and 4.3 show the general form of these variations. The distance Z is varied in steps of 0.50 cm. Details of these method of measurement is given in section 3.7. Extreme care is taken in maintaining the symmetry of the flange system and keeping the detector crystal exactly along the axis. Graphs connecting P_e and Z are

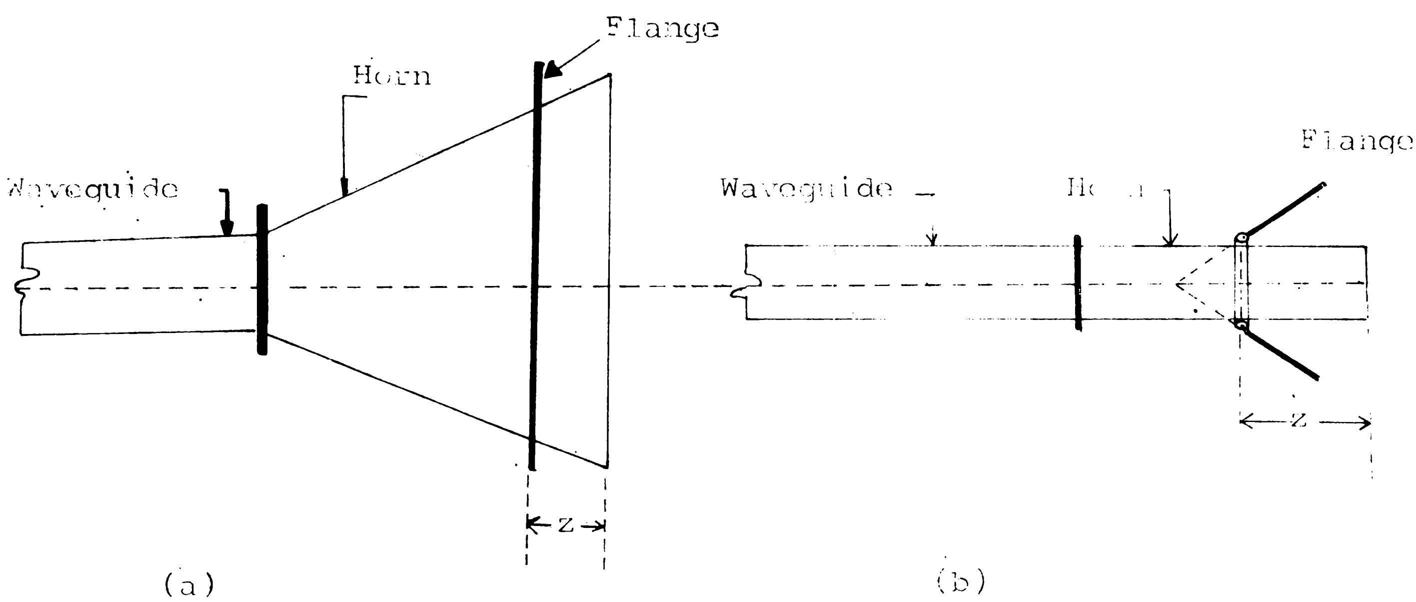

FIGURE 4-1(A)

FLANGED H-PLANE SECTORAL HORN

(a) View in the H-plane

(b) View in the E-plane

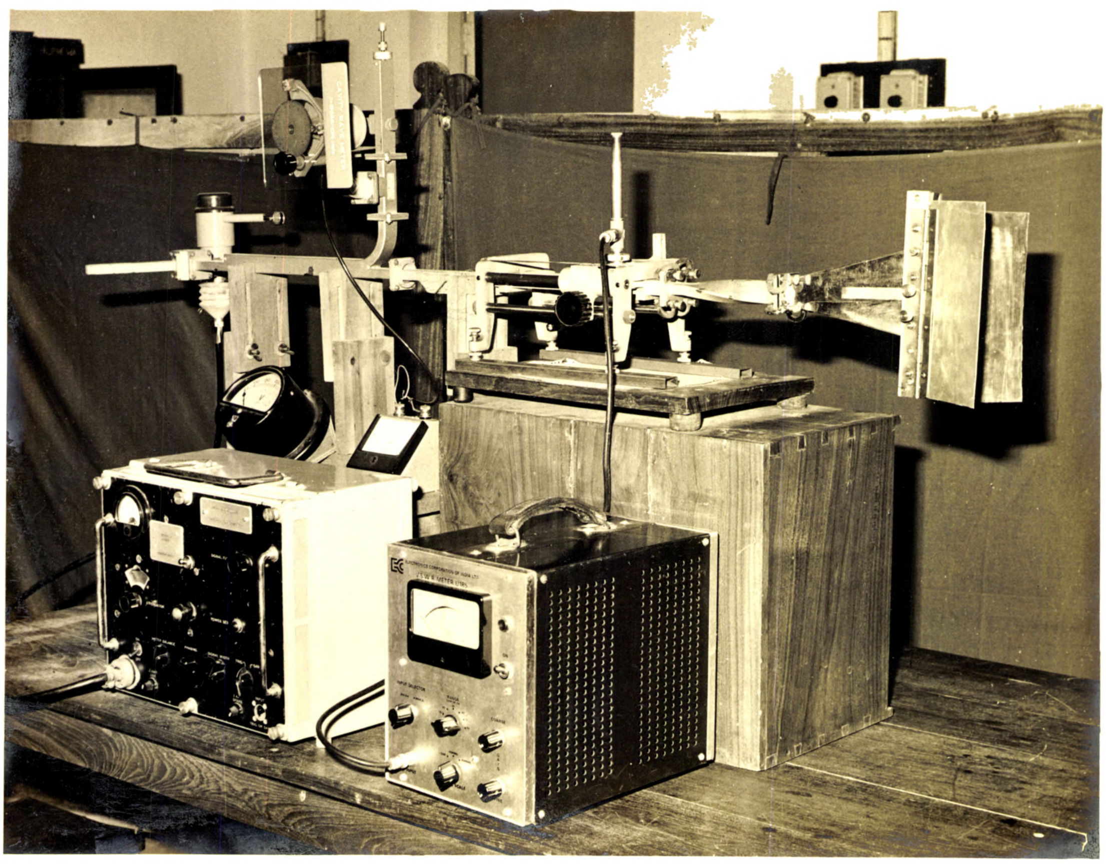

FIGURE 4.1(B)

Set up for the measurement of on-axis power

TABLE 4.1 Variation of On-axis Power with Position of Flange

Flange distance from horn aperture Z cm	Normalised on-axis power P_0	
	Horn H1, Freq. 9.4 GHz, W/λ = 3, 2α = 60°	Horn H3, Freq.9.4.GHz, W/λ = 2, 2α = 90°
0	0.73	0.53
0.3	1.00	--
0.5	0.49	0.40
1.0	0.018	0.27
1.5	0.00	0.12
2.0	0.26	0.08
2.5	0.57	0.37
3.0	0.73	0.63
3.2	0.77	--
3.5	0.69	0.86
4.0	0.55	1.00
4.5	0.60	0.99
5.0	0.51	0.92
5.5	0.26	0.75
6.0	0.20	0.60
6.5	0.37	0.45
6.7	0.41	--
7.0	0.30	0.33
7.5	0.24	0.19
8.0	0.29	0.17
8.5	0.45	0.17
9.0	0.33	0.25
9.5	0.26	0.40
10.0	0.45	0.55
10.5	0.36	--
10.8	0.24	--
11.0	0.22	--
11.5	0.36	--
12.0	0.44	--
12.5	0.25	--

TABLE 4.2 Variation of On-axis Power with Position of Flange

Flange distance from horn aperture Z cm.	Normalised on-axis power P_o	
	Horn H2 Freq. 9.4 GHz W/λ = 2 2α = 90°	Horn H4 Freq. 7.5 GHz W/λ = 2.5 2α = 60°
0	0.30	0.26
0.5	0.06	0.18
1.0	0.32	0.15
1.5	0.47	0.13
2.0	0.78	0.21
2.5	1.00	0.31
3.0	0.56	0.45
3.5	0.12	0.64
4.0	0.14	0.74
4.5	0.09	0.86
5.0	0.42	0.97
5.5	0.61	1.00
6.0	0.39	0.80
6.5	0.18	0.55
7.0	0.31	0.51
7.5	0.29	0.49
8.0	0.21	0.47

TABLE 4.3 Variation of On-axis Power with Position for Flange

Flange distance from horn aperture Z cm	Normalised on-axis power P_0	
	Horn E1 Freq. 9.40 GHz W/λ = 3.7 2α = 60°	Horn E2 Freq. 9.4 GHz W/λ = 3.0 2α = 40°
0	0.84	0.89
0.5	1.00	0.96
1.0	0.83	1.00
1.5	0.60	0.71
2.0	0.39	0.25
2.5	0.21	0.45
3.0	0.10	0.59
3.5	0.10	0.73
4.0	0.14	0.54
4.5	0.21	0.63
5.0	0.36	--
5.5	0.49	--
6.0	0.61	--
6.5	0.40	--
7.0	0.24	--
7.5	0.21	--
8.0	0.29	--
8.5	0.39	--
9.0	0.36	--

plotted for different definite values of flange angle with flanges of different widths using various sectoral horns operating at different frequencies.

These observations are made on both H-plane and E-plane sectoral horns. Figures 4.2 and 4.3 are showing the results for a few H-plane and E-plane sectoral horns respectively.

It is observed from P_e-Z curves which have the approximate shape of damped sinusoidal variations in general, that there are distinct flange positions with respect to the aperture, where P_e reaches maximum values. Whereas for certain other positions it reaches minimum values. These positions are called the "optimum position (or O-position"). and "minimum position (or M-position") respectively. The flange kept at the aperture is said to be at the "A-position". This position provides a reference for comparison with the above two positions. The distances of O-position and M-position from the aperture are represented by Z_e and Z_m respectively. These values can be readily obtained from the P_e-Z plots. From the different O and M positions we take the most dominant position for further study of radiation patterns.

It can be argued from the P_e-Z graphs that a flange at O-position may give a favourable set up for axial concentration of energy and hence a focussing of the

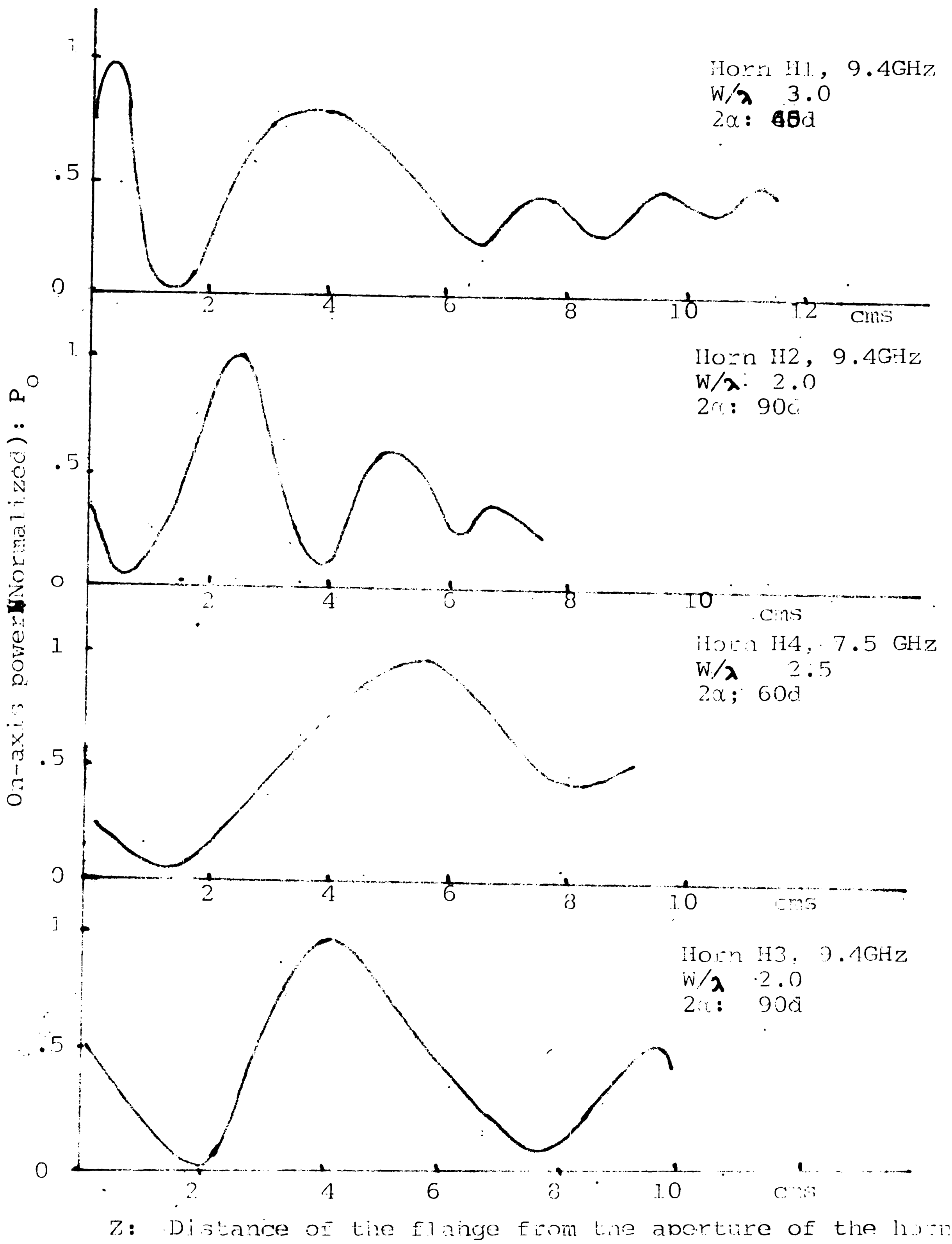

FIGURE 4-2
VARIATION OF THE ON-AXIS POWER OF FLANGED SECTORAL HORN WITH THE POSITION OF THE FLANGE

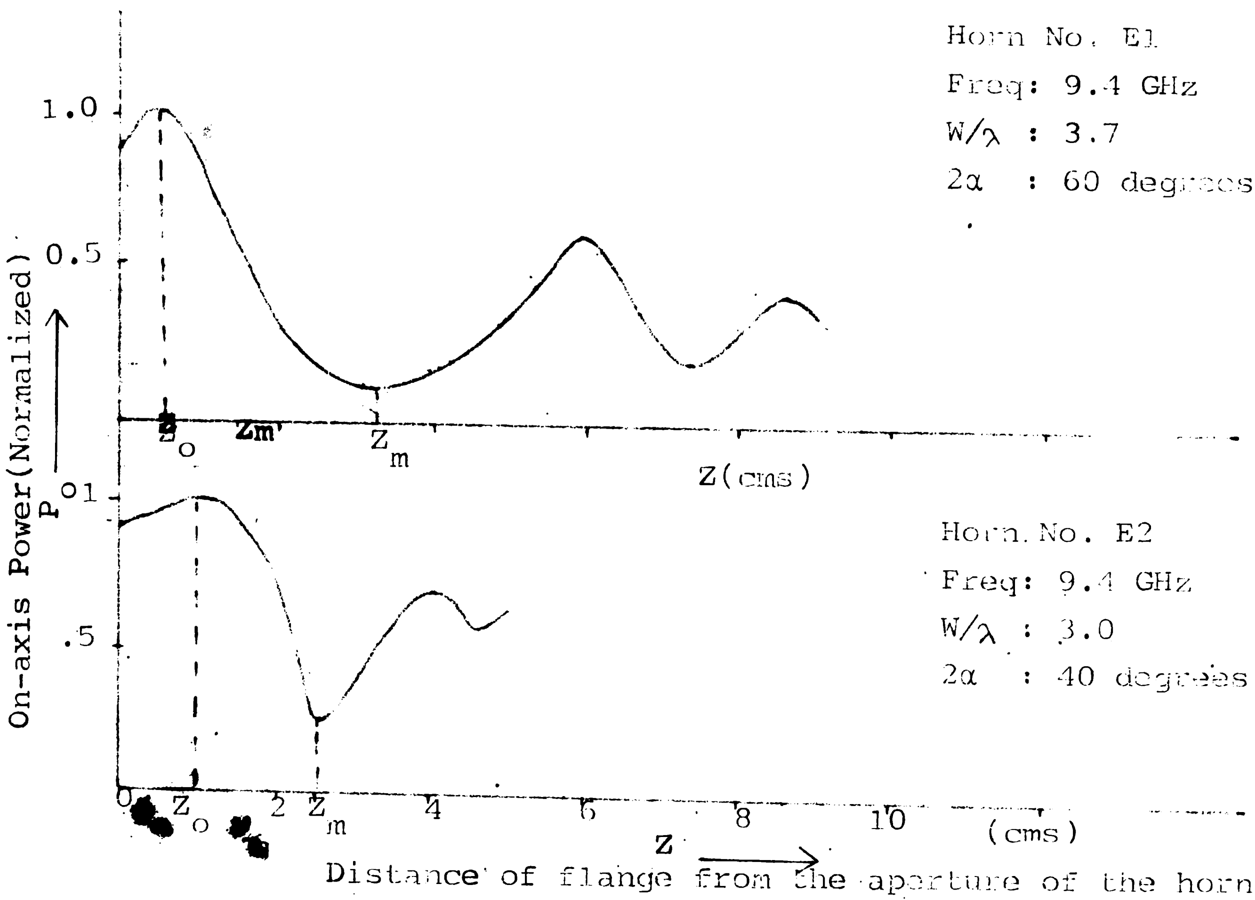

FIGURE 4-3
VARIATION OF ON-AXIS POWER OF FLANGED SECTORAL HORNN
WITH THE POSITION OF THE
FLANGE

beam from the horn. On the other hand, a flange at M-position may avoid axial flow of energy, resulting a beam splitting or beam broadening. This is taken as the next point for investigation.

4.3 Effect of Flange Position on Beam Shape: Variation of Radiation Patterns at Different Positions of the Flange System. Change in HPBW

As indicated in the preceeding section, the variation of on-axis power with the position of the metallic flange with respect to the aperture is a clue for the possibility of beam shaping or sectoral electromagnetic horn antennas. Both the H and E-plane sectoral horns are subjected to intensive study in this respect. The changes in radiation patterns are observed in the plane perpendicular to the plane of flare of the horns. The flange system will not make any change in the radiation patterns of the horns in the plane of flare. Thus, for the H-plane sectoral horn, the variation effected by the flange system will be only in the E-plane patterns. The H-plane patterns of the H-plane sectoral horn remain unaffected by the flange system. Similarly, for the E-plane sectoral horns, E-plane radiation patterns remain unaffected, while the drastic changes are observed only for the H-plane radiation patterns. This behaviour of the flange system is illustrated in Fig. 4.4, presenting the natural

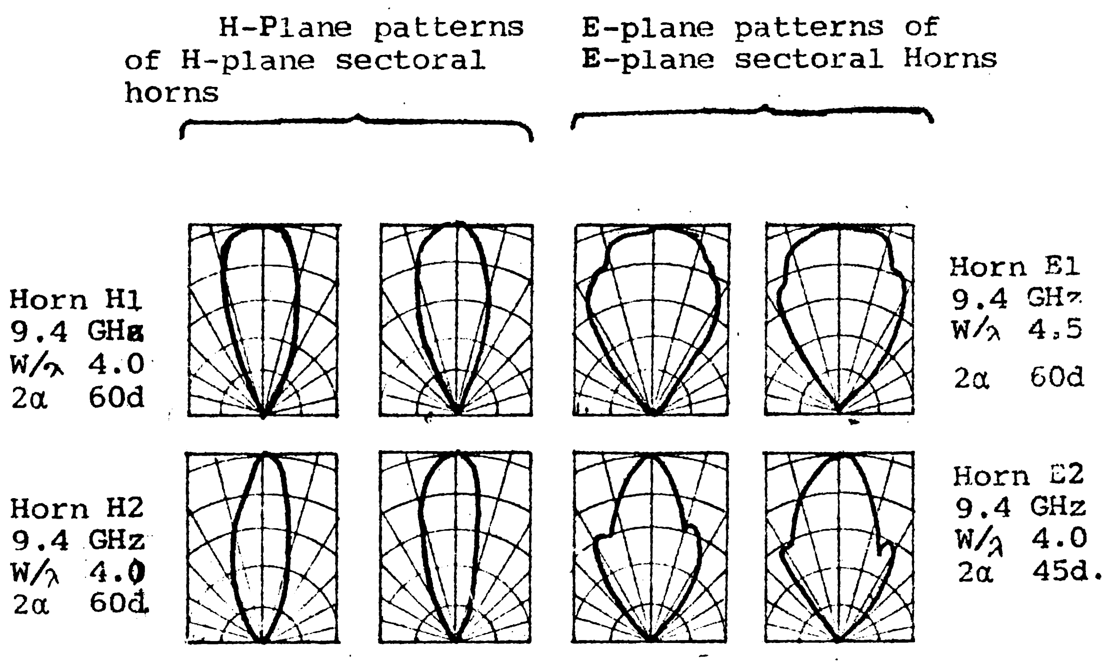

FIGURE 4.4

RADIATION PATTERNS OF SECTORAL HORNS WITH AND WITHOUT FLANGES
The flange system does not make any significant change in the radiation patterns in the plane of flare of the sectoral horns.

radiation patterns in the respective plane with and without flange system. Interpretation of this phenomenon will be given in a subsequent chapter, where theoretical explanations are presented.

4.3A Variation of E-plane Radiation Patterns of H-plane Sectoral Horn with Respect to the Position of a Flange System.

*To study the effect of flange position on the E-plane radiation pattern of the H-plane sectoral horn, the natural E-plane patterns of the horns are obtained first. These are taken as the reference patterns. The radiation patterns are recorded by the method described in section 3.7. A waveguide twist is conveniently used to make the E-plane horizontal. The test antenna system is used as a receiver, which is capable of rotating about a vertical axis passing through the apex of the flange system. After plotting the natural pattern of the horn a flange system of a particular width and angle is symmetrically mounted on it at the A-position. Similar measurements are repeated with the same flange at the 'O' and 'M' positions which are determined from the P_e-Z graph of the horn. These measurements are repeated with the same horn but with flanges of different included angle and flange lengths. A number of frequencies are tried for ascertaining the results.

TABLE 4.4 Measured E-plane Radiation Pattern at various Positions of Flange

Horn H1; Freq: 9.4 GHz; $W/\lambda = 2$, $2\alpha = 90°$

Bearing angle $\theta°$	Normalised power at angle θ			
	Natural pattern (without flange)	with flange		
		At aperture	At O-position	At M-position.
0	1.00	1.00	1.00	0.1
5	0.98	0.83	0.54	0.16
10	0.95	0.74	0.22	0.42
15	0.95	0.70	0.03	0.48
20	0.89	0.63	0.01	1.00
25	0.82	0.58	0.00	0.88
30	0.74	0.39	0.015	0.68
35	0.68	0.26	0.05	0.52
40	0.59	0.21	0.09	0.46
45	0.64	0.19	0.10	0.36
50	0.50	0.16	0.08	0.24
55	0.45	0.10	0.058	0.16
60	0.41	0.06	0.048	0.06
65	0.27	0.03	0.039	0.04
70	0.35	0.00	0.01	0.00
75	0.27	0.00	0.00	0.00
80	0.23	0.00	0.00	0.00
85	0.18	0.00	0.00	0.00
90	0.16	0.00	0.00	0.00

E-PLANE RADIATION PATTERNS OF H-PLANE SECTORAL HORNS

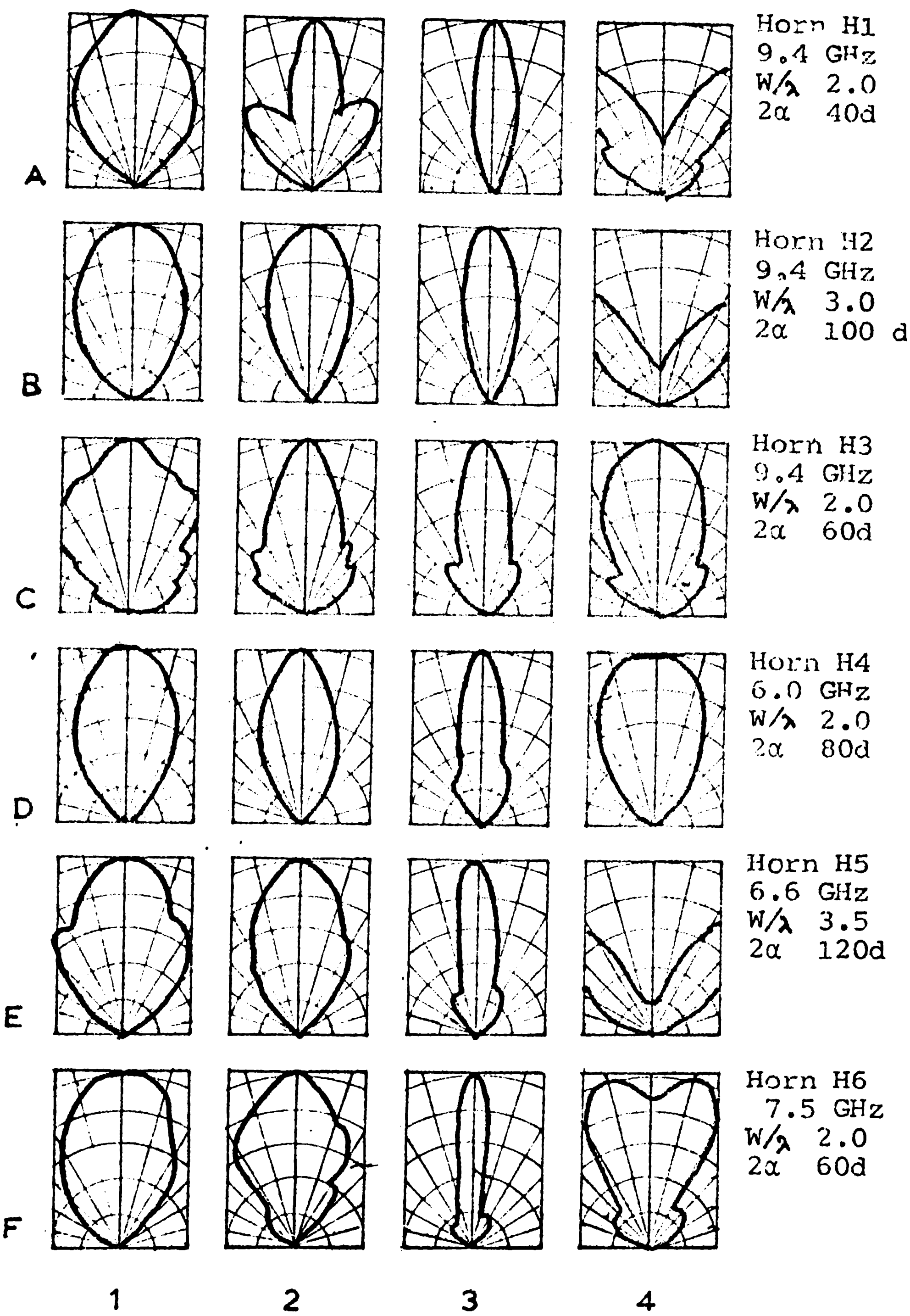

FIGURE 4-5

NATURAL AND MODIFIED E-PLANE RADIATION PATTERNS OF H-PLANE SECTORAL HORNS

1. Natural pattern(without flange system)

2,3,4: Modified patterns with flange at the Aperture, O-position and M-position respectively.

A set of sample observations is given in Table 4.4. The readings are normalised so that the patterns will have the same maximum (unity) irrespective of the different maximum power available in each case. A few sets of radiation patterns are represented in Fig. 4.5.

4.3B <u>Variation of H-plane Radiation Patterns of E-plane Sectoral Horns with respect to the Position of the Flange System</u>

As in the case of the H-plane sectoral horns the effect of the flange position on the H-plane radiation patterns of the E-plane sectoral horn is studied by keeping the flange at different positions with respect to the aperture. For taking these patterns with the set up described in Chapter III, the transmitting horn is attached to the waveguide system. The horn antenna under test with the flange system is used as the receiver and is arranged on the turntable such that the E-plane pattern can be conveniently taken.

A few observations are given in Table 4.5. Fig. 4.6 represents a set of H-plane radiation patterns of the E-plane sectoral horns used in this investigation.

It can be seen that the E-plane radiation patterns of the H-plane sectoral horns and H-plane radiation patterns of E-plane sectoral horns are adjustable to a greater extent by the flange technique. At 0-position the beams

TABLE 4.5 Measured H-plane Radiation Pattern at various Positions of Flange

Horn E1 Freq: 9.4 GHz; W/λ = 2.5 ; 2α = 50°

Bearing angle $\theta°$	Normalised power at angle θ			
	Natural pattern (without flange)	with flange		
		At aperture	at O-position	At M-position
0	1.0	1.00	1.00	0.38
5	0.98	0.82	0.89	0.34
10	0.88	0.55	0.63	0.41
15	0.78	0.40	0.52	0.59
20	0.67	0.26	0.38	0.79
25	0.59	0.15	0.38	0.79
30	0.56	0.15	0.20	1.00
35	0.42	0.19	0.14	0.93
40	0.30	0.21	0.13	0.79
45	0.27	0.23	0.09	0.69
50	0.20	0.13	0.09	0.62
55	0.13	0.13	0.05	0.48
60	0.10	0.13	0.02	0.41
65	0.067	0.13	0.00	0.30
70	0.05	0.09	0.00	0.17
75	0.02	0.02	0.00	0.11
80	0.00	0.00	0.00	0.07
85	0.00	0.00	0.00	0.03
90	0.00	0.00	0.00	0.00

H-PLANE RADIATION PATTERNS OF E-PLANE SECTORAL HORNS

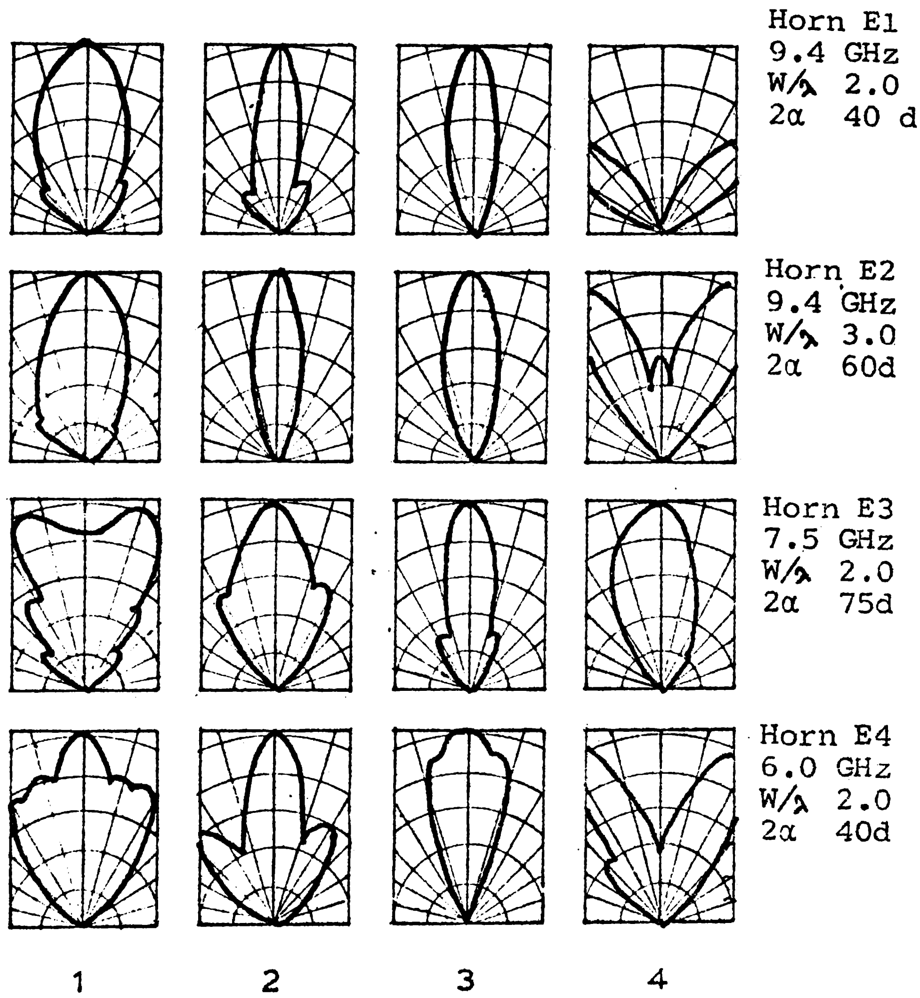

FIGURE 4-6

NATURAL AND MODIFIED H-PLANE RADIATION PATTERNS OF E-PLANE SECTORAL HORNS

1. Natural pattern(without flange system)
2,3,4: Modified patterns with flange at the Aperture, O-position and M-position respectively.

are invariably sharpened or focussed while at M-position the patterns are broadened or split up into major side lobes. The extent to which this effect is observed is seen from tables 4.6 and 4.7 in which the half power beam widths of the systems are tabulated.

4.4 Variation in VSWR for the Different Positions of the Flange System

The impedance conditions of the flanged sectoral horns are studied by observing the VSWR of the system. The horn under test is fitted at the end of the micro-wave test set up as shown in figure 3.2. The VSWR is measured with the horn. Keeping the flanges at the O-position and M-position, the observations are repeated. It is observed that the VSWR of the horn is not considerably affected by the flange system. In some cases slight decrease in VSWR was observed when the flange is at O-position. This result holds for both H and E-plane sectoral horns. These results are presented in the table 4.8.

4.5 Possibility of Beam Tilting by Asymmetry Imposed on the Flange System.

a) Axis asymmetry. In the earlier sections, the flanges used were all symmetric with respect to the horn radiator. But we may think of imposing asymmetries on the system. For example, an axis asymmetry can be imposed by tilting the flange axis off the horn axis.

TABLE 4.6 Half power Beam Widths of the E-plane Patterns of H-plane Sectoral Horns with and without Flanges

Horns	Frequency GHz	Flange width W/λ	Flange angle 2α	Half power beam width in the E-plane (deg)			
				Natural	with flanges		
					at A	at O	at M
H1	9.4	2	40°	80°	30	27	90*
H1	9.4	3.7	100°	80°	46	28	80*
H2	9.4	3.0	100°	92	66	40	84*
H3	7.5	2.0	50°	98	69	47	73
H3	6.0	2.5	60°	128	58	20	75
H4	6.0	2	80°	90	48	19	64
H4	6.6	2	140°	84	52	20	55
H5	7.5	3.7	120°	88	63	29	108*

* Indicates that the beam is split. Beam width in this case is taken as the sum of the half power beam widths of the lobes.

TABLE 4.7 Half-power Beam Width of H-plane Patterns of E-plane Sectoral Hors with and Without Flanges

Horns	Frequency GHz	Flange width W/λ	Flange angle 2α	Half power beam width in the H-plane (deg)			
				without flange (natural)	with flanges		
					At A	At O	At M
E1	9.4	2	40°	60°	23	30	100*
E1	9.4	3	60°	60°	24	26	98°*
E2	9.4	2.5	75°	48°	50°	29°	50
E2	9.4	2	75°	72°	50°	33°	67°*
E3	6.0	2	40°	70°	31	25°	52*
E4	7.5	3.5	40°	68°	60°	31°	50°
E5	7.5	3	60°	77°	57°	29°	48°
E6	6.66	3.5	60°	83°	60°	41°	73*

*Indicates that the beam is split. Beam width in this case is taken as the sum of the half power beam widths of the lobes.

--78--

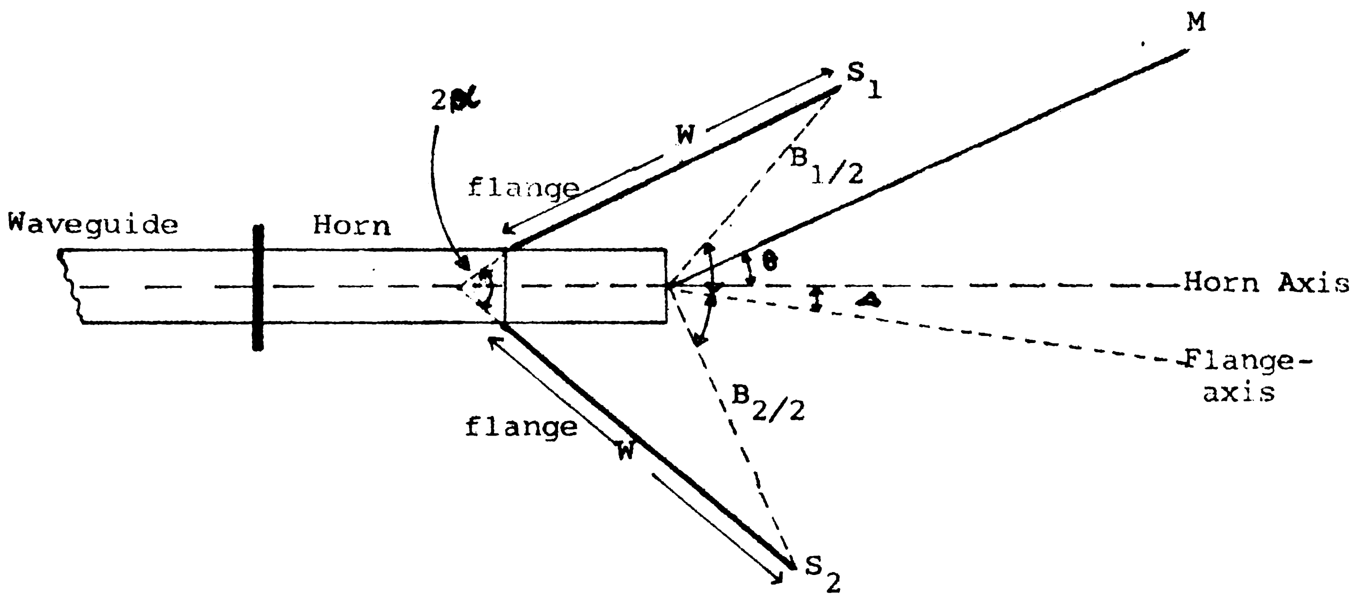

FIGURE 4-7

REPRESENTATION OF A FLANGE SYSTEM WITH AXIS ASYMMETRY

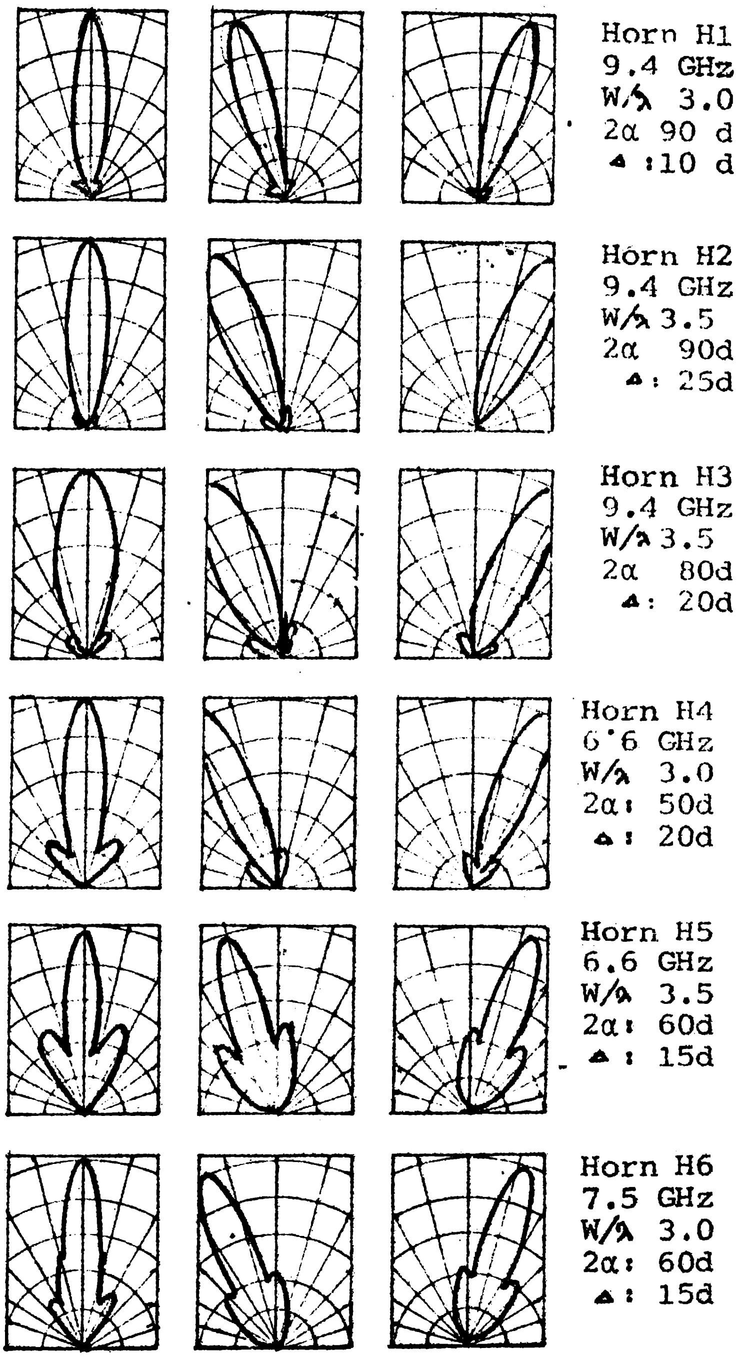

(a) (b) (c)

FIGURE 4-8

RADIATION PATTERNS SHOWING TILTING OF BEAMS

(a)Shaped beam with symmetrical flange at 0-position
(b) Flange axis tilted towards left
(c) Flange axis tilted towards right.

Fig.4.7 shows the flange system with axis asymmetry. Let the angle between the two axes be Δ . The resultant beam-shape of this asymmetric system is investigated as follows.

The asymmetric system of the flange of elements of the same material and of equal flange widths, is moved to an optimum position as determined earlier. Using the system as a receiver of CW signal from a standard pyramidal horn, the radiation patterns are plotted. A set of sample observations is given in Table 4.9. For $\Delta = 15°$, 20° and 25° the radiation patterns taken in different cases are shown in Figure 4.8.

It can be seen that the focussed beam is undergoing a definite tilt due to this asymmetry. It is interesting to note that the resultant beam is effectively tilted towards the flange axis from the horn axis.

b) Asymmetry in flange width. Another type of asymmetry which can be imposed on a flange system is the width asymmetry. This means that we are putting the flange elements of the same material with different widths, say W_1 and W_2. The axis of the flange is made to be the same as the horn axis. The optimum position for such a flange system is obtained from the data available with a flange system of mean width $W = \frac{W_1 + W_2}{2}$. The radiation patterns corresponding to the optimum position are

TABLE 4.8 Variation of VSWR of Flanged Sectoral Horn for various Positions of Flange System

Frequency used : 9.4 GHz

Horn	W/λ	2α deg	VSWR without flange	VSWR Flange at O-position	VSWR Flange at M-position
H1	2.5	45	1.41	1.30	1.57
H1	2.5	60	1.41	1.32	1.60
H2	3.5	90	1.45	1.38	1.52
H2	2.5	120	1.45	1.41	1.54
E1	2	60	1.237	1.265	1.296
E1	2.5	45	1.237	1.273	1.292
E2	2	30	1.40	1.41	1.46
E2	3	75	1.40	1.41	1.44

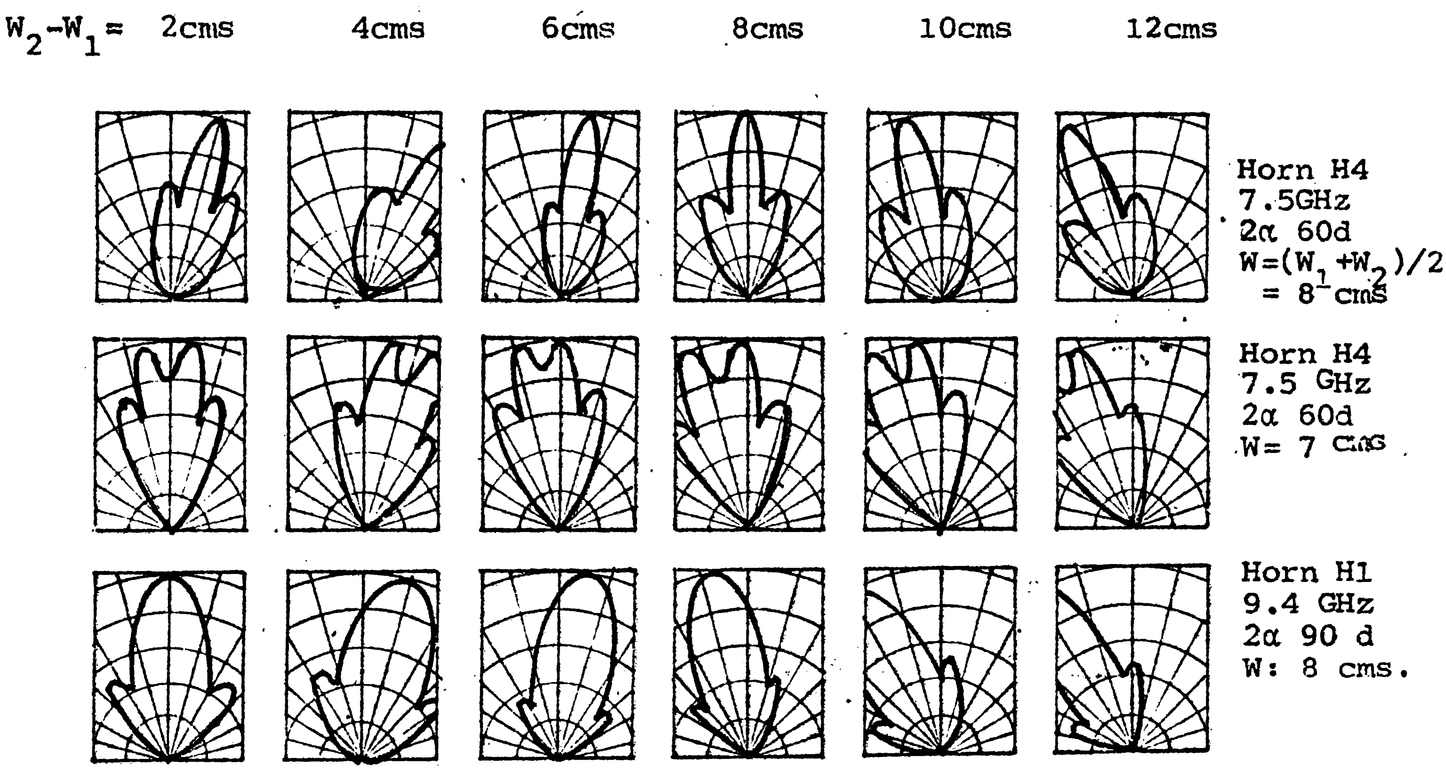

FIGURE 4-9

TILTING OF BEAM BY ASYMMETRY IN FLANGE WIDTH plotted. It is observed that the beam is undergoing a tilt by this asymmetric flange also. For different values of $(W_2 - W_1)$, the patterns are recorded. The mean width $\frac{({}^2W_1 + {}^1W_2)}{2}$ is kept constant throughout. The tilt of the beam is found to be towards the side of the smaller flange element for smaller values of $(W_2 - W_1)$. But, as this quantity is increased the tilt becomes zero at some stage and then goes to the side of the longer element. The result has been confirmed with results obtained for different horns and frequencies. In figure 4.9 these patterns are shown.

c) Asymmetry in amplitude of excitation of the flange elements. If the flange elements are of different materials we get a flange system which may give secondary radiators of unequal amplitudes. This also may be treated as a system with asymmetry. The widths of the elements will be the same and its axis collinear with the horn axis. In the present investigation, on one side, flange element of aluminium is used, while on the other side, a perspex element of the same width and thickness as that of the metal element is used. Keeping the flange at the 0-position, the radiation pattern is plotted. The patterns thus obtained for different horns and flange parameters are shown in Figure 4.10. Table 4.10 gives observations taken for plotting a few such radiation patterns.

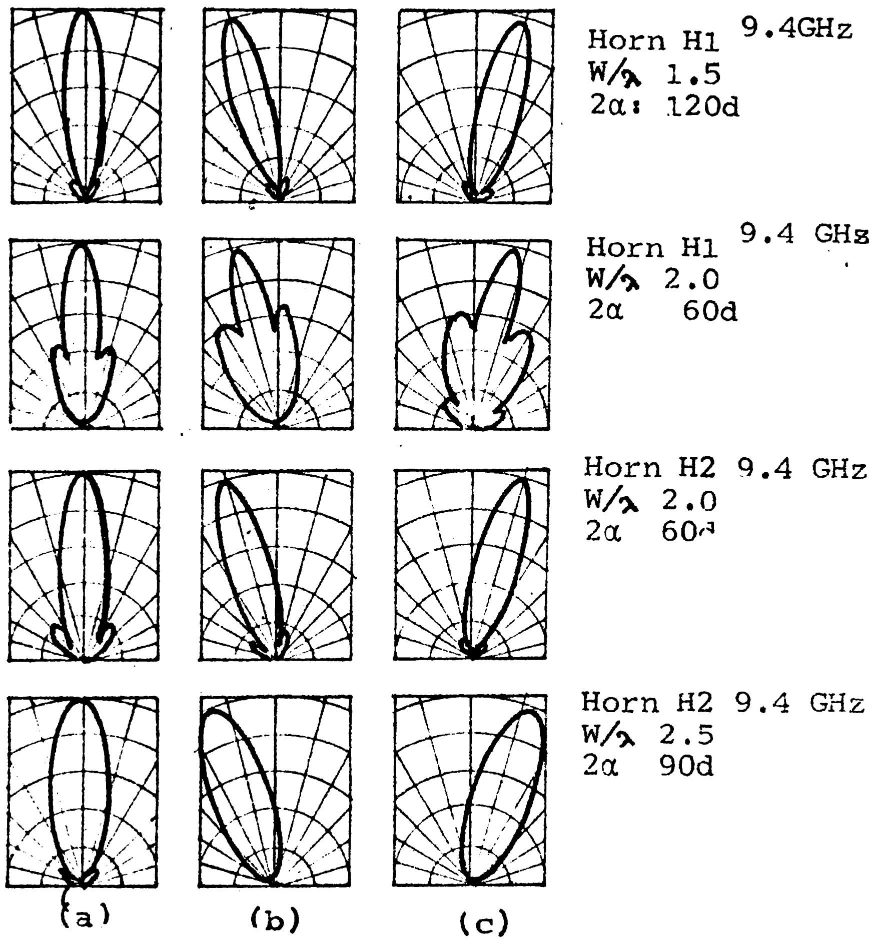

FIGURE 4-10
BEAM TILTING BY AMPLITUDE ASYMMETRY

(a)Both flange elements metallic
(b)Metallic flange on left side
(c)Metallic flange on right side.

TABLE 4.9 Measured Radiation Pattern of a System with Axis Asymmetry

Horn H1; Frequency 9.4 GHz; W/λ = 1.5, 2, 2α = 90°
Z = 2 cm, 3 cm.

Bearing angle $\theta°$	Power P_θ (Galvanometer reading)			
	Δ = 15°		Δ = 25°	
	Left	Right	Left	Right
0	38	38	54	54
5	90	6	79	33
10	90	4	102	36
15	104	14	98	70
20	117	25	78	145
25	96	23	68	128
30	34	31	47	80
35	10	29	35	88
40	19	20	28	100
45	34	16	26	100
50	45	10	24	64
55	23	5	19	30
60	21	0	19	17
65	21	0	17	22
70	10	0	16	15
75	5	0	10	15
80	5	0	8	10
85	0	0	2	7
90	0	0	0	0

TABLE 4.10 Measured Radiation Pattern with Flange Element asymmetry (Amplitude asymmetry)

Horn H1; Freq. 9.4 GHz; $W/\lambda = 2$; $2\alpha = 60°$

Bearing angle $\theta°$	Normalised Power P_θ		
	Both Metallic	Metallic flange left	Dielectric flange right
0	1.00	0.62	0.62
5	0.85	0.77	0.50
10	0.53	0.85	0.34
15	0.27	0.94	0.26
20	0.19	1.00	0.17
25	0.18	0.94	0.12
30	0.15	0.79	0.08
35	0.14	0.62	0.07
40	0.08	0.41	0.05
45	0.06	0.29	0.05
50	0.05	0.18	0.045
55	0.03	0.11	0.04
60	0.01	0.07	0.03
65	0.01	0.032	0.02
70	0.01	0.01	0.00
75	0.01	0.00	0.00
80	0.00	0.00	0.00

It can be observed that the tilt produced by this asymmetry is towards the side containing the metal flange. This tilt is most significant for smaller flange angles.

From the foregoing section, it is evident that the flange system is capable of shaping the beam from a sectoral electromagnetic horn antenna. The different parameters involved can be conveniently adjusted for controlling the beam shape to any desired pattern. A beam thus focussed can be even tilted to any side by imposing one or more asymmetric conditions on the system.

B. Results Obtained with Corner Reflector System

4.6. Variation of On-axis Power with Distance of the Primary Feed from the Apex of the Corner Reflector System.

In this case the primary feed is a half wave dipole fed through a co-axial cable, from a microwave source. The corner reflector system is simply two metallic sheets oriented at an angle 2α. The feed dipole is parallel to the apex-line of the corner reflector system. Radiation patterns of such system have been thoroughly studied by many reseearch workers[40-46]. However a systematic study of the corner reflector system in comparison with the flanged sectoral horn has not yet been attempted.

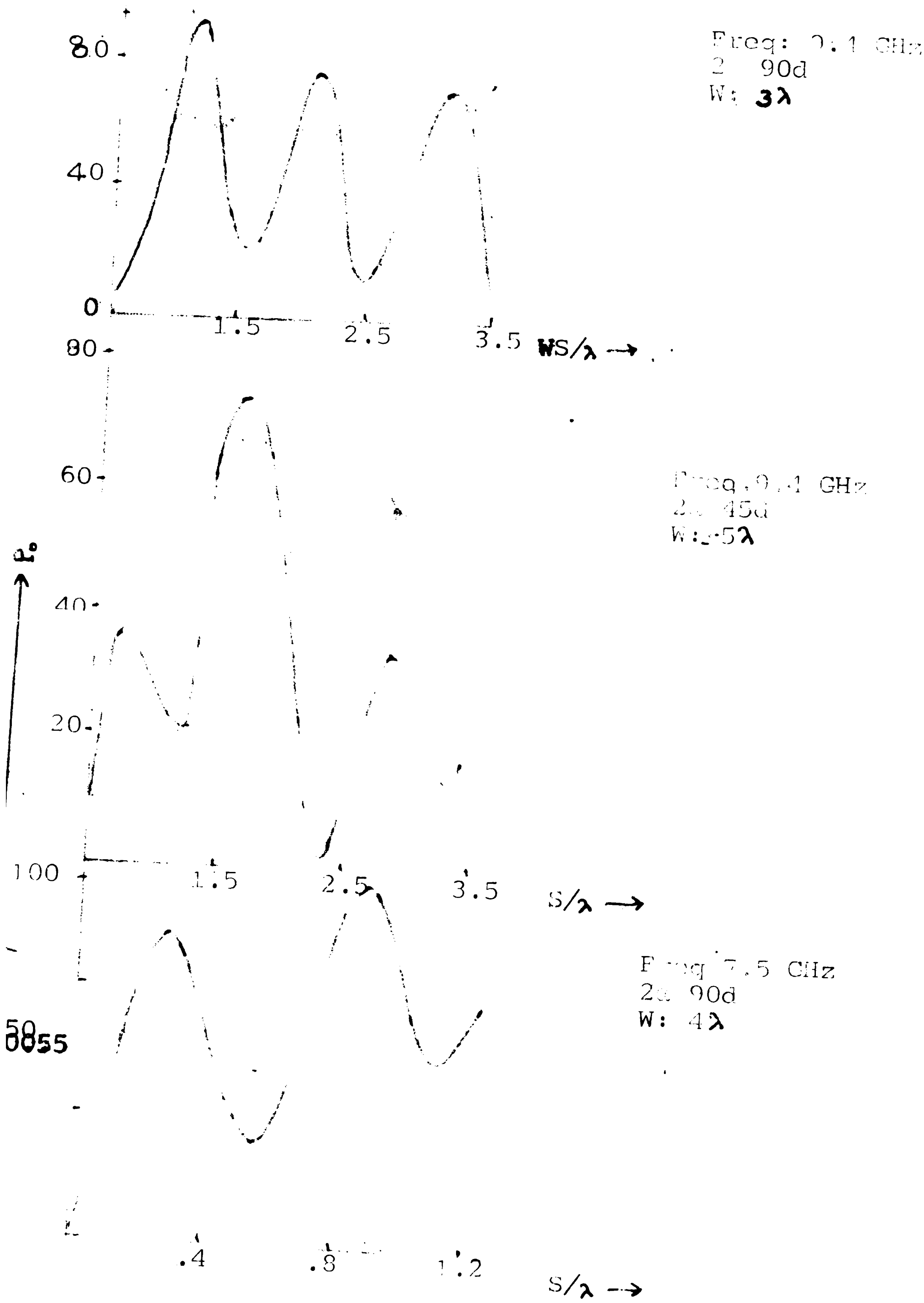

FIGURE 4-11
VARIATION OF ON-AXIS POWER WITH THE POSITION OF THE PRIMARY FEED DIPOLE OF A CORNER REFLECTOR SYSTEM

Hence the present observations are taken in step by step procedure adopted for flanged sectoral horns.

The variation of the on-axis power with distance 'S' of the primary feed is obtained by keeping a detector crystal at a point along the axis in the far field region. The distance 'S' is varied in regular steps and the variation of P_e, the on-axis power is noted. It is interesting to note that P_e undergoes periodic variations giving distinct maximum and minimum on-axis power. These positions can be easily obtained from the graph. Sample observations are given in Table 4.11. For various angles of the corner reflector system these results have been verified. Figure 4.11 shows graphical representation of these results.

4.7 Variation of Radiation Patterns at Different Positions of the Primary Feed.

The rapid variations in the on-axis power with respect to the distance 'S' of the primary feed is suggesting the possibility of beam shaping as in the case of flanged sectoral horns. To test this conclusion, H-plane radiation patterns of the corner reflector system are taken for different values of 'S'. These are presented in figure 4.12. Typical observations for plotting the radiation patterns are given in Table 4.12(a) and 4.12(b).

TABLE 4.11 Variation of On-axis power P_o with the Primary Feed Dipole

Frequency : 9.4 GHz.

Distance of dipole from the apex in λ	On-axis power (Galvenometer reading) W = 3λ, 2α = 60°	W = 3λ; 2α = 90°
0	110	11
0.1	260	22
0.2	38	30
0.3	34	32
0.4	27	38
0.5	29	67
0.6	32	88
0.7	21	88
0.8	33	53
0.9	44	16
1.0	59	20
1.1	73	35
1.2	71	28
1.3	62	22
1.4	56	44
1.5	42	75
1.6	23	70
1.7	8	50
1.8	1	8
1.9	5	7
2.0	10	18
2.1	13	21
2.2	16	18
2.3	18	21
2.4	17	9
2.5	13	7
2.6	12	10
2.7	11	48
2.8	15	68
2.9	29	56
3.0	28	35
3.25	12	5
3.5	9	6

TABLE 4.12(a) Measured Radiation Patterns of Corner Reflector System

Frequency : 9.4 GHz; $2\alpha = 45°$; Width $= 3\lambda$

Bearing Angle $\theta°$	Normalised power	
	At Optimum position	At Minimum position
0	1.00	0.46
5	0.700	0.30
10	0.16	0.66
15	0.13	0.50
20	0.16	0.06
25	0.14	0.59
30	0.13	1.00
35	0.12	0.94
40	0.10	0.49
45	0.09	0.49
50	0.07	0.23
55	0.06	0.15
60	0.03	0.11
65	0.01	0.09
70	0.00	0.03

TABLE 4.12(b) Measured Radiation Patterns with Corner Reflector

$W/\lambda = 2$; $2\alpha = 90°$

Frequency : 7.5 GHz

Bearing angle $\theta°$	Normalised power: Optimum position	Normalised power: Minimum position
0	1.00	0.2
5	0.70	0.13
10	0.31	0.08
15	0.13	0.30
20	0.16	0.75
25	0.13	1.00
30	0.12	0.82
35	0.15	0.48
40	0.11	0.16
45	0.09	0.10
50	0.06	0.08
55	0.31	0.60
60	0.01	0.043
65	0.01	0.011
70	0.00	0.00

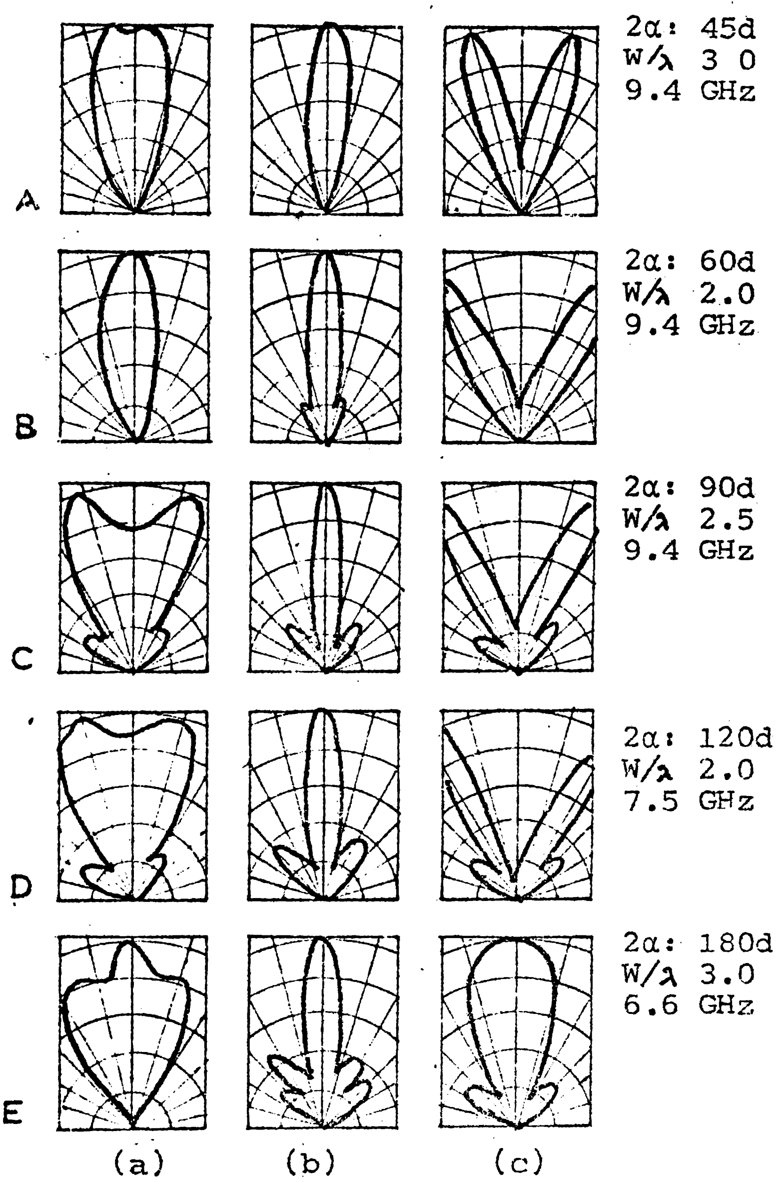

FIGURE 4-12

RADIATION PATTERNS OF CORNER REFLECTOR ANTENNAS
AT DIFFERENT POSITIONS OF
THE DIPOLE FEED

(a) Arbitrary position(Not corresponding to maxim minimum of on-axis power)
(b) Optimum position of the feed
(c) Minimum position of the feed.

It can be seen that the radiation patterns are undergoing noticeable variations as 'S' is varied. At the optimum positions of the primary feed the radiation patterns are narrowed down with an effective focussing, while at M-positions the beams are broadened or split into major side lobes. The results are testified at different frequencies using a number of corner reflector systems of various parameters.

For a quantitative analysis the half power beam widths of the radiation patterns for different positions of the primary feed are tabulated. This is given in Table 4.12 (c).

4.8 Variations in VSWR at Different Positions of the Primary Feed from the Apex of the Corner Reflector.

Using a slotted line and a tunable probe the VSWR of the corner reflector system is measured. The distance 'S' is varied in regular steps and the corresponding VSWR is measured precisely. The variation of VSWR with 'S' is plotted and a few such graphs are shown in Figure 4.13. It can be seen that the VSWR is varied considerably with distance 'S'. At certain positions the VSWR is minimum while at some other positions they are very high. The positions of minimum VSWR are indicating an improvement in the matching condition while its increase

TABLE 4.12(c) HPBW of the Radiation Pattern of Corner Reflector System

Freq. GHz	W/λ	Corner angle 2α in deg.	HPBW in deg.		
			inter-mediate posn.	at 0 position	at M-position
9.4	3	45	28	17	32
9.4	2	60	42	12	56
9.4	2.5	90	70	12	68
7.5	2	120	43	15	59
7.5	3	180	50	27	58
7.5	4	120	63	39	52

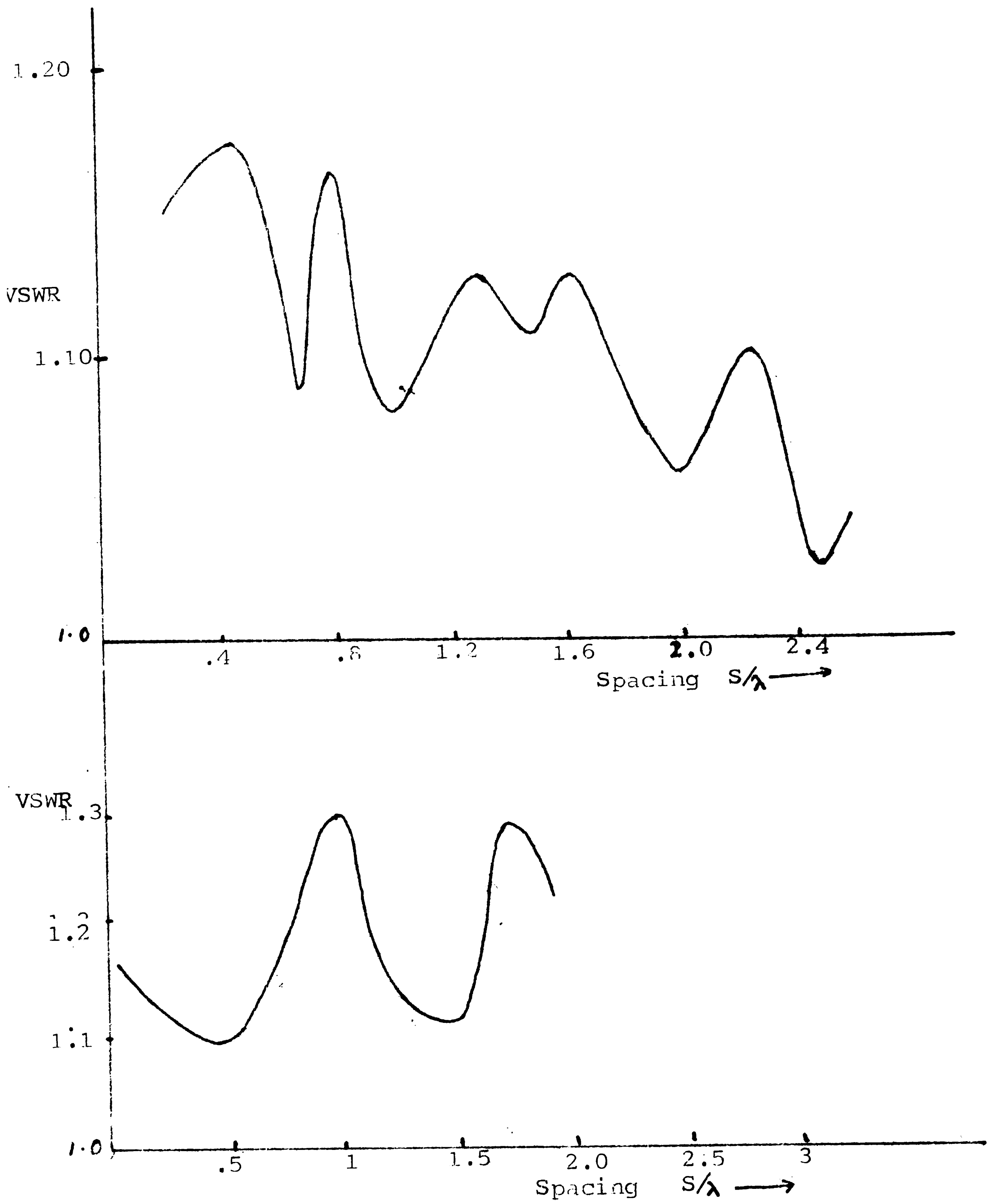

FIGURE 4.13
VARIATIONS OF V.S.W.R WITH THE POSITION OF DIPOLE FEED

indicates worsening of the same. It can be seen that a better matching of the system is corresponding to an optimum position of the primary feed giving a focussing of the beam.

4.9 Beam Tilting by Asymmetric Corner Reflector System

a) Off-axis primary feed. The feed dipole is slightly displaced from the axis of the corner reflector. The distance 'S' from the apex of the corner reflector is adjusted to correspond the value for the optimum beam focussing. This is obtained from the earlier investigation of the variation of the on-axis power. It has been observed that the resultant beam is tilted to the side opposite to the side containing the primary radiator. A few patterns taken with different corner reflector systems are presented in Figure 4.14.

b) Width asymmetry. It has been observed that the difference in widths of the corner reflector element is also a cause for producing a beam tilt. Keeping CR elements of varying widths, radiation patterns are plotted when the primary feed is kept at O-position for the on-axis power. The resultant radiation pattern is found to be tilted away from the axis towards the side containing the shorter element. As the CR angle is increased the tilt becomes more and more insignificant as shown in the Figure 4.15. For greater values of $(W_2 - W_1)$ also the beam tilt is not very significant.

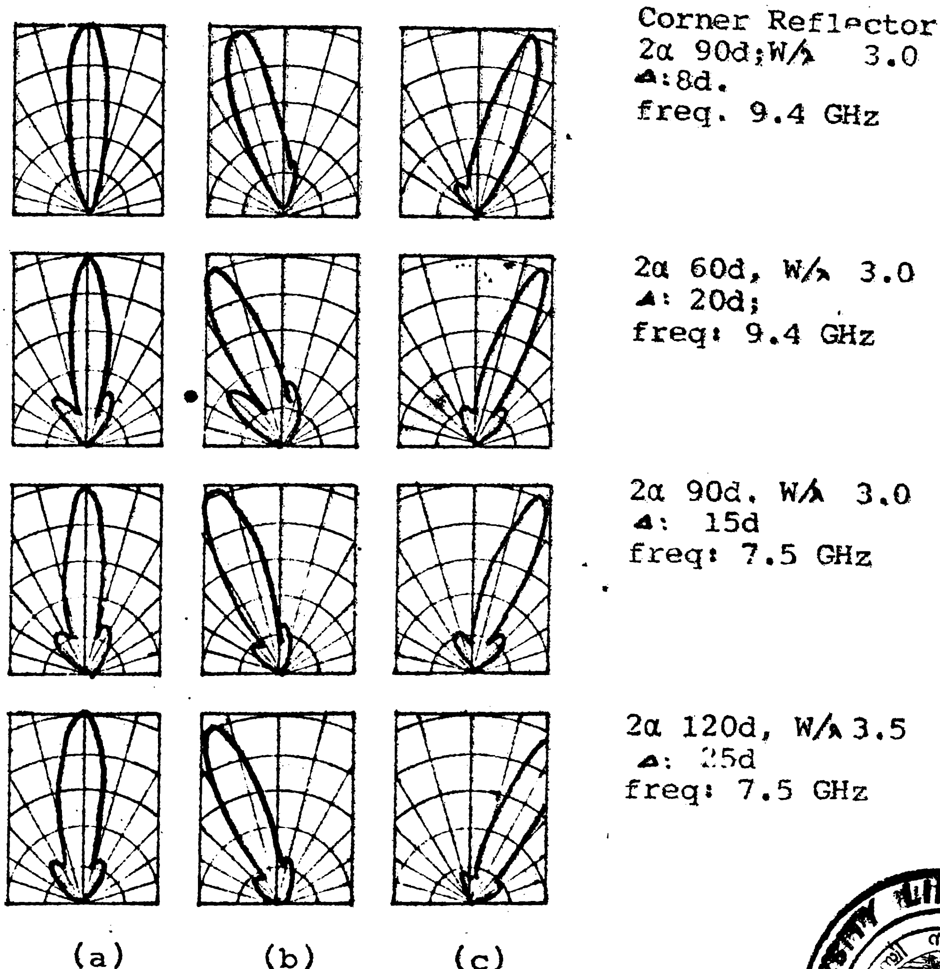

FIGURE 4-14

Beam tilting of corner reflector system by off-axis primary feed.

(a) Primary feed in the axis of the CR system.
(b) Primary feed on the right side at an angle Δ of the CR axis
(c) Primary feed on the lect side at an angle Δ of the CR axis.

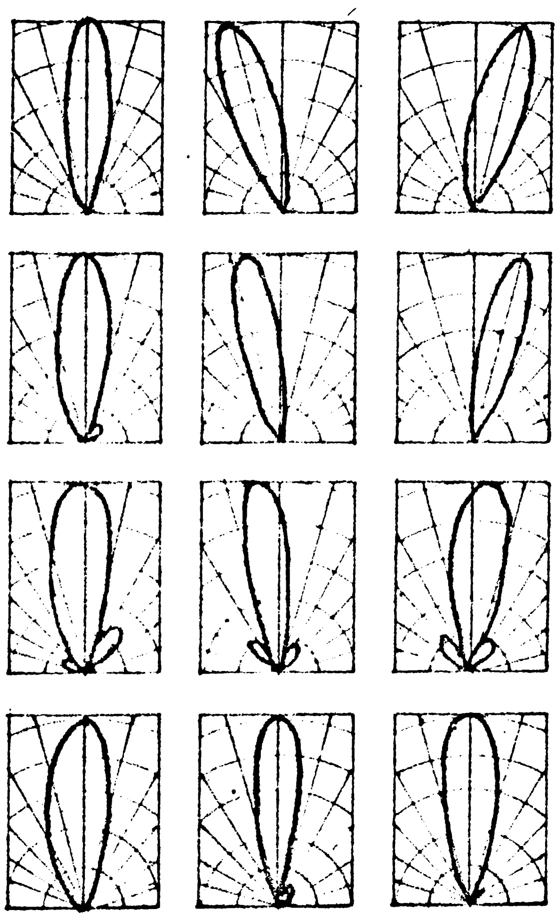

FIGURE 4-15

Beam tilting of Corner reflector antennas by reflector elements of different widths.

(a) Symmetric flange of equal width $W=(W_1+W_2)/2$ on both sides
(b) Shorter element on left side.
(c) Shorter element on right side.

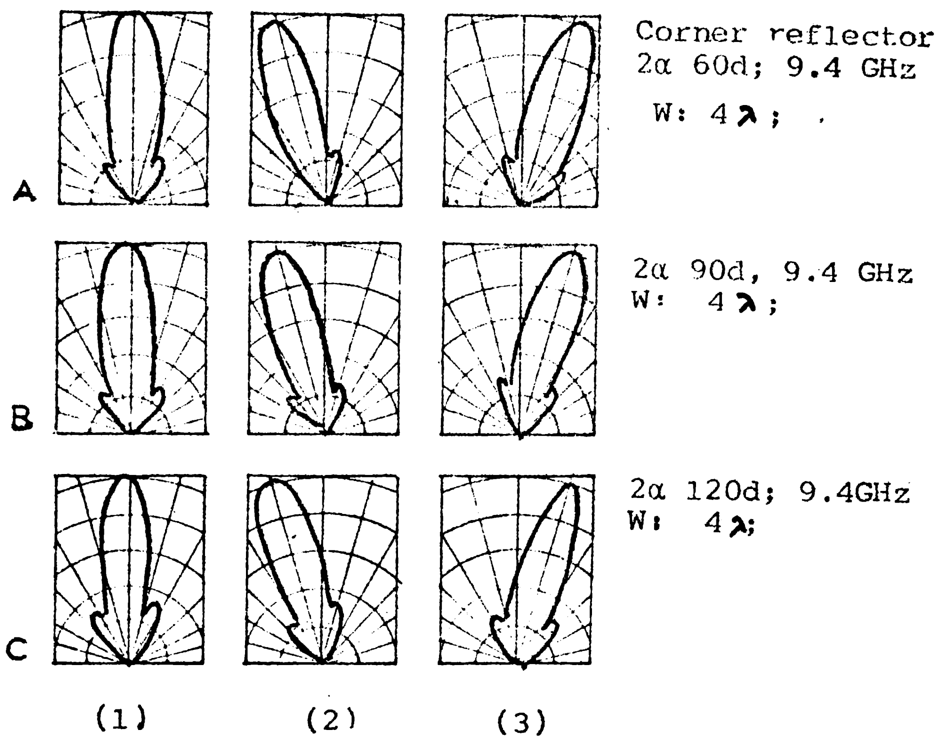

FIGURE 4.16

Beam tilt of corner feflector antennas by reflector elements of different materials

(1) Both reflector elements metallic
(2) Metallic element on left side
(3) Metallic element on right side.

c) <u>Asymmetric reflector element</u>. Keeping CR elements of different materials but of the sems thickness and widths another type of asymmetry can be imposed in the system. In the present investigation a perspex element of the same width and thicknees as the aluminium element is used to make the asymmetric element. Here the conductivity and hence the reflectivity of the elements for the electromagnetic waves will be different. The resultant beam shape of this complex system is studied by plotting the radiation patterns when the primary dipola feed is kept at the optimum position. It has been observed that the beam is tilted towards the side containing the metal element. The tilted radiation patterns of a few such asymmetric CR systems are given in Figure 4.16.

The above experimental results obtained with flanged sectoral horns and corner reflector antennas show striking resemblances in many respects. An exhaustive comparative study of these resemblances is made in the next chapter.

CHAPTER V

COMPARATIVE ANALYSIS OF THE EXPERIMENTAL RESULTS

5.1 Introduction

This chapter extensively gives a comparative analysis of the results presented in the preceeding chapter. The flanged sectoral horns and the corner reflector systems are found to be giving similar results in almost all aspects investigated in the present study. The variation of the on-axis power with respect to the position of the primary feed, changes in the radiation patterns with respect to the flange or corner reflector parameters, changes in beam shape due to various asymmetries imposed on the system are all found to be identical. A systematic analysis of these similarities is presented in the following sections.

5.2 Variation of On-axis Power with the Distance of the Primary Feed from the Apex of the Flange or Corner Reflector System.

From the results presented in sections 4.2 and 4.6 it can be seen that the on-axis power of the both flanged

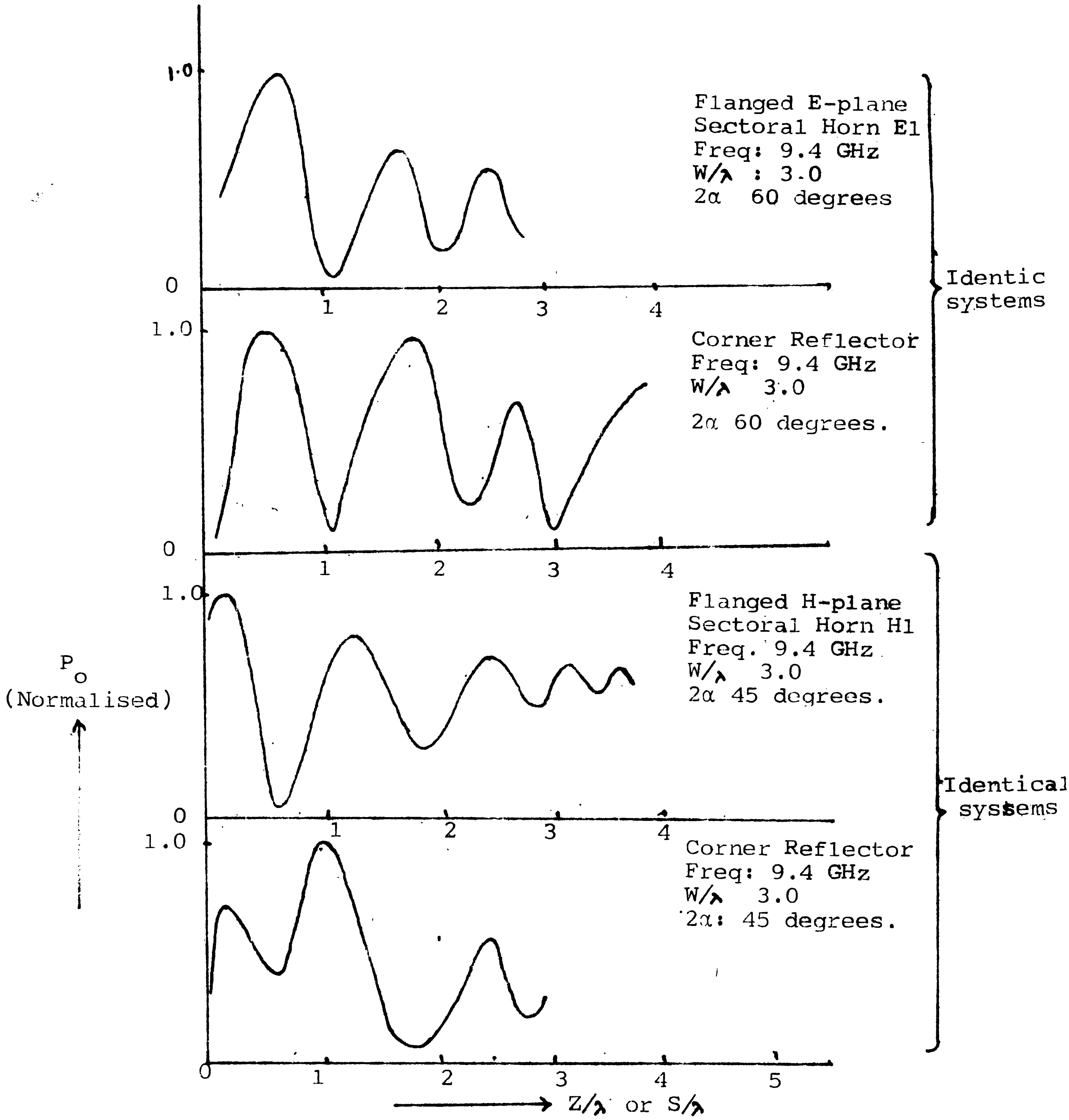

FIGURE 5-1.A
COMPARISON BETWEEN FLANGED SECTORAL HORNS AND CORNER REFLECTOR SYSTEMS: VARIATION OF ON-AXIS POWER.

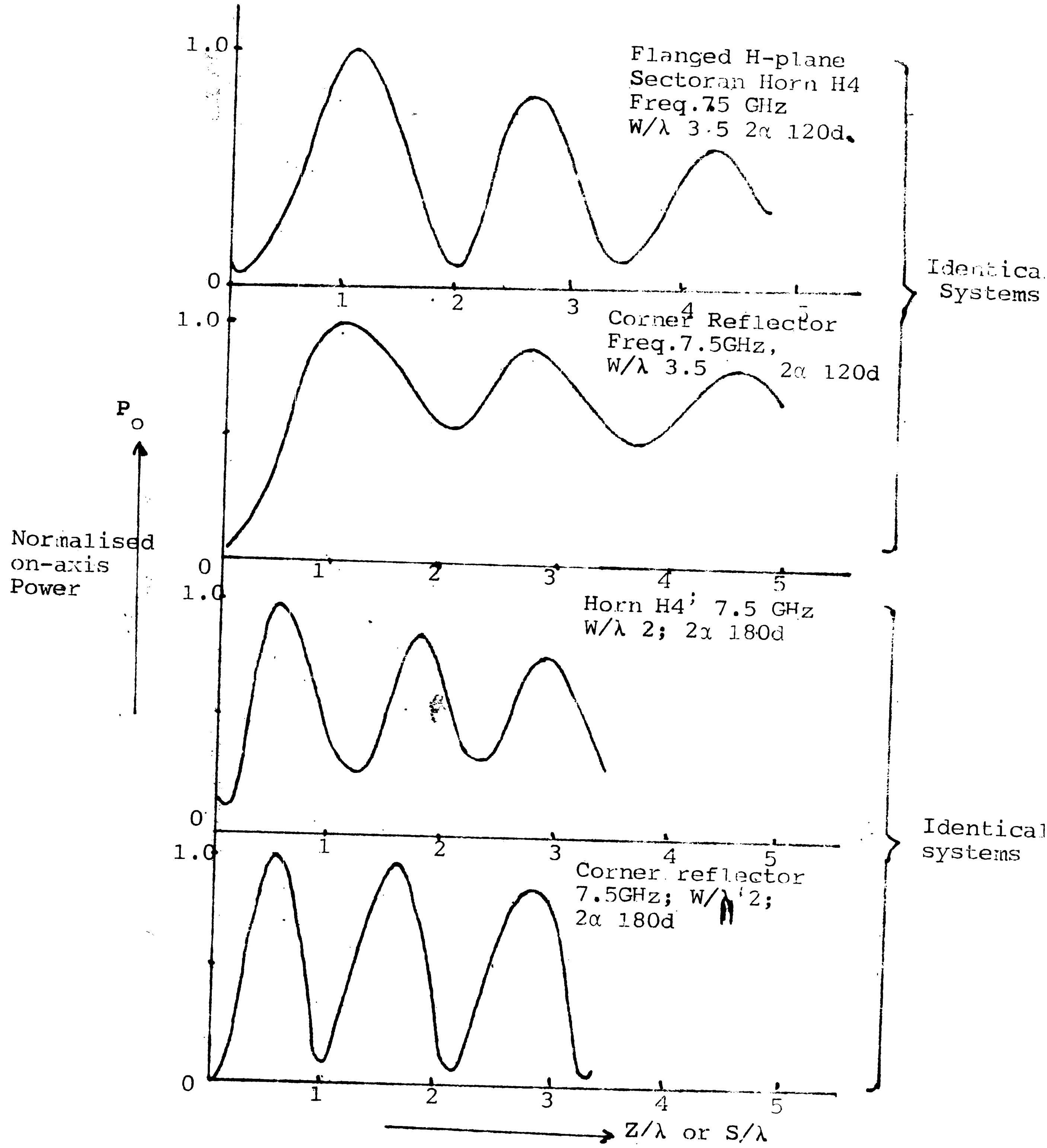

FIGURE 5-1.B.
COMPARISON BETWEEN FLANGED SECTORAL HORNS AND CORNER REFLECTOR SYSTEMS: VARIATION OF ON-AXIS POWER.

sectoral horns and corner reflector systems varies with the distance z or S, which is the distance of the primary feed (aperture of the horn or the dipole, as the case may be) from the apex of the flange or corner reflector system. In both the cases, the on-axis power has sharp maxima and minima for distinct values of Z or S. For two identical systems operating at the same frequency, variation of on-axis power is compared. This is given in Figures 5.1 A and 5.1 B. For various horns and corner reflectors operating at different frequencies, this has been verified as shown in the sets of graphs in the above figures. It can be seen that the positions of the primary feed corresponding to maximum or minimum on-axis power are almost identical under the same conditions for both flanged sectoral horns and corner reflector systems.

5.3 Variations in Radiation Patterns

For symmetric metallic flanges and corner reflector systems, variations effected in the radiation patterns by the changes in distance of the primary feed are compared for identical systems. Figure 5.2A represents radiation patterns of identical flange and CR systems for different values of 'S'.

The general variations of patterns are the same in both the cases. For example, a flange or a corner reflector of any angle kept at 0-position (maximum on-

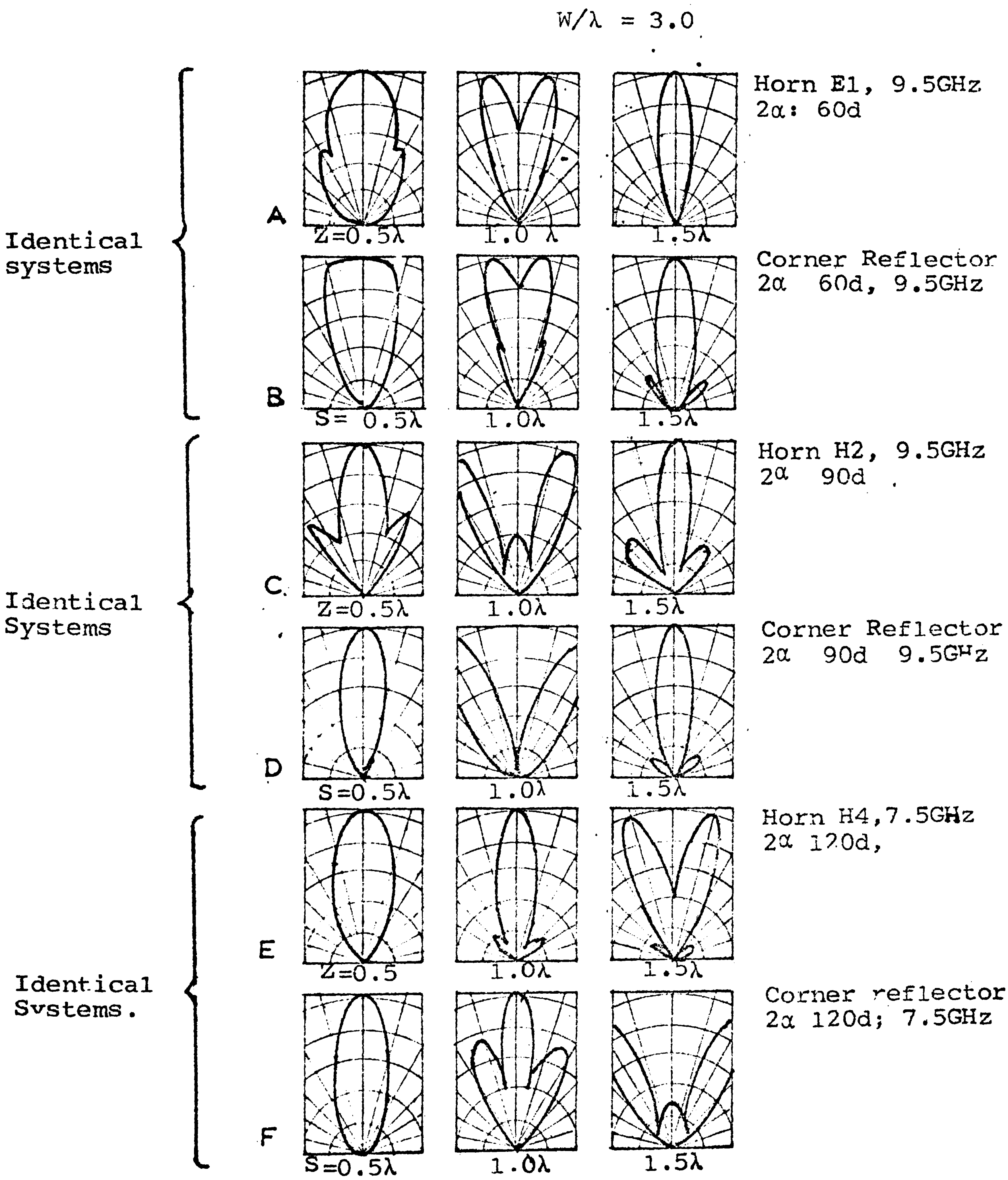

FIGURE 5-2-A
RADIATION PATTERNS OF FLANGED SECTORAL HORNS AND CORNER REFLECTOR SYSTEMS FOR CORRESPONDING VALUES OF Z OR S.

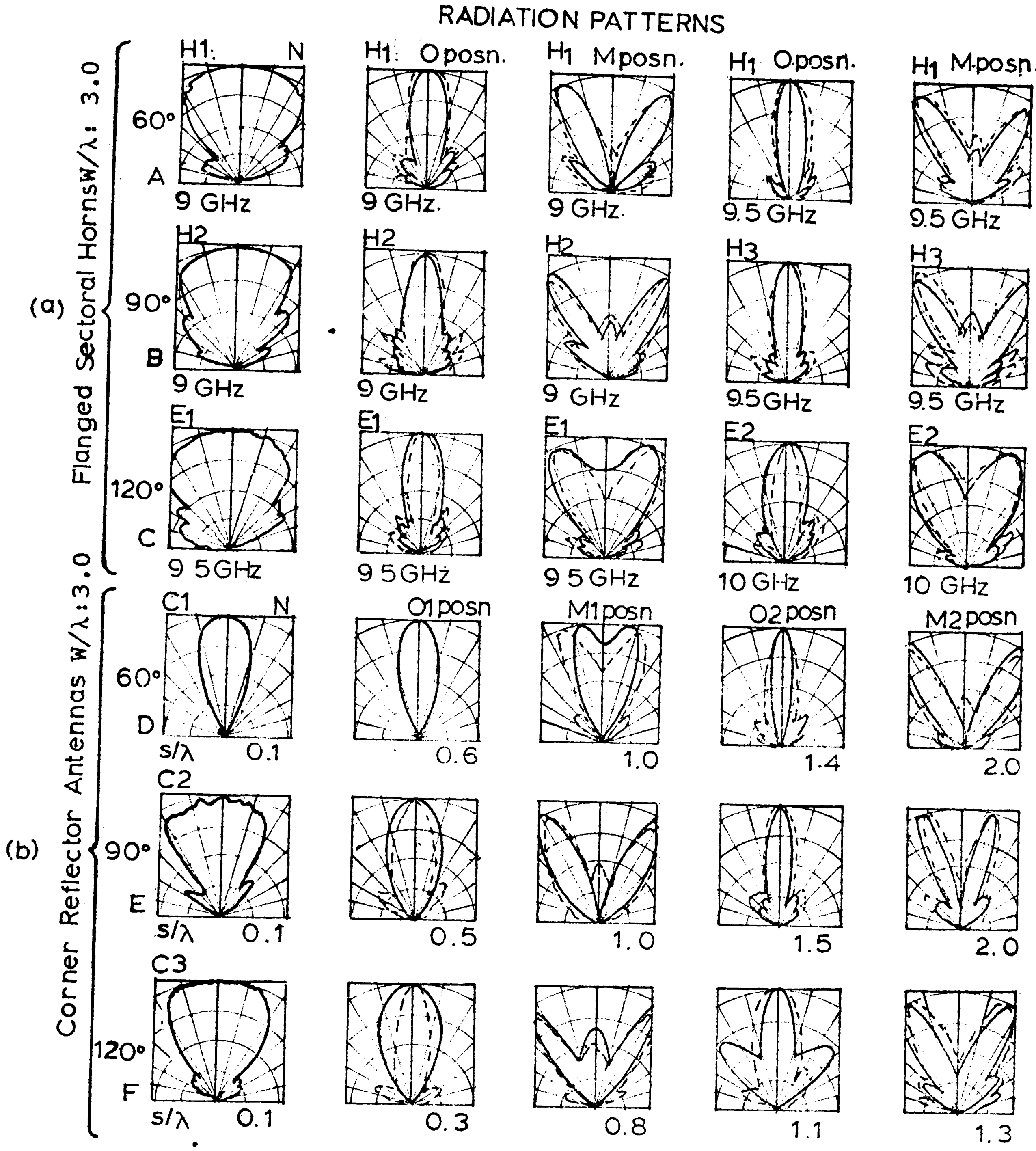

FIGURE 5-2·B·

COMPARISON BETWEEN THE RADIATION PATTERNS OF IDENTICAL FLANGED SECTORAL HORNS AND CORNER REFLECTOR SYSTEMS: AT O-POSITIONS THE BEAMS ARE SHARPENED AND AT M POSITIONS THEY ARE BROADENED OR SPLIT INTO MAJOR SIDE-LOBES.

axis power) will sharpen the radiation pattern. On the other hand, if it is kept at M-position (minimum on-axis power) beam will be broadened or split into prominent sidelobes as shown in Figure 5.2 B. Comparison of radiation patterns of the two systems having identical conditions reveals this facts very clearly.

5.4(a) <u>Beam Tilt by Flange or Corner Reflector Axis Asymmetry</u>.

The flanges on the sectoral horns are adjusted such that the axis of the flange system is different from the horn axis. The radiation patterns of such a system for flanges at O-position are plotted for various horns and frequencies. These patterns are compared with the patterns obtained using identical corner reflectors. A comparative analysis of the results is given in Figure 5.3.

It can be seen that the beam is undergoing a tilt towards the axis of the flange or corner reflector system. Thus the behaviours of the flanges and the corner reflector system are similar in this aspects also.

5.4(b) <u>Width Asymmetry</u>.

Flange or corner feflector elements of unequal widths make asymmetric systems. Here the unequal widths of the elements make the system uneven or asymmetric. In both the flange and corner reflector systems, the result-

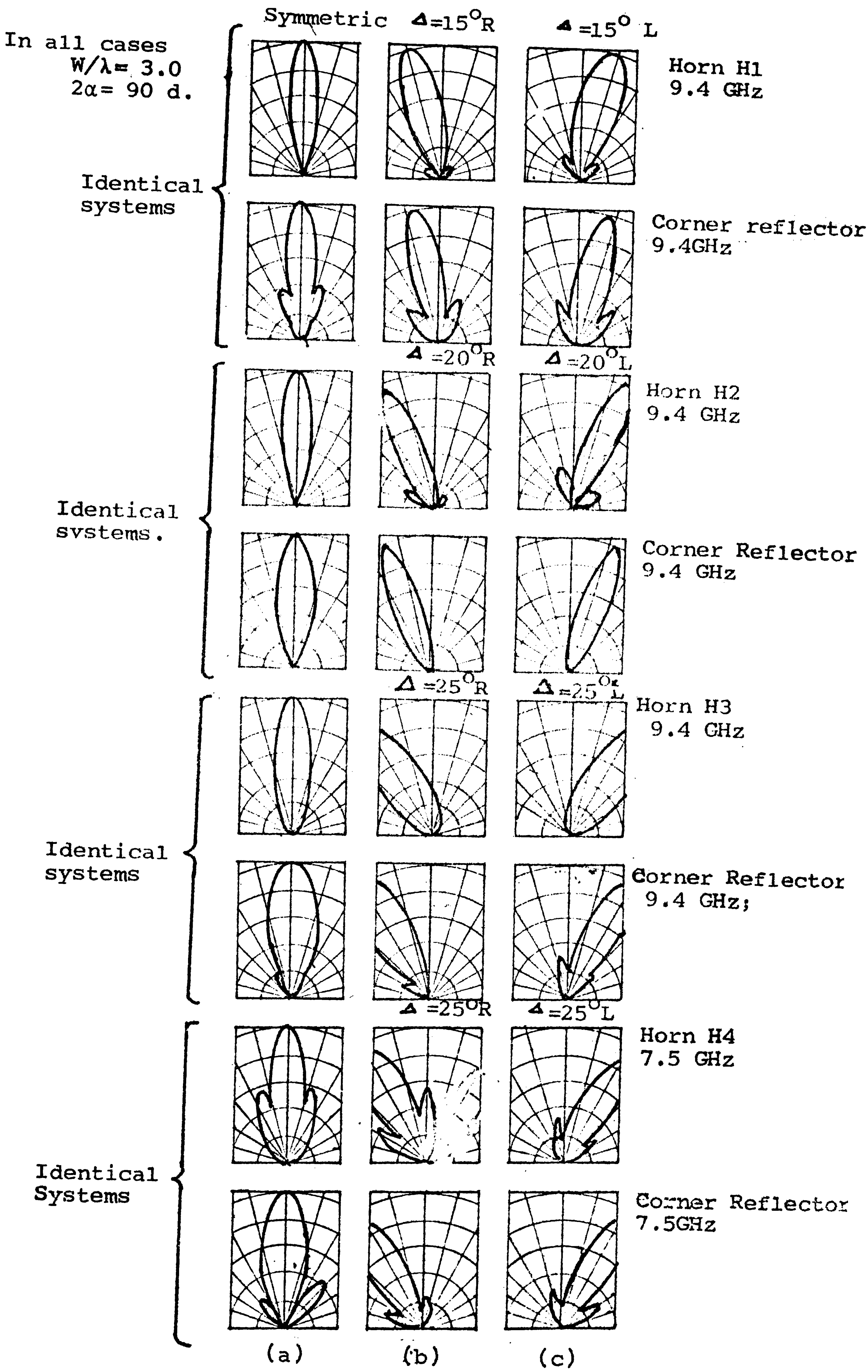

FIGURE 5-3
BEAM TILT BY AXIS ASYMMETRY: (a) Symmetric system; (b) Flange/CR axis tilted to right; (c) Flange/CR axis tilted to left.

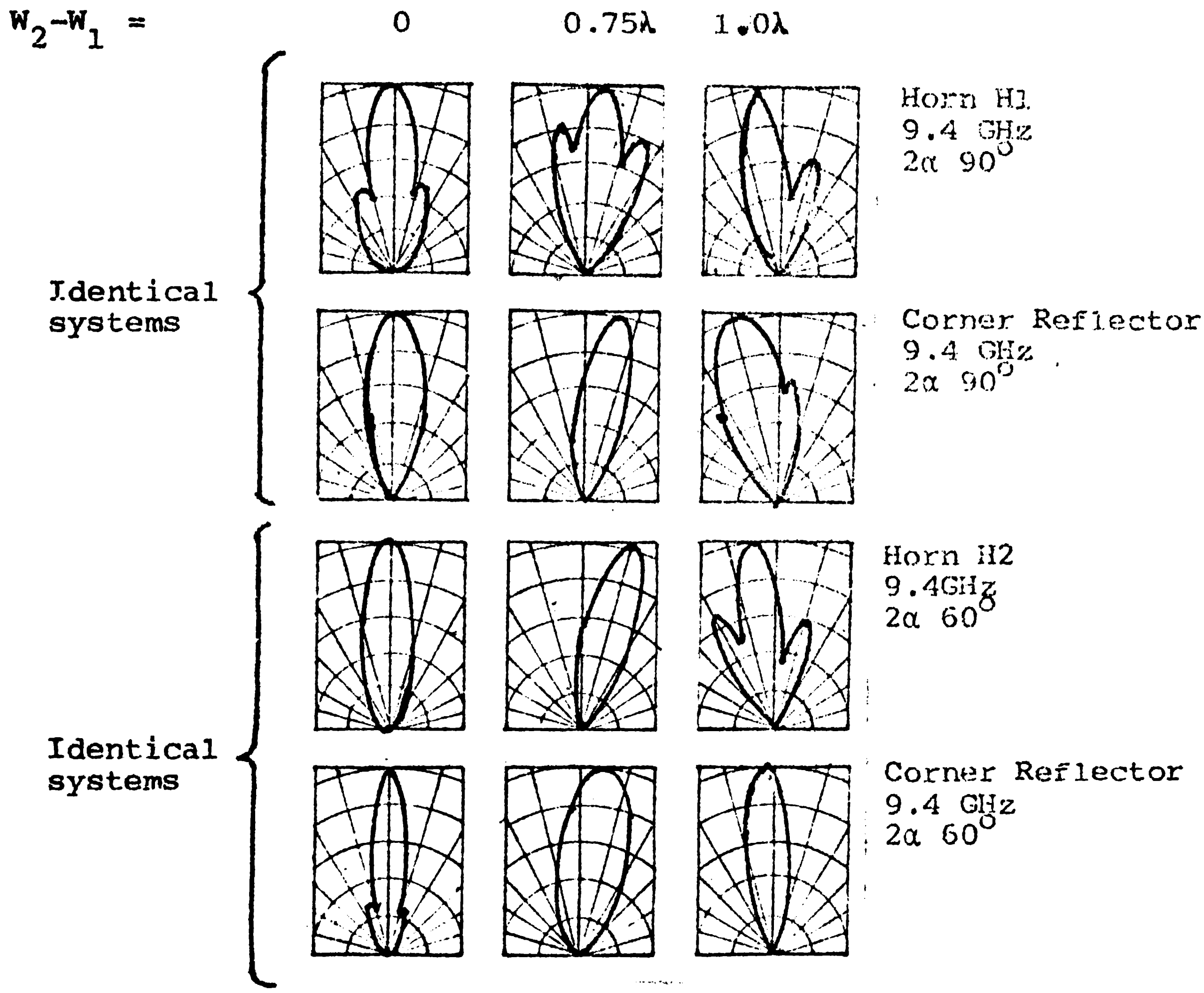

FIGURE 5-4

BEAM TILT BY WIDTH ASYMMETRY OF FLANGE AND CORNER REFLECTOR ELEMENTS.

ant beam is found to be tilted towards one side depending upon the mean difference $(W_2 - W_1)$ and the average width $\left(\frac{W_1 + W_2}{2}\right)$. In the flange system with moderate values of $(W_2 - W_1)$ the tilt is towards the side containing the smaller flange element. However, with increase in (W_2-W_1) the tilt becomes irregular. For corner reflector system for moderate values of $(W_2 - W_1)$ the tilt is towards the side containing the smaller elements as in the case of the flange system. This comparative analysis is presented in Figure 5.4.

5.4(c) Amplitude Asymmetry

The effects of dissimilar flange or corner reflector elements on either side~~s~~ of the primary radiator are investigated in section 4.5 c and 4.9c. This asymmetry is achieved by keeping a metal element on one side and an equivalent (same width and thickness) element made of a different material (for example perspex) on the other side. The resultant beam at the optimum position of the primary feed is found to be tilted away from the common axis. The tilt is invariably towards the side containing the metal element. This result is common for both the flanged sectoral horns and corner reflector systems as shown in Figure 5.5.

5.5 Conclusion

The different aspects of the results obtained

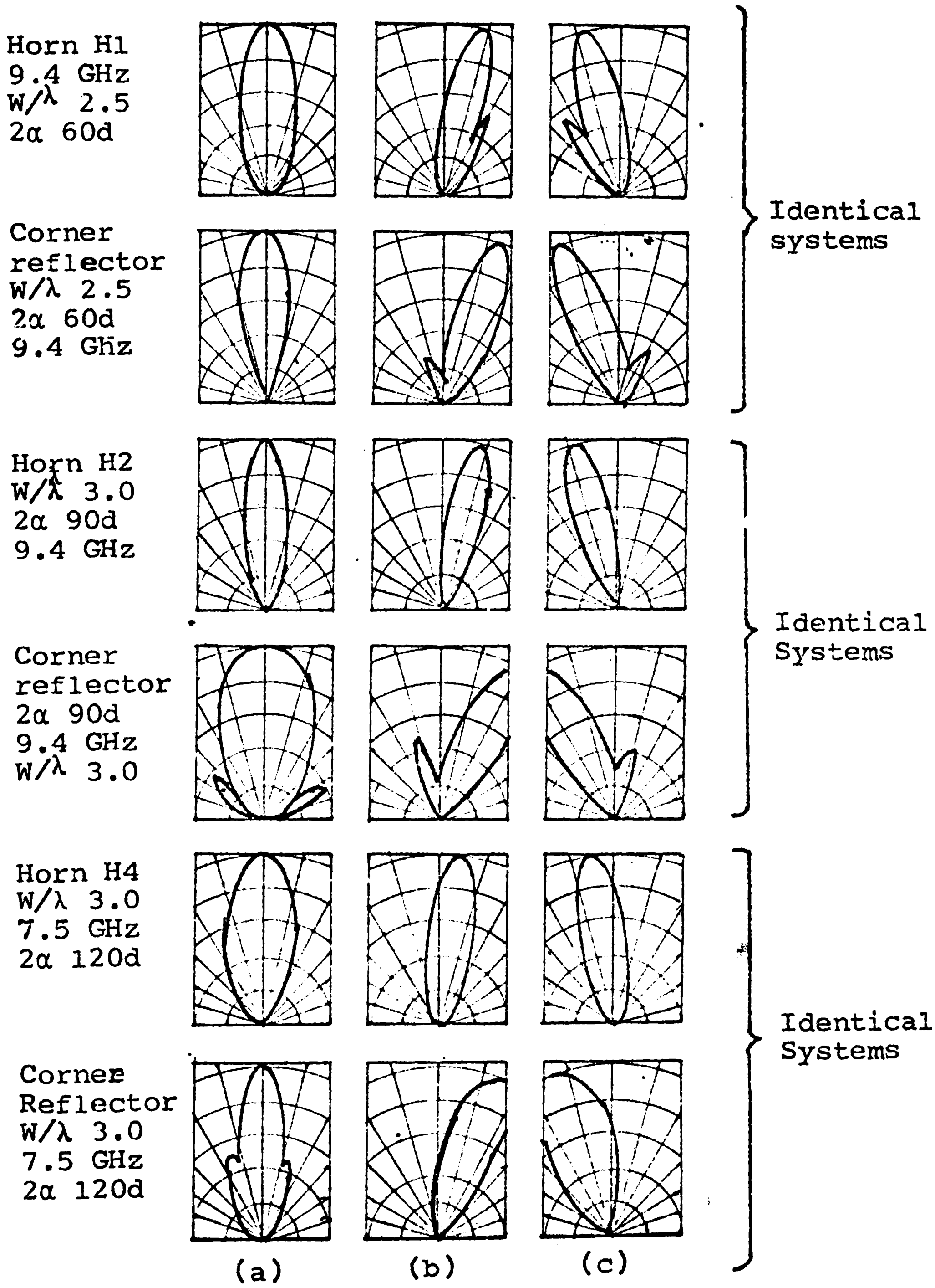

FIGURE 5-5

BEAM TILTING OF FLANGED SECTORAL HORNS AND CORNER REFLECTORS BY AMPLITUDE ASYMMETRY

(a) Metal elements on both sides
(b) Metal element on the right side
(c) Metal element on the left side

with flanged sectoral horns and corner reflector systems undoubtedly prove that there is close resemblance between the actions of the two systems. The flanges attached to a sectoral electromagnetic horn can be interpreted as nothing but corner reflectors. The main difference between the two systems is that a linear dipole is used as the primary feed in corner reflectors while the primary feed is a narrow aperture for the flanged sectoral horn. In spite of this fundamental difference in the mechanical structure of the systems, the results show very clear resemblances in all aspects. It may be recalled that in the earlier theoretical analysis of flanged sectoral horn by Owen and Reynolds[36] and Butson and Thompson[37] the narrow aperture of the sectoral horn is approximated to a linear source. Accepting this suggestion, we may proceed further, to conclude that the flanges attached to a sectoral horn are corner reflectors. This simplified approach is really advantageous since there is no consideration about the nature of the flare of the horn. Thus for the E-plane and H-plane sectoral horns, the corner reflector theory is applicable. In the theory suggested by earlier workers, the edges of the flanges are assumed to be acting as secondary radiators and the theory is suitable only to explain results with H-plane sectoral horns.

A detailed study of the theoretical aspect of the two systems is given in the following chapter. The application of the corner reflector theory for the flanged horn antennas solves the problem of explaining the results available with E-plane sectoral horns.

CHAPTER VI

THEORETICAL CONSIDERATIONS

6.1 Introduction

The possibility of modifying radiation patterns from sectoral horn antennas has been investigated by a number of research workers. The flange technique in its earlier form has been adopted with considerable success by Owen and Reynolds[36], Butson and Thompson[37], Nair and Srivastava[38,39] and many others. Additional attempts by introducing more variable parameters into the system were also reported. In explaining these effects the "Line Source Theory" has been adopted. According to this theory the edges of the metallic flange elements act as secondary radiators, while aperture of the sectoral horn is taken as a primary linear source. But this theory seems to be inadequate for explaining the effects of metal flanges on both E and H-plane horns. The line source theory can be applied only to H-plane sectoral horns since the edges of the flange elements are parallel to the H vector which satisfies the condition for radiation. But for E-plane sectoral horn this condition cannot be satisfied and hence the effects of flanges on E-plane sectoral horn remain unexplained. The present attempt is to correlate the effects exhibited by the flanges both on H and E-plane sectoral horns with the corner reflector theory. The consistence of the experimental results in the two systems has already been pointed out in the previous chapters.

6.2. Theory of the Flanged Sectoral Horns

a) Line Source Theory

b) Modified Line Source Theory.

a) Line Source Theory. According to the suggestion made by Owen and Reynolds the two edges of the conducting flange can be considered as two secondary radiators while the aperture of the horn may be taken as a primary radiator. The expression for the power P_θ at any point making an angle θ with the horn axis is derived as follows:

Let S be the primary radiator and S_1 and S_2 the two secondary radiators. The angle subtended by S_1 and S_2 at S be 2α. As given in Figure 6.1(a) P is a point in the far field corresponding to a bearing angle Assuming that the intensity of field from the primary as unity, K is taken as the amplitude of the field at P due to each of the secondary radiators.

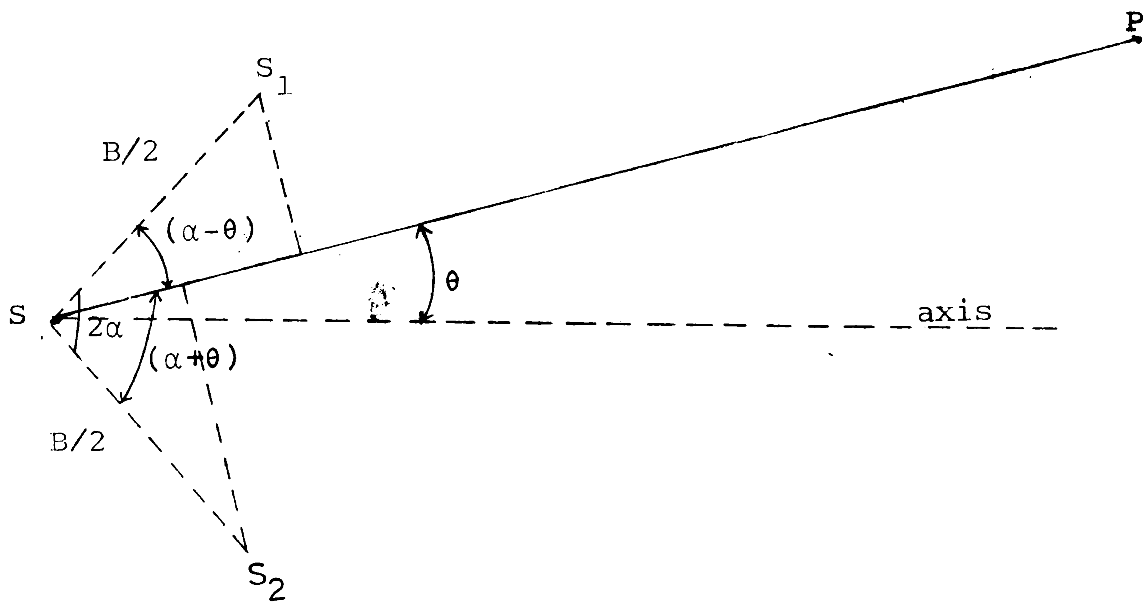

(a) Representation of Primary and Secondary sources.

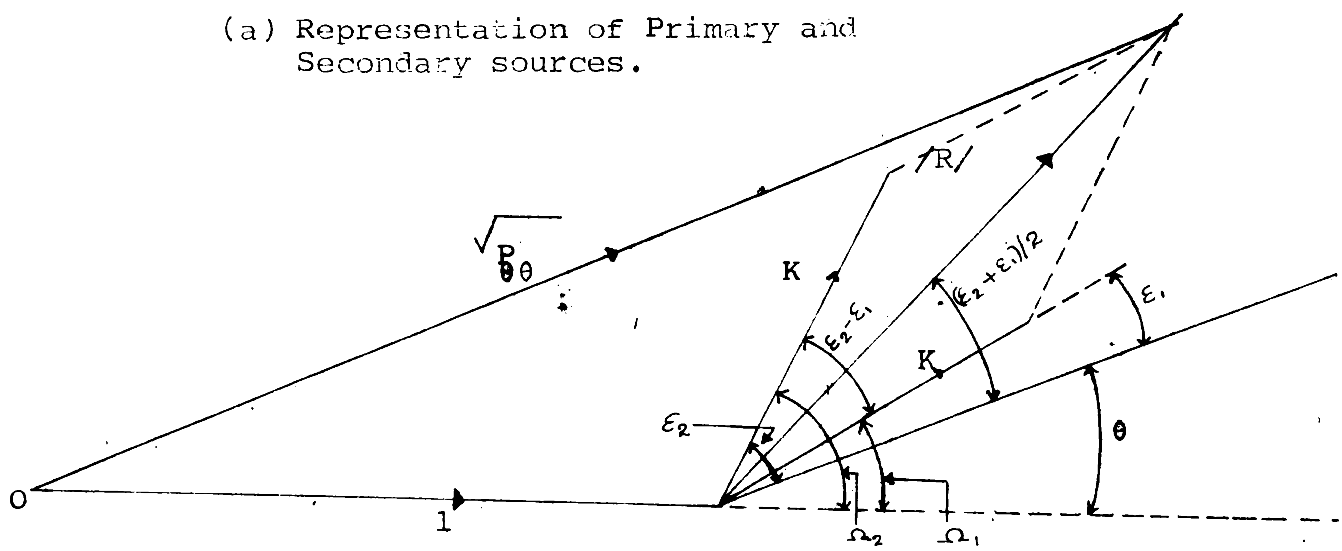

(b) Vector diagram of fields at P.

FIGURE 6-1.

Representation of primary and secondary sources and the vector diagram of fields at a point.

Let $\frac{B}{2}$ = distance of each secondary source from the primary.

φ = the phase difference of each secondary radiator with respect to the primary due to the path $\frac{B}{2}$, i.e.

$\varphi = \frac{\pi B}{\lambda}$ which is a constant.

Ω_1 = net phase change of the field at P due to S_1, relative to the primary.

Ω_2 = net phase change of the field at P due to S_2, relative to the primary.

ε_1 = phase difference of the radiator from S_1 due to the difference in path affected at P

i.e. $$\varepsilon_1 = \frac{\pi B}{\lambda} \cos(\alpha - \theta) \qquad (6.1)$$

similarly $$\varepsilon_2 = \frac{\pi B}{\lambda} \cos(\alpha + \theta) \qquad (6.2)$$

so that

$$\varepsilon_2 - \varepsilon_1 = \frac{2\pi B}{\lambda} \sin\alpha \sin\theta \qquad (6.3)$$

$$\varepsilon_2 + \varepsilon_1 = \frac{2\pi B}{\lambda} \cos\alpha \cos\theta \qquad (6.4)$$

The corresponding vector diagram of field reaching P can be represented as shown in Figure 6.1.(b). The resultant amplitude of the two secondary radiators is given by

$$|R|^2 = K^2 + K^2 + 2K^2 \cos (\Omega_2 - \Omega_1) \qquad (6.5)$$

But $\Omega_2 - \Omega_1 = \mathcal{E}_2 - \mathcal{E}_1$

$$\therefore |R|^2 = 4 K^2 \cos^2 \left(\frac{\mathcal{E}_2 - \mathcal{E}_1}{2} \right)$$

therefore

$$|R| = 2 K \cos \left(\frac{\pi B}{\lambda} \sin\alpha \sin\theta \right) \qquad (6.6)$$

The resultant amplitude of the field at P due to the primary and the two secondary radiators is given by $\sqrt{|P_\theta|}$

i.e. $|P_\theta| = 1^2 + |R|^2 + 2 |R| \cos \left(\frac{\mathcal{E}_2 + \mathcal{E}_1}{2} - \varphi \right)$

substituting the values of $|R|$ and $\mathcal{E}_2 + \mathcal{E}_1$ we get

$$|P_\theta| = 1 + 4 K \cos \left(\frac{\pi B}{\lambda} \sin\alpha \sin\theta \right) \times \left\{ \cos\left[\left(\frac{\pi B}{\lambda} \cos\alpha \cos\theta \right) + \varphi \right] + K \cos \left(\frac{\pi B}{\lambda} \sin\alpha \sin\theta \right) \right\}$$

which is the power delivered by the flanged horn antenna at a point P making an angle θ with the horn axis.

b) Modified Line Source Theory. In the line source theory presented above, the aperture of the horn is taken as a linear source. This approximation is not true especially in the case of E-plane sectoral horns. Hence a modified theory is attempted for. Here we consider the aperture of the horn as area through which electromagnetic energy is radiated. Let E_o be the mean amplitude of excitation existing at the aperture. In the far field the intensity at a point is given by Jordan[48] as

$$E_a = \left(\frac{E_o A_E A_H}{2 \lambda r} \right) \frac{(\sin u)}{u} (1 + \cos\theta) \, \mathrm{Exp}(-j \beta r)$$

(6.7)

where λ = the free space wavelength of radiation

r = distance of point 'M' from the antenna system,

$\beta = \frac{2\pi}{\lambda}$

$u = (A_E \sin\theta \;/ \lambda)$

A_E, A_H = widths of the aperture in the E and H-planes respectively

and E_o = field existing at the aperture of the antenna.

putting E_o = 1, the above equation can be written as

$$E_a = \frac{A_E A_H}{2 r} \; \frac{\sin(\pi A_E \sin\theta / \lambda)}{\pi A_E \sin\theta / \lambda} (1 + \cos\theta) \, \mathrm{Exp}\left\{ j\left(\frac{\pi}{2} - Br\right)\right\}$$

(6.8)

The resultant field at M (figure 6.2) due to the two secondary radiators, each having an amplitude K and phase difference $\left(\frac{\pi B}{\lambda} \right)$ is given by Nair et.al[38] as

$$E_f = 2 K \cos(\hat{P}/2),$$

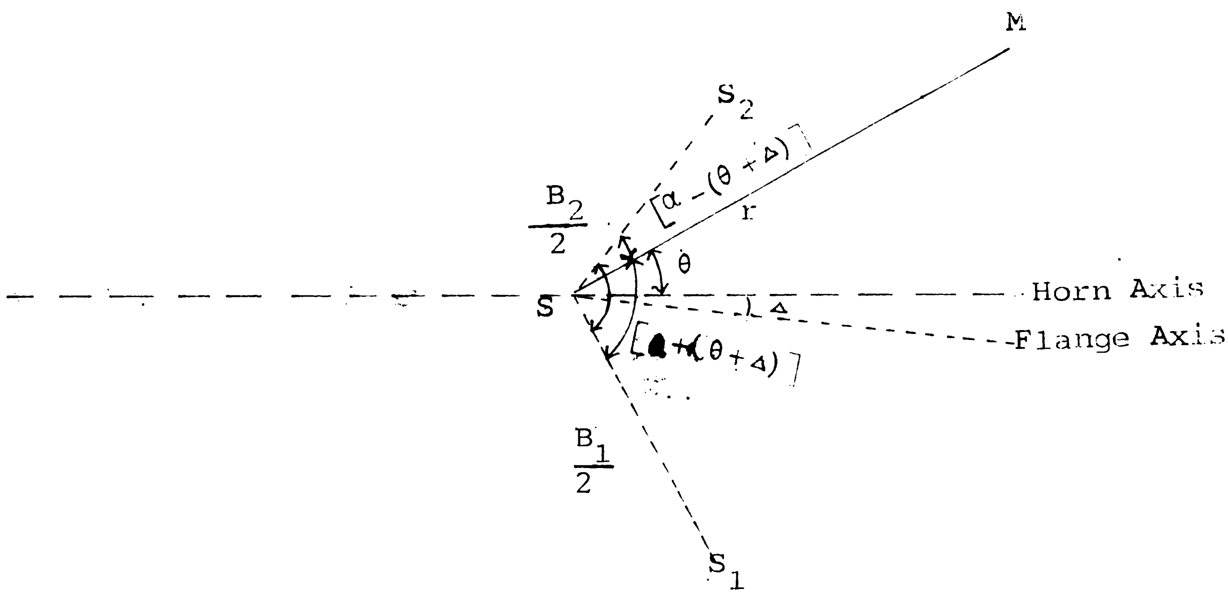

FIGURE 6-2

Primary and Secondary radiators in Flanged Sectoral Horns.

where $\hat{P} = B\hat{A}C = (\varphi_1 - \varphi_2) + (\varphi_1' - \varphi_2')$

φ_1, φ_2, φ_1' and φ_2' are the angles defined as in the above reference.

E_f when expressed in the complex form is

$$E_f = |E_f| \exp(-j\beta r) = (2K \cos \hat{p}/2)$$

$$\times \exp(-j\beta r) \qquad (6.9)$$

If E is the resultant field at M due to both E_a and E_f then $E = |E_a| + |E_f|$

Adding them as phasors we may write

$$E = \left[|E_a|^2 + |E_f|^2 + 2|E_a| \cdot |E_f| \cos(\varepsilon_2 - \varepsilon_1) \right]^{1/2} \qquad (6.10)$$

where $\varepsilon_1 = (\pi/2 - \beta r)$

and $\varepsilon_2 = -\beta r$,

so that $(\varepsilon_2 - \varepsilon_1) = \pi/2$

therefore $E = \left[|E_a|^2 + |E_f|^2 \right]^{1/2}$ (6.14)

Hence the power at the point M may be written as

$$P_\theta = |E_a|^2 + |E_f|^2 \qquad (6.12)$$

Therefore the resultant E-plane power pattern of the horn with the double secondary antenna system can be written as

$$\hat{P}_\theta = \left[2\ K \cos\ (\hat{P}/2)\right]^2 + \left[\frac{A_E\ A_H \sin\ (\pi\ A_E \sin\theta\ /\lambda\ )}{2\ \lambda\ r\ (\pi\ A_E \sin\theta\ /\ \lambda\ )} \times (1 + \cos\theta\ )\right]^2 \qquad (6.13)$$

The values of $\hat{P}$ may be substituted depending upon the nature of flange system. For a symmetric flange system kept at the aperture, $\hat{P} = \frac{(2\pi B)}{\lambda} \sin\alpha \sin\theta$ as given by Nair et.al.[38] and in which case eq.(6.13) may be written as

$$P_\theta = \left[2\ K \cos\ (\frac{\pi B}{\lambda}\ \sin\alpha\ \sin\theta\ )\right]^2 + \left[\frac{A_E\ A_H \sin\ (\ \pi\ A_E \sin\theta\ /}{2\ \lambda r\ (\pi A_E \sin\theta\ /\lambda} \times (1 + \cos\theta\ )\right]^2 \qquad (6.14)$$

This may be taken as a more appropriate expression for the radiation patterns of flanged horn antenna system, since we have not made any otar simplified assumption that the primary aperture is a linear source. Computations of radiation patterns on the basis of this theory revealed more closeness with experimental results.

However, even this modification is not suitable for E-plane sectoral horns, since orientation of field vectors with respect to the edges of the flange element is not congenial for electromagentic radiation. Let us now see the possibility of applying the corner reflector theory to this probelm.

6.3 Theory of the Corner Reflector Antenna

From the assumption that the reflecting planes are perfectly conducting and infinite in extent and by using the method of images, Kraus[40] derived expressions for gain and directional patterns of corner reflector antennas. Kraus showed that very small spacing of the driven radiator from the apex of the corner reflectors will adversely affect the gain of the systems. The spacing will have an upper limit also, above which the beam splits up to sidelobes. Thus the gain and directional patterns of the system can be conveniently adjusted by varying the spacing 'S' or the corner reflector angle 2α or both.

Later investigation by Moullin[47] gave a more theoretical background and design data of corner reflector antennas. Following again the method of images, he proved that the directional pattern of a CR system can be expressed in the form of a series of Bessel functions as:

$$\frac{E}{E_o} = 4n(-1)^{n/2} \Big[J_n (K) \cos n\theta + J_{3n} (K) \cos 3n\theta + J_{5n} (K) \cos 5n\theta + \ldots . \Big] \tag{6.15}$$

when n is even and

$$\frac{E}{E_o} = 4\, nj(-1)^{\frac{(n-1)}{2}} \Big[J_n (K) \cos n\theta - J_{3n} (K) \cos 3n\theta + J_{5n} (K) \cos 5n\theta - \ldots . \Big] \tag{6.16}$$

when n is odd. Here

E = electric field at any point with bearing angle θ ,

E_o = maximum electric field,

n = $\pi/2\alpha$, where 2α = corner angle,

K = vector distance = $2\pi S/\lambda$, where S is the distance of the driven linear radiator from the apex and λ the wavelength of radiation

j = complex quantity $\sqrt{-1}$ and

J = Bessel function of the order indicated by the suffix and argument shown in brackets.

It is seen that the expressions (6.15) and (6.16) are valid only when a system of perfect images exists, i.e. only when n is an integer. If this condition is not satisfied, sufficient number of terms of the infinite series must be added in the expression given by

$$\frac{E}{E_o} = 4n \Big[\mathrm{Exp}\,(nj\pi/2)\; J_n\,(K)\;\cos\; n\theta + \mathrm{Exp}\,(3nj\pi/2)\; J_{3n}\,(K)\;\cos\; 3n + \ldots \Big] \qquad (6.17)$$

For these fractional n values, there will be two field components with 90° phase variations. No values of K will make the forward field zero. For all values of n, the axial field fluctuates periodically as K is continuously increased.

In the present study, identical flanges and corner reflector systems are taken for experimental investigation. For example, for a flanged sectoral horn, a flange or included angle 60° is taken. To find the effect of corner reflectors, conducting elements of the same width and angle are used. Experimental results with respect to on-axis power and radiation patterns are then compared. As already pointed out, there were striking resemblances in all the aspects and hence we may conclude that the behaviour of the metallic flanges on corner reflectors is similar to, or the same as, the corner reflector system. Here again the primary aperture of the horn is behaving as a linear radiator kept within the corner reflector elements. In many similar cases these patterns are compared. As shown in Figures 5.2 to 5.5, we can see that they all are giving conclusive proof for this deduction.

The variation of on-axis power with respect to the distance 'S' it can be obtained by solving equation (6.17). From a recent computation by Proctor[46], distances of the primary feed from the apex of the corner reflector systems giving maximum and minimum on-axis power values are obtained. These are compared with corresponding values of Z, experimently obtained for flanged sectoral horns. In table 6.1. this quantitative analysis is shown, giving theoretical values of 'S' and experimental

TABLE 6.1 Comparison between Theoretical and Experimental values of Z giving Maximum and Minimum On-axis power.

No.	Horn	Freq. GHz.	CR/Flange / angle 2α	Distance of the primary feed from the aped in λ: CORNER REFLECTOR (Theoretical values) Optimum	CORNER REFLECTOR (Theoretical values) Minimum	FLANGED HORN (From experiment) Optimum	FLANGED HORN (From experiment) Minimum
1	H1	9.4	45°	0.85	0.12** 1.58**	1.00	1.6
2	E1	9.4	60°	0.60	0.00** 1.00**	0.61	1.1
3	H2	9.4	90°	0.5	0.00* 1.00*	0.53	1.1
4	H4	7.5	180°	0.75	0.50** 1.00**	0.70	1.2

*From Proctor[46] and Moullin[47]

**Both values are probable according to computed graphs.

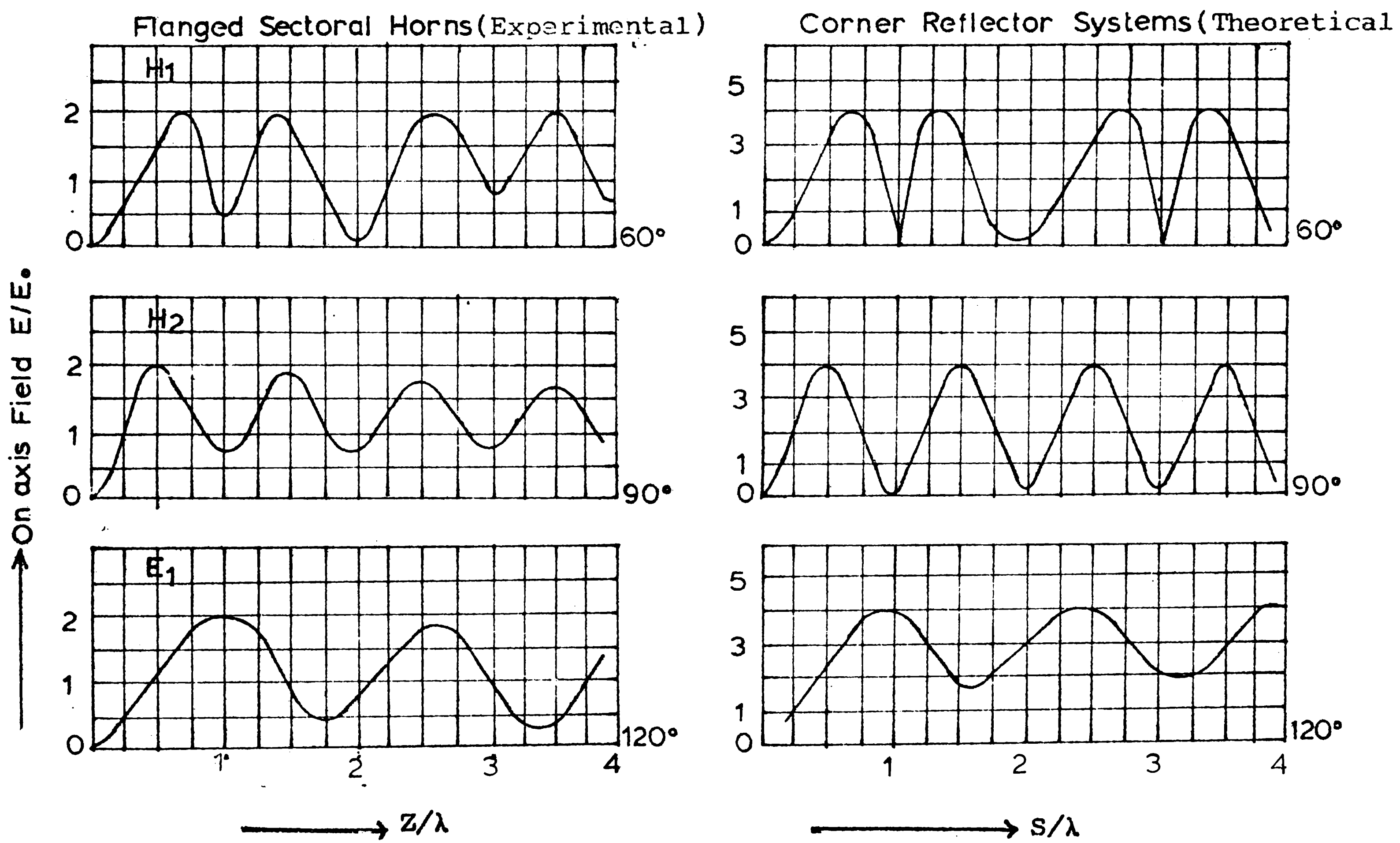

FIGURE 6.3

Variation of on-axis power of flanged sectoral horns are compared with theoretical values obtained in the Corner reflector theory.

values of Z, for optimum and minimum on-axis power. We can see that the experimental values are very close to the theoretical values obtained from the corner reflector theory. Figure 6.3 presents a set of these theoretical and experimental values. As far as the radiation patterns are concerned, sharpening and broadening of the patterns are effected by flanges or corner reflector systems in the same manner. If the spacing between the apex and the driven radiator is corresponding to a maximum of the on-axis power the beam will be sharpened. On the other hand, the beam will be split or broadened if the spacing corresponds to a minimum of on-axis power. This aspect has been verified by experiments and the results were presented in Chapter V.

The asymmetries which are causing beam tilt in the flanged sectoral horns can be explained on the basis of the line source theory. If W_1 and W_2 are the widths of the flange elements on the two sides, the resultant pattern can be derived, using the method given by Koshy _et.al._[49]

Figure 6.4 represents a sectoral horn fitted with an asymmetric flange system. As the flange is moved back from the aperture O to some arbitrary position O' through a distance Z, the secondary radiators take positions S_1' and S_2'. The phases of excitation of S_1 and S_2 with respect to the primary are

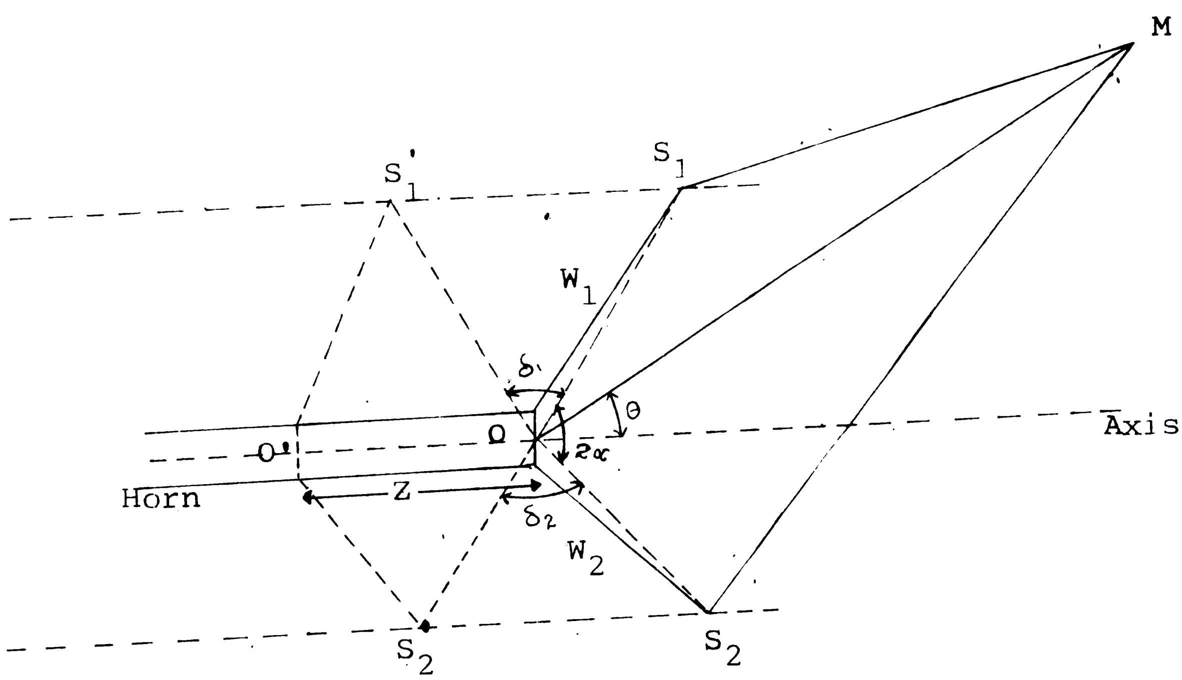

FIGURE 6-4

Representation of Flanged sectoral horn with asymmetric flange system.

$$\varphi_1 = (2\pi/\lambda)\ (W_1^2 + Z^2 - 2\,W_1\,Z\cos\alpha)^{1/2} \qquad (6.18)$$

$$\varphi_2 = (2\pi/\lambda)\ (W_2^2 + Z^2 - 2\,W_2\,Z\cos\alpha)^{1/2} \qquad (6.19)$$

For a distant point M in space with bearing angle θ there is additional phase difference φ_1' between S_1 and the primary due to unequal paths.

$$\varphi = (2\pi/\lambda)\ OS_1 \left[\cos(\alpha - \theta)\cos\delta_1 - \sin(\alpha - \theta) \times \sin\delta_1\right] \qquad (6.20)$$

But

$$\cos\delta_1 = (W_1 - Z\cos\alpha)/\,OS_1$$

$$\sin\delta_1 = Z\sin\alpha\,/\,OS_1$$

Therefore

$$\varphi_1' = (2\pi/\lambda)\quad (W_1 - Z\cos\alpha)\cos(\alpha - \theta) - Z\sin\alpha\ \sin(\alpha - \theta) \qquad (6.21)$$

The phase difference at M between S_2 and the primary is given by

$$\varphi_2' = (2\pi/\lambda)\quad (W_2 - Z\cos\alpha)\cos(\alpha + \theta) - Z\sin\alpha\ \sin(\alpha + \theta) \qquad (6.22)$$

Figure 6.5 shows the vector represtation of the flanged system. OA, AC and AB are the field vectors at M due to the primary and secondary sources S_1 and S_2 respectively. The resultant field R due to S_1 and S_2 is given by

$$R = 2 K \cos 1/2 (\varphi_1 - \varphi_2 + \varphi_1' - \varphi_2') \qquad (6.23)$$

The resultant power P_θ at M is given by

$$P_\theta = OD^2 = 1 + R^2 - 2 R \cos \widehat{OAD}$$

$$\text{and} \quad \widehat{OAD} = \pi - 1/2 (\varphi_1 + \varphi_2 + \varphi_1' + \varphi_2')$$

Therefore

$$P_\theta = 1 + R^2 + 2 R \cos 1/2 (\varphi_1 + \varphi_2 + \varphi_1' + \varphi_2') \qquad (6.24)$$

Here it is assumed that the antenna aperture acts as a line source of amplitude unity and the edges of the flange elements as two secondary sources excited to an amplitude K. Substituting and rearranging equation (6.24) the expression P_θ is obtained in terms of λ, W_1, W_2, Z, α and θ. If the flange axis is turned through an angle from the horn axis, the flange axis becomes the axis of reference and the bearing angle is $(\theta + \Delta)$. P_θ for such an asymmetric system is obtained by replacing the θ terms with $(\theta + \Delta)$ in the expression (6.24). Thus the most general expression for P_θ is obtained as

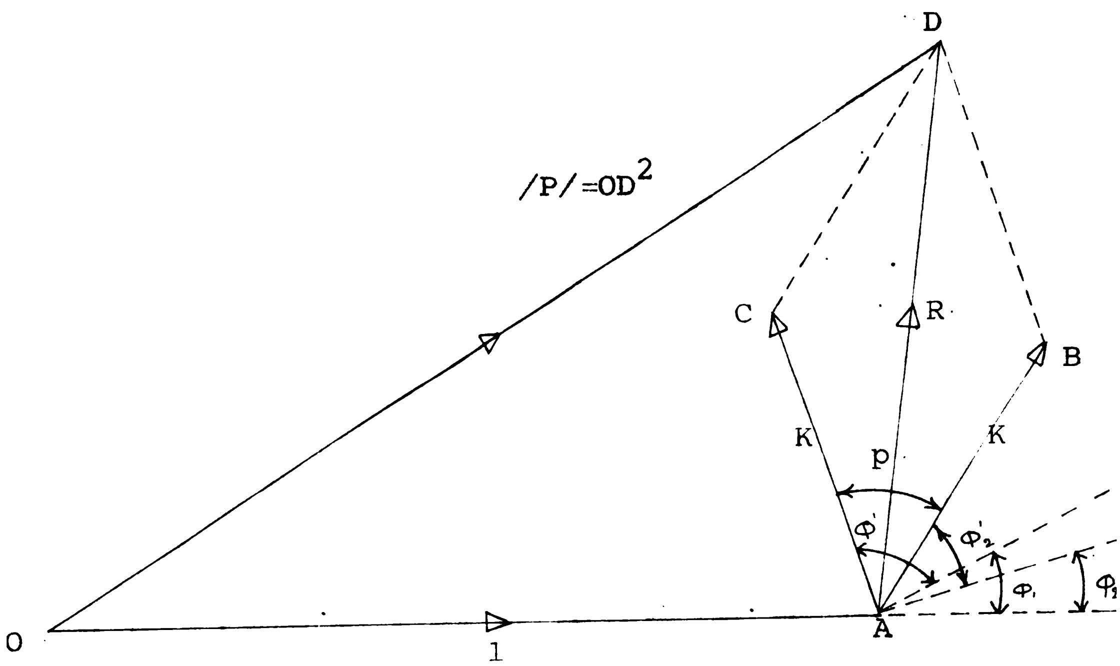

FIGURE 6-5

Vector diagram of fields due to a flanged sectoral horn.

$$
\begin{aligned}
P \;=\; 1 \;+ & \Big\{ 4\,K \cos(\pi/\lambda) \Big[(W_1^2 + Z^2 - 2\,W_1\,Z \cos\alpha)^{1/2} \\
& - (W_2^{\,2} + Z^2 - 2W_2\,Z \cos\alpha)^{1/2} \\
& + (W_1 - W_2) \cos\alpha \;\cos(\theta + \Delta) \\
& + (W_1 + W_2) \sin\alpha \;\sin(\theta + \Delta) \Big] \Big\} \\
& \times \Big\{ K \cos(\pi/\lambda) \Big[(W_1^{\,2} + Z^2 - 2\,W_1\,Z \cos\alpha)^{1/2} \\
& - (W_2^{\,2} + Z^2 - 2\,W_2\,Z \cos\alpha)^{1/2} \\
& + (W_1 - W_2) \cos\alpha \;\cos(\theta + \Delta) \\
& + (W_1 + W_2) \sin\alpha \;\sin(\theta + \Delta) \Big] \\
& + \cos(\pi/\lambda) \;(W_1^{\,2} + Z^2 - 2\,W_1\,Z \cos\alpha)^{1/2} \\
& + (W_2^{\,2} + Z^2 - 2W_2\,Z \cos\alpha)^{1/2} \\
& + (W_1 + W_2) \cos\alpha \;\cos(\theta + \Delta) \\
& + (W_1 - W_2) \sin\alpha \;\sin(\theta + \Delta) - 2Z \cos(\theta + \Delta) \Big] \Big\}
\end{aligned}
\qquad (6.25)
$$

In actual calculations this expression has to be multiplied with an overall obliquity factor $(1 + \cos\theta)$.

By introducing different conditions in various cases, variation of on-axis power, beam shaping of radiation patterns and beam tilting by different types of asymmetries can be effectively explained. If the flange elements have equal widths i.e. $W_1 = W_2 = W$ the above equation becomes

$$P_\theta = 1 + \left\{ 4\,K \cos\left[\left(\frac{2\pi W}{\lambda} \right) \sin\alpha \quad \sin\,(\theta + \Delta) \right] \right\}$$
$$\times \left\{ K \cos\left[\left(\frac{2\pi W}{\lambda} \right) \sin\alpha \quad \sin\,(\theta + \Delta) \right] \right.$$
$$\cos\,(2\pi/\lambda)\left[(W^2 + Z^2 - 2\,W\,Z\cos\alpha)^{1/2} \right.$$
$$\left.\left. W\cos\alpha \quad \cos\,(\theta + \Delta) - Z\cos\,(\theta + \Delta) \right] \right\}$$

(6.26)

To get the expression for the variation of on-axis power P_0 with the position Z of the flange, put $\theta = 0$ and

$\Delta = 0$

$$\therefore P_0 = 1 + 4\,K^2 + 4\,K\cos\,(2\pi/\lambda)$$
$$\times \left[(W^2 + Z^2 - 2\,W\,Z\cos\alpha)^{1/2} + W\cos\alpha - Z \right]$$

(6.27)

This is same as the equation derived by Nair <u>et.al.</u>[38]

Thus, from the analysis of the general expression the following conclusions can be drawn.

a) Variation of on-axis power P_0 with the position of flange

The positions of maxima and minima can be evaluated from the above equation. For simplicity, let us take the included angle equal to 180°. Then the above equation is reduced to

$$P_o = 1 + 4K^2 + 4K\cos\left(\frac{\pi B}{\lambda} - \frac{2\pi Z}{\lambda}\right)$$

But $\frac{B}{2} = \sqrt{W^2 + Z^2}$

$$P_o = 1 + 4K^2 + 4K\cos\left[\frac{2\pi}{\lambda}(W^2 + Z^2)^{1/2} - \frac{2\pi Z}{\lambda}\right] \qquad (6.28)$$

Thus it is seen that P_o varies sinusoidally about P as Z is changed. The maxima and minima are obtained when

$\frac{2\pi}{\lambda}(W^2 + Z^2)^{1/2} - \frac{2\pi Z}{\lambda}$ is $2n\pi$ and $(2n+1)\pi$, respectively, where n is any integer including zero.

From the above equation the theoretical value of Z giving maximum and minimum on-axis power are calculated.

The distance Z_o of the flange from the aperture for the optimum position is

$$\frac{2\pi}{\lambda}(W^2 + Z_o^2)^{1/2} - \frac{2\pi Z}{\lambda} = 2n\pi \qquad (6.29)$$

$$\therefore Z_o = \frac{W^2}{2n} - \frac{n}{2}$$

Similarly for the minimum value of P_o

$$Z_m = \frac{W^2}{(2n+1)\lambda} - \frac{(2n+1)\lambda}{4} \qquad (6.30)$$

Values of Z giving different order maxima and minima are given in Table 6.2. Table 6.3 is giving theoretical and experimental value of Z_o and Z_m for different values of n.

TABLE 6.2 Values of Z for different order Maxima and Minima in terms of Width W of flange and wavelength λ for an included angle 180°

n	$Z_o = \frac{W^2}{2n\lambda} - \frac{n\lambda}{2}$	$Z_m = \frac{W^2}{(2n+1)\lambda} - (2n+1)\frac{\lambda}{4}$
0	∞	$\frac{W^2}{\lambda} - \frac{\lambda}{4}$
1	$\frac{W^2}{2\lambda} - \frac{\lambda}{2}$	$\frac{W^2}{3\lambda} - \frac{3\lambda}{4}$
2	$\frac{W^2}{4\lambda} - \frac{2\lambda}{2}$	$\frac{W^2}{5\lambda} - \frac{5\lambda}{4}$
3	$\frac{W^2}{6\lambda} - \frac{3\lambda}{2}$	$\frac{W^2}{7\lambda} - \frac{7\lambda}{4}$

The experimental values given in the above table are those of the H-plane sectoral horns. In the case of E-plane sectoral horns the values of Z_m and Z_o obtained from experiment are found to be much different from the theoretical values thus predicted. As the H vector is perpendicular to the edges of the flange elements the assumption of the secondary sources at these positions is not valid according to Butson and Thompson[37]. This disparity in the case of E-plane sectoral horns can be solved if we adopt the corner reflector theory based on the method of images. As shown earlier in Chapter V the corner reflector theory gives better results in the case of both E-plane and H-plane sectoral horns. This is evident from the graphs presented in Figures 5.1 and 6.3.

However the line source theory is capable of explaining the observed phenomena in flanged H-plane sectoral horns to a considerable extent. The experimental patterns for the sectoral horns with flanges at the aperture, at O-position and M-positon are given in Figures 6.6(A) and 6.6(B). (The experimental patterns in these figures are repoduced from Figures 4.5 and 4.6). By substituting for $Z = 0$ for the aperture position, $Z = Z_o$ for optimum position and $Z = Z_m$ for the minimum position, the corresponding radiation patterns are computed. These are shown in the figure in green lines.

H-Plane Sectoral Horn H1
9.4GHz, W/λ= 2.0
2α : 40d.

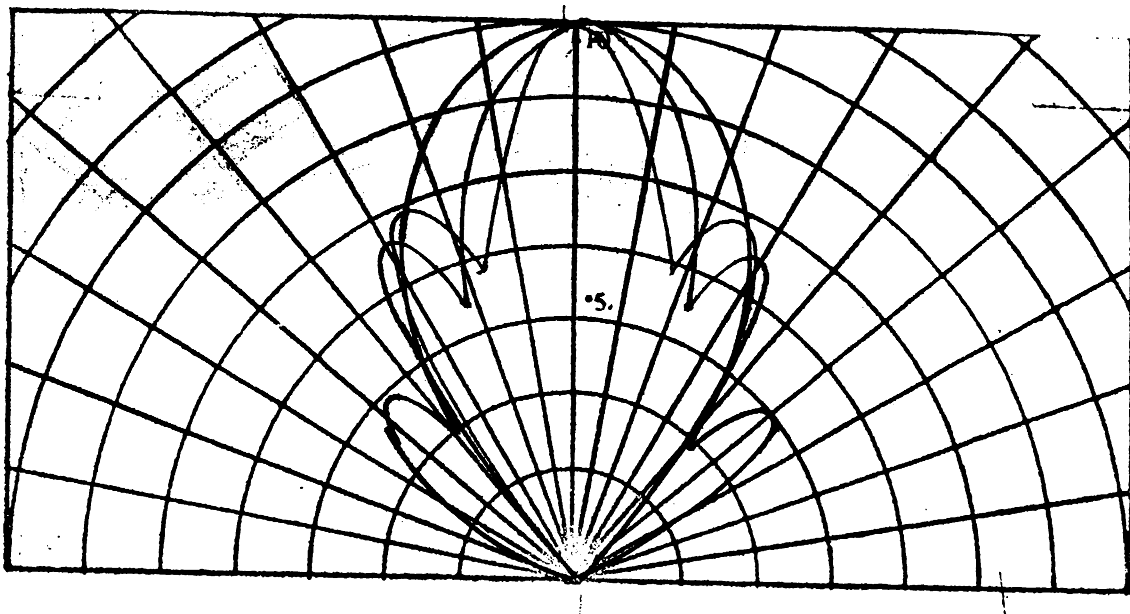

Flange at the Aperture of the Horn
$Z=0$

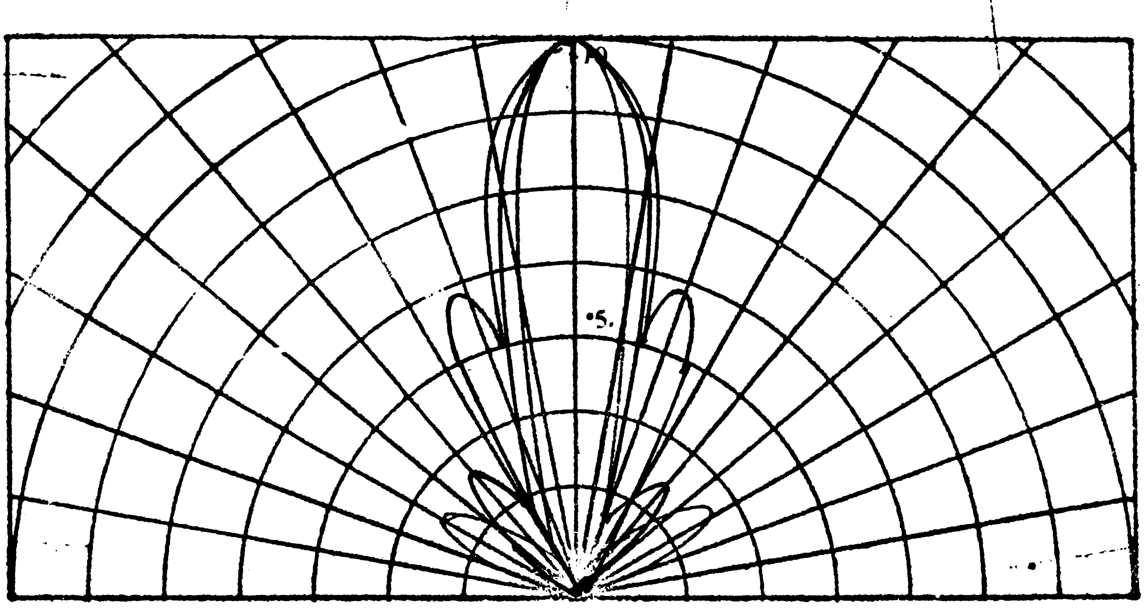

Flange at the O-Position.
$Z=Z_o$

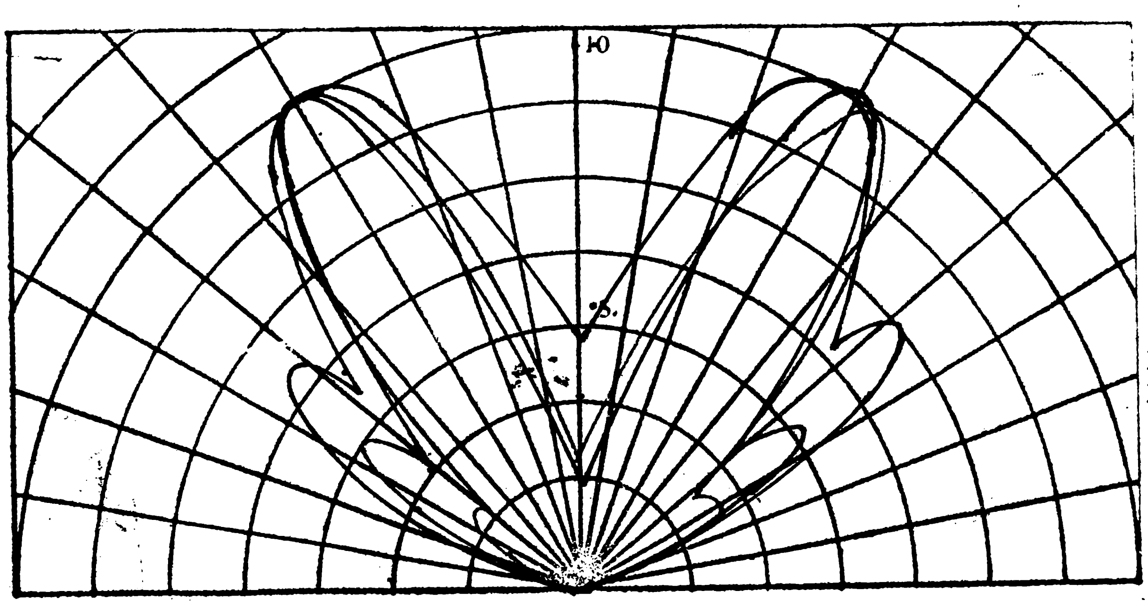

Flange at the M-Position.
$Z=Z_m$

FIGURE 6-6 A.

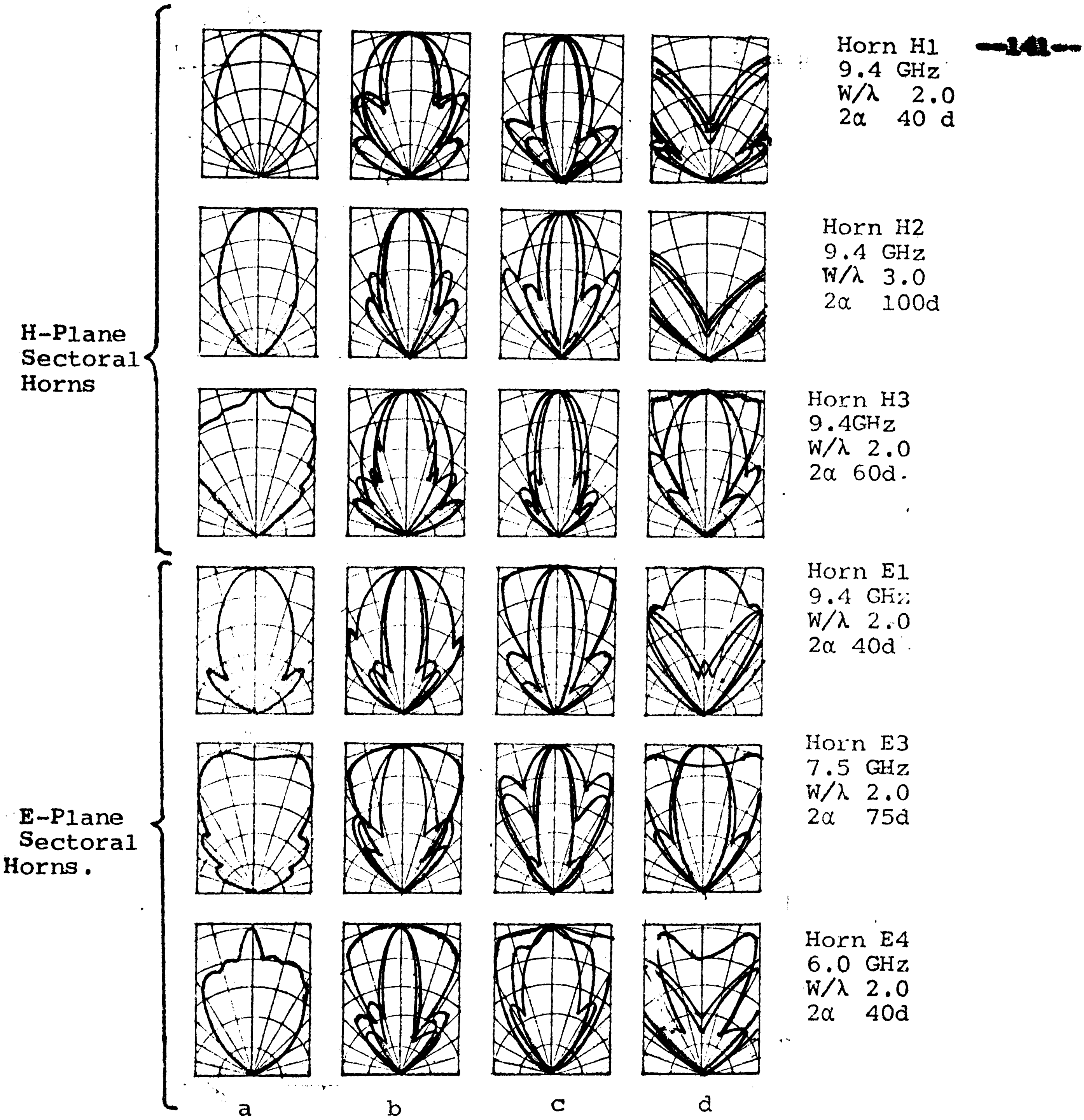

FIGURE 6-6.B.

A comparative study of the Line-Source theory and Corner Reflector theory applied to flanged Sectoral Horn Antennas.

a. Natural patterns of the horns; b. Patterns with flange at the aperture; c. Patterns with flange at O-position; d. Patterns with flange at M-position.

▬▬ Experimental Patterns; —— Theoretical patterns comput[e] using Line Source Theory; —— Theoretical patterns computed using Corner reflector theory.

TABLE 6.3 For a few flanges of included angle $2\alpha = 180°$, the theoretical and experimental values of Z at O-position and M-position.

λ(cm)	W(cm)	n = 1				n = 2				n = 3			
		Z_o		Z_m		Z_o		Z_m		Z_o		Z_m	
		T	E	T	E	T	E	T	E	T	E	T	E
3.2	3.2	0.00	0.00	-1.40	-1.44	-2.41	-2.52	-3.4	-3.5	-4.10	-4.39	-5.21	-5.40
	4.0	+0.92	0.68	-1.18	-1.32	-1.93	-2.03	-3.09	-3.12	-4.00	-4.23	-4.95	-5.08
4.0	4.0	0.00	0.00	-1.58	-1.74	-3.00	-3.31	-4.11	-4.27	-5.30	-5.55	-6.43	-6.21
	5.0	+1.18	--	-1.46	-1.67	-2.40	-2.70	-3.7	-4.01	-4.93	-5.11	-6.17	-6.11
5.0	5.0	0.00	0.00	-2.00	-2.20	-4.77	-4.87	-5.25	-5.46	-6.66	-7.00	-8.08	-8.52
	10.0	+8.3	--	+2.02	--	0.00	0.00	-2.37	-2.44	-4.24	-4.44	-5.97	-6.13

T = Theoretical value.

E = Experimental value.

Positive value for Z is not permissible.

For n = 0 the values of Z for optimum and minimum position are not consistent.

It can be seen that the experimental radiation patterns are very close to the theoretical patterns on line source theory for the H-plane sectoral horns. But the patterns differ enormously in the case of E-plane sectoral horns.

A plot of the radiation patterns for the same flanged horns evaluated on the basis of corner reflector theory using equation (6.17) is shown as red lines in the graphs in Figures 6.6(A) and 6.6(B). We can see that these theoretical patterns are very close to the experimental patterns obtained for both H and E-plane sectoral horns. Hence we may conclude undoubtedly that the corner reflector theory is most appropriate to explain the effect of metal flanges on sectoral horns.

However, the corner reflector theory is not suitable to explain the observed beam tilting effects by asymmetric flange or corner reflector system. As pointed out earlier, the geometry of the corner reflector system demands the feed antenna to be at the bisector of the angle formed by the reflector elements. As this condition will be violated by the asymmetric excitation the corner reflector theory seems to be inadequate to explain the consequent beam tilting. It may be noted that an extension of the line source theory can be used to explain these beam tilting effects with considerable success.

6.4 Conclusion

For symmetric systems of flanged E and H-plane sectoral horns the corner reflector theory is most suitable to explain the beam shaping. The difficulty in explaining the results with E-plane sectoral horns is thus solved by this uniform theory. However the effects shown by asymmetric flange systems are not explainable by the corner reflector approach. In such cases we may have to stick on the line source theory as indicated above.

CHAPTER VII

CONCLUSIONS

7.1 Introduction

From the exhaustive experimental and theoretical study presented in the previous chapters, few interesting conclusions are drawn and these are presented in this chapter. The significance of these conclusions is of great importance in antenna feed systems in which a sectoral horn is used as the primary feed. The primary radiation patterns can be conveniently shaped by the corner reflector technique.

For a symmetrical flanged sectoral horn antenna the corner reflector analogy is most suitable. The two flange elements act as reflecting elements casting images of the primary. The resultant beam pattern will depend upon the position of the primary feed from the apex, and the included angle.

The importance of this conclusion is that it provides an easier explanation for the behaviour of both H and E-plane sectoral horns. The line source theory which was originally used to explain the results obtained with flanged H-plane sectoral horns was not capable of explaining the behaviour of flanged E-plane sectoral horns. But the corner reflector theory is applicable for both types of the sectoral horns. Hence this approximation can be taken as a solution for the hitherto unexplained results available in the case of E-plane sectoral horns.

The beam tilting exhibited by flanged sectoral horns due to asymmetric excitation is finding easier explanation in the line source theory. The very definition of corner reflector demands a primary feed along the bisector of the corner angle and the consequent formation of images. Hence the results obtained with asymmetric systems are explainable with the line source theory only. However further attempts can be made to modify corner reflector theory to incorporate these asymmetric parameters.

7.2 Importance of the Work

Beam shaping of the primary horn radiat~~ion~~or by the Corner reflector technique is of importance in many ways. Proper aligning of a primary feed horn with a large secondary reflector antenna is a painstaking job for antenna experts. But a corner reflector fitted on the horn has a number of parameters which are variable to obtain the desired alignment.

Impedance matching for the complex system of a primary feed and a secondary reflector can also be achieved by corner reflector technique. The axial flow of energy in the horn can be minimised by the flange parameters. This results in minimum reflection back to the horn from the reflector and the consequent reduction in VSWR. Preliminary observations in this aspect proved that this is possible to a considerable extent.

Even when the horn is used as the main radiator in small radar and navigational aid, the corner reflector technique can be used for effective beam shaping.

7.3 Scope for further work

The investigation presented in this thesis offers much scope for further work in this field. Some of the problems which are considered and subjected to preliminary investigation have already been mentioned. The following is a brief description of the problems connected with this study for further investigation in the field.

a) The effect of beam shaping of primary horn feed due to corner reflector technique on secondary reflector antennas is a problem which requires further elaborate study. When the sectoral horn is used as a primary feed, the corner reflector fitted on it can change the beam shape. How this primary beam variation is affecting the resultant beam from the secondary reflector (which is usually a paraboloid) has not been investigated. It is presumed that the resultant beam shape will change in accordance with the primary beam variation. Some preliminary observations in this regard are presented in Appendix A_2.

b) The impedance matching between a secondary reflector and the primary horn feed is another subject of study. The reflected energy, from the secondary radiators in to the primary horn, primarily depends on the beam shape of the horn. Since this beam shape can be altered by the corner reflector fitted on the horn, the reflection from the secondary radiator and hence the VSWR can be considerably decreased. This will result in a better impedance matching.

c) As pointed out earlier, the corner reflector theory seems to be inadequate to explain the effects shown by asymmetric systems. A theoretical study in this respect can be pursued to modify the corner reflector theory to incorporate the asymmetric parameters.

d) The effect of the corrugated corner reflector elements has not been investigated. In such systems we get additional parameters like depth of corrugation, width and thickness of walls. The effect of these parameters together with that due to other parameters like length, angle, and position of the primary feed can be investigated in detail. Considering the importance of corrugated metal conductors in surface wave propagation, this will be a study of significant importance.

****
****
****

A P P E N D I C E S

1. Beam Shaping of Sectoral Horn Antennas by Compound Flange System.

2. Effect of Flanged Sectoral Horn Primary Feeds on the Radiation Patterns of Secondary Reflector Antennas.

APPENDIX A_1

BEAM SHAPING OF SECTORAL HORN ANTENNAS BY COMPOUND FLANGE SYSTEM*

Abstract: Flanges with different amplitudes of excitation are named as compound flanges. These flanges are found to be effective in modifying the radiation patterns of sectoral horn antenna. Dielectric flanges are functioning in the same way as that of metallic flanges having the same parameters. A compound flange system with a metallic element on one side and a dielectric one on the other side is observed to have a very significant tilting effect on the beam. Relevant radiation patterns are presented and a theoretical explanation is given.

1. Introduction

The effect of metal flanges on radiation patterns is a subject of interest in telecommunication field. Nair and Srivastava[56] and Nair et.al.[58] pointed out that the radiation patterns of a sectoral horn can be shaped according to one's desire. Butson and Thompson[37] studied the

*Published as a paper in Indian J. Radio Space Phys. Vol 5 Sept. 1976. pp 254-256.

effect of flange length and flange angle. It has been pointed out that the axis asymmetry and width asymmetry can produce beam tilt. Another type of asymmetry namely amplitude asymmetry has been suggested by Koshy et.al.[39] The two secondary radiators formed by the edges of flanges will have different amplitudes of excitation if they are of different materials. This suggestion has been taken up for the present investigation.

2. Experimental Setup and Techniques

The method of measurements is the same as described by Nair and Srivastava[56]. The flange system consists of a rectangular frame to which the flange elements can be conveniently attached. Provisions are made to vary the flange width and flange angle. As dielectric elements perspex plates of thickness 0.1 cm. were used while aluminium plates of same thickness were used as the metal elements. Figure 1 shows flanged sectoral horn.

3. Experimental Results

When a symmetric dielectric flange system is used it has been observed that E-plane radiation patterns of H-plane sectoral horns will be changed as in the case of metal flanges. The on-axis power fluctates with the position of the flange relative to the aperture of the horn, showing sharp maxima and minima as shown in Figure 2. The corresponding positions of the flanges are called the opti-

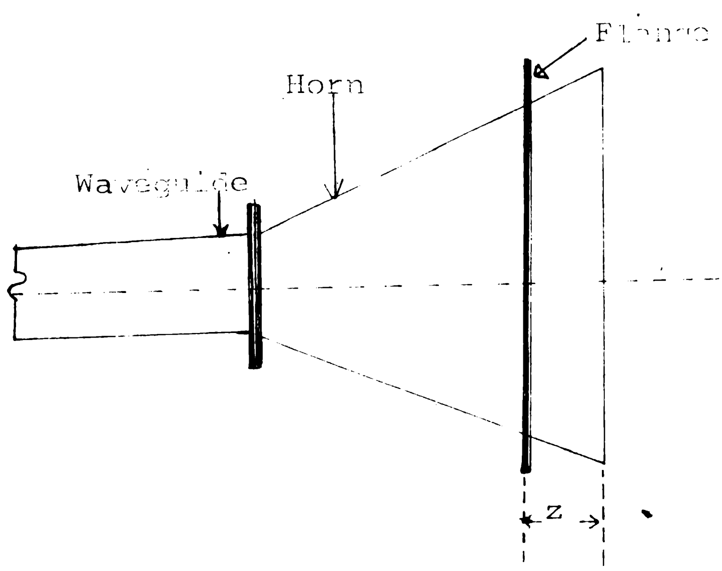

FIGURE -1 (APPENDIX I)

REPRESENTATION OF A FLANGED SECTORAL HORN

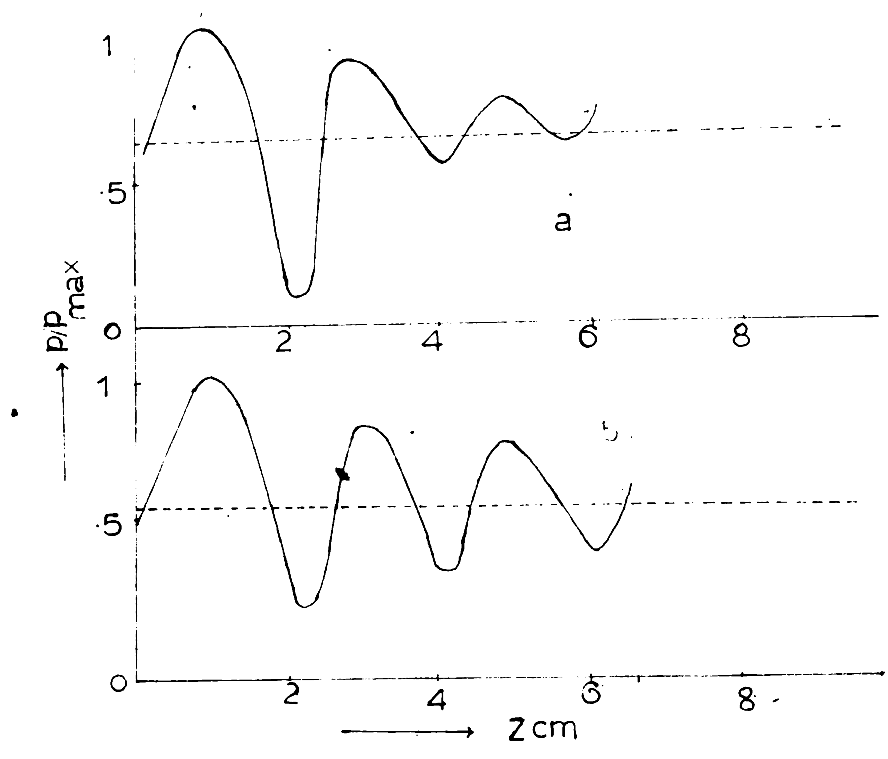

FIGURE-2(APPENDIX I)
Variation of on-axis power of the flanged h[illegible] of the flange with respect to the a[illegible]ture.
a.Horn H1; flange length 6.3 cm; flange angle 90°
b.Horn H2; flange length 5.5 cm; flange angle 60°

Table 1--Half-power Beam Widths of Horns with and without Metallic and Dielectric Flange System

Flange length W cm.	Flange angle 2α deg.	Beam widths of modified E-plane radiation patterns (in deg) with metallic flanges, Horn H1	with metallic flanges, Horn H2	with dielectric flanges, Horn H1	with dielectric flanges, Horn H2
		(93)	(82)	(93)	(82)
6.3	45	42	21	64	68
	60	22	20	40	52
	90	20	18	38	56
	120	16	16	38	64
5.5	45	34	38	62	64
	60	23	28	45	55
	90	26	24	52	40
	120	30	20	54	42

Note: The values in paranthesis below the column headings H1 and H2 indicate the natural E-plane radiation pattern in deg. Frequency: 9.98 GHz; Horn H1: Radial length 17.5 cm, flare angle 25°, H-plane aperture 10 cm, E-plane aperture 1.0 cm; Horn H2: Radial length 9.5 cm, flare angle 60°, H-plane aperture 12 cm, E-plane aperture 1.0 cm.

mum position or O-position and minimum position or M-position respectively.

The behaviour of dielectric flanges on E-plane radiation patterns of H-plane sectoral horns is investigated by keeping the flanges at O-position and M-position as shown in Figure 3. For a comparison the half power beam widths of the natural patterns and that of the modified beams due to metallic and equivalent dielectric flanges are tabulated in Table 1.

Using a compounded flange system with a metallic flange on one side and a dielectric element on the other side the variation of the on-axis power is studied. All other asymmetries are avoided. The O-position and M-position are determined. Radiation patterns at O-position are plotted. It has been observed that the beams are tilted towards the metallic flange element. This is presented in figure 3(c) and 3(d). The results of the detailed investigations are tabulated in Table 2. The tilting is less prominent at larger values of flange angle.

Theoretical Explanation

According to the theory suggested by Owen and Reynolds[36] the two edges of the flanges act as secondary radiators. The resultant pattern of the system can be obtained by combining the radiations from the primary aperture of the horn and the two secondary radiators. For

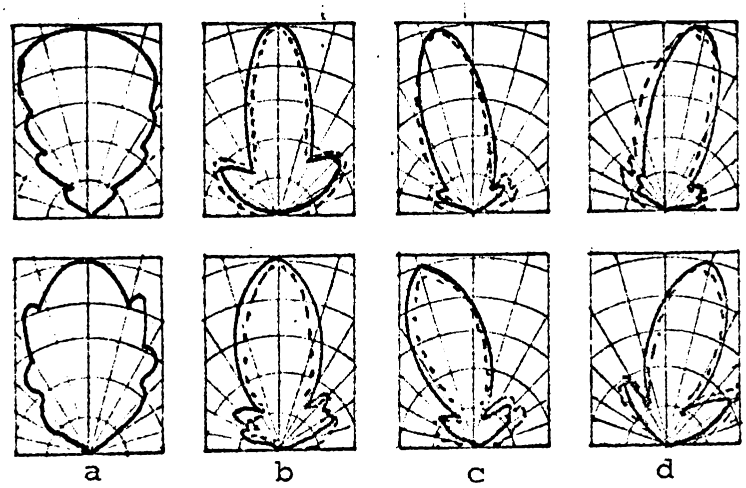

Horn H1, 9.4 GHz
W: 6.3 cms;
2α: 90^{o}

Horn H2, 9.4 GHz
W: 5.5 cms;
2α: 60^{o}

FIGURE 3.(APPENDIX I)
Natural and Modified radiation patterns

a.Natural pattern, (b)modified pattern with a symmetric dielectric flange at O-position;(c)focussed beam tilted by an asymmetric flange system when the dielectric flange element is on the right side and (d) focussed beam tilted by an asymmetric flange system when the dielectric element is on the left side. (The tilting is invariably towards the side in which the metallic element is attached)

Table 2 - Beam Tilt by Asymmetric Flange System

Flange length (in cm)				Flange angle 2α deg	Beam tilt (in deg) L: towards left, R: towards right	
Metallic		Dielectric			Horn	
Left	Right	Left	Right		H1	H2
6.3	-	-	6.3	45	18 L	21 L
-	6.3	6.3	-	45	20 R	18 R
6.3	-	-	6.3	60	14 L	14 L
-	6.3	6.3	-	60	12 R	10 R
6.3	-	-	6.3	90	8 L	9 L
-	6.3	6.3	-	90	5 R	6 R
6.3	-	-	6.3	120	0	0
-	6.3	6.3	-	120	0	3 R
5.5	-	-	5.5	45	20 L	17 L
-	5.5	5.5	-	45	17 R	15 R
5.5	-	-	5.5	60	15 L	12 L
-	5.5	5.5	-	60	14 R	10 R
5.5	-	-	5.5	90	4 L	9 L
-	5.5	5.5	-	90	6 R	6 R
5.5	-	-	5.5	120	2 L	4 L
-	5.5	5.5	-	120	0	3 R

the compound flange system the amplitudes of excitation of the two secondary radiators are assumed to be different say, K_1 and K_2. For a symmetric compound flange system the power P_θ at a distant point of bearing angle θ is given by Koshy et.al[39] as

$$P_\theta = 1 + K_1^2 + K_2^2 + 2 K_1 K_2 \cos \hat{p} + 2 \left\{ \left[\cos \frac{\pi B}{\lambda} \times \left\{ 1 + \cos (\alpha - \theta) \right\} \right] \times (K_1 + K_2 \cos \hat{p}) + \left[\sin \frac{\pi B}{\lambda} \left\{ 1 + \cos (\alpha - \theta) \right\} \right] (K_2 \sin \hat{p}) \right\}$$

where $\hat{P}$ is the phase difference between the two secondary sources, 2α is the flange angle and λ is the wavelength of radiation. The value of K_1 has been estimated by Butson and Thompson[37] as 0.077. Using the same method and substituting for K_1, the amplitude of excitation K_2 of the dielectric is extrapolated to be 0.026. The theoretical patterns are agreeing well with the experimental patterns in Figure 3.

5. Conclusion

From the above experimental results it may be concluded that dielectric flanges are also effective in controlling the E-plane radiation patterns of H-plane sectoral horns. The beam can be effectively tilted easily with a compound flange system.

APPENDIX A_2

Effect of Flanged Sectoral Horn Primary feeds on the Radiation Patterns of Secondary Reflector Antennas*

Abstract - Preliminary experimental results confirming the effects of flanged sectoral horn feeds on the radiation patterns of a paraboloidal reflector are presented. The flange-position of the primary horn feed is found to have a very significant effect on the beam shape of the secondary radiator. Radiation patterns for different flange parameters have been presented.

Experimental and theoretical investigations on flanged sectoral horns have been publised and the basic properties of such systems as revealed from these investigations may be summarized as follows:

(i) A flange system kept at 'O' position effects maximum focussing of the beam.

(2) At 'M' position, the flange causes broadening or splitting of the beam.

* Published as a paper in Jour.of the Inst. of Elect. and Telecom. Engrs. 1977 Vol 23 No.3 pp 148-149.

(3) Asymmetries of flange system in orientation, flange width or conductivity may ultimately cause a beam tilt from the axis of the horn.

The experimental confirmation of the first two results given above is obtained from the early works of Nair and Srivastava[56]. A detailed study on the relative position of metal flanges on the radiation patterns was made by Nair et.al.[38] and they showed that the beam may be narrowed, broadened or split up, depending on the position of the flange relative to the aperture of the horn. Regarding the flange-asymmetry, a theoretical study was made by Koshy et.al[49]. It was shown by S.B. Singh et.al.[39] that flange-width asymmetry as well as flange-axis asymmetry was effective in beam tilt. The width-asymmetry can focus, broaden or tilt the beam depending on the position of the flange system. Theoretical curves by Nair et.al. agree well with the experimental curves. A third asymmetry, namely the asymmetry in amplitude of excitation of the flange, suggested by Koshy et.al[49] is under investigation.

The effect of flanged sectoral horn radiators used as primary feeds to illuminate secondary reflector antennas like paraboloids has not been investigated so far. This paper presents the results of such a study. Flanged sectoral horns mounted at the focus of a large paraboloidal reflector gave interesting results. Radiation patterns for different flange-parameters have been presented.

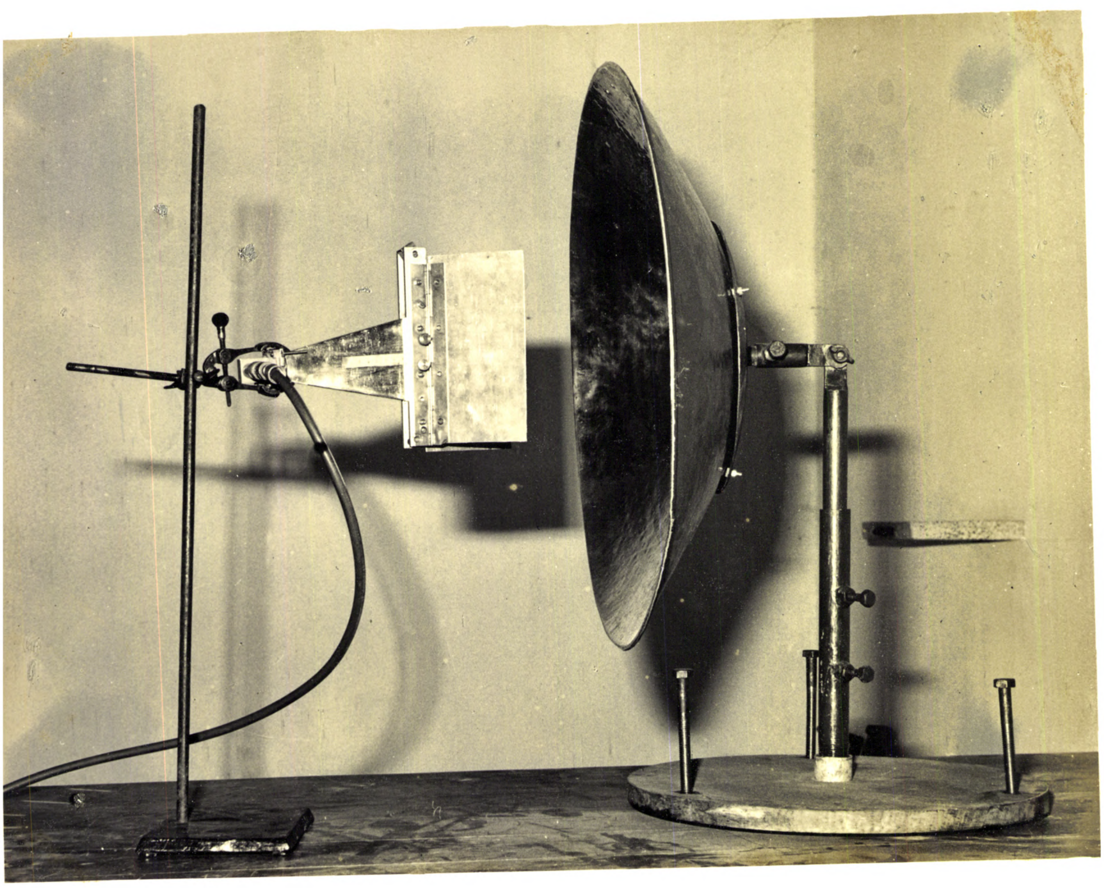

FIGURE 1(A)(Appendix II)

Sectoral Horn and Paraboloidal Reflector

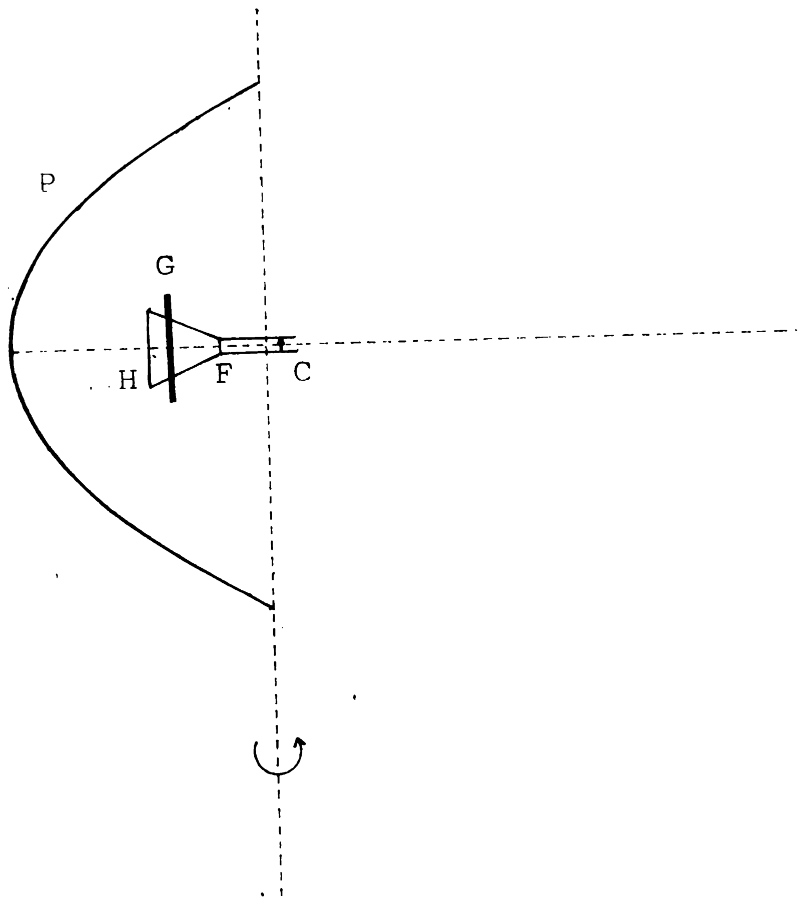

FIGURE 2B(APPENDIX-II)
Experimental arrangement of flanged primary horn feed and paraboloidal reflector used as a receiver.

P:Paraboloidal reflector; H:Horn; G:Flange; F:Cocal point of the paraboloid; C.Crystal mount. The whole system is capable of rotating about a vertical axis as shown by the arrow mark.

The experimental arrangements consist of a large aluminium paraboloidal reflector mounted on a stand which can be rotated about a vertical axis. The flanged horn can be ekpt at the focus of the paraboloid, to act as the primary feed. For plotting the radiation patterns of this system, it is used as a receiver of C.W. signal from a large standard pyramidal horn. Figure 1 represents an outline of the experimental set up. For plotting the secondary radiation pattern, the paraboloid with the flanged horn is used as a receiver. To measure the received power, a germanium crystal (IN 21 or IN 23) properly mounted is kept at a point along the axis of the horn is used. The output of the crystal detector is applied to a very sensitive microgalvanometer whose deflection is proportional to the crystal current and hence the power of the received signal at the point where the crystal is kept. The patterns are manually plotted by noting the received power corresponding to different orientations of the receiver axis with respect to the transmitter axis. A flange system, as explained by Nair *et.al.*[56] may be arranged at the 'M-position' or'O-position' of the primary horn feed. Variations in the secondary radiation patterns of the paraboloid due to different flange-parameters (namely, flange-length, flange-angle, relative position of the flange with the aperture of the horn etc.) are studied.

Results

The study of effects of flanges attached to primary

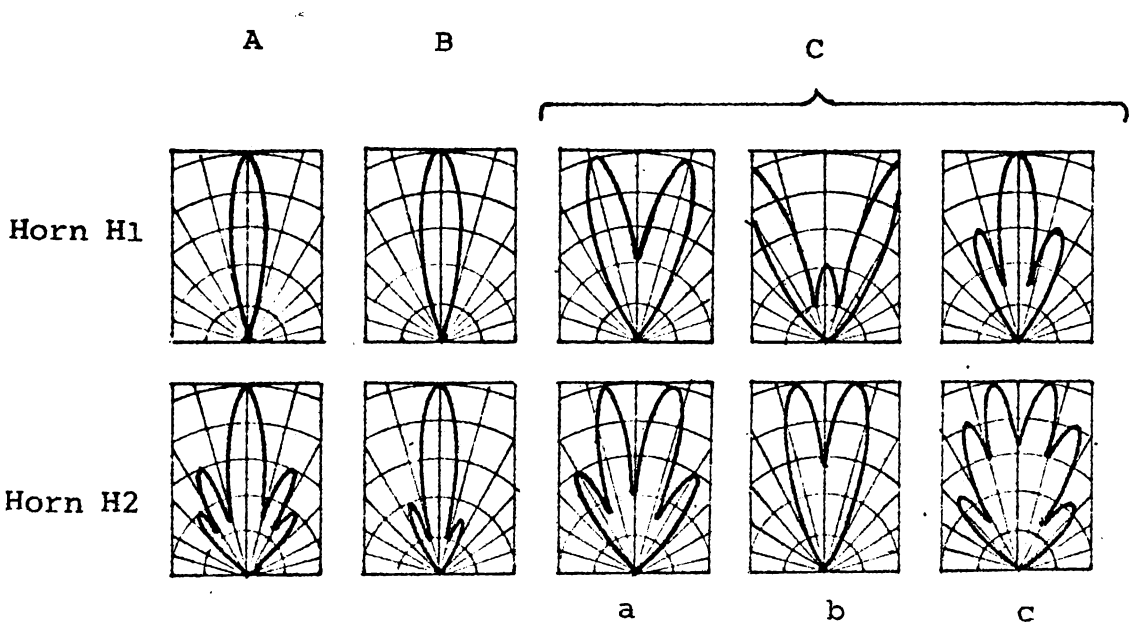

FIGURE 2(APPENDIX-II)

Natural and modified E-plane radiation patterns of a paraboloidal radiator with flanged H-plane horn primary feed.

A:Natural E-plane pattern of the system when no flange is attached to the feed horn; B. Modified pattern when the flange is at O-position of the horn; C:Modified patterns when the flange is at M-position

Paraboloidal Reflector: Focal length: 20 cms; aperture diameter: 65 cm.

Flange parameters: For Horn H1: Flange length 6.4 cms; $2\alpha=60^{O}$(for O-posn) For M-Positions corresponding to figures C(a),(b) and (c),6.4cms,60 degrees, 5.5 cms.60degrees and 5.5cms 90 degrees respectively. For Horn H2, flange parameters are the same as for H1.

horn feeds on the secondary radiation patterns of reflector antennas revealed very interesting results. A representative set of radiation patterns is given in fig.2. The patterns plotted are those in the E-plane. A close analysis of the results reveals the following facts: (i) the optimum directivity of the system is not affected by a flange, when it is at the O-position of the horn. This is found to be true for any value of flange-angle and flange-length. But at M-position, the flange has got a very dominant role in shaping the secondary radiation pattern. (ii) The secondary radiation pattern from the reflector antenna can be split or broadened with proper selection of flange widths and flange angles.

Conclusions

The results clearly show that the secondary radiation patterns from a reflector antenna can be shaped to a considerable extent by the flange technique which was originally developed for primary horn feeds only[56]. Eventhough an enhanced focussing or sharpening of the secondary pattern is not possible by the flange, it can broaden or split the pattern to any desired shape by slight adjustment of flange parameters. This may have practical applications in matching and aligning very large communication and radar antennas.

R E F E R E N C E S

REFERENCES

1(a) Love, A.W. "Electromagnetic Horn Antennas" IEEE Press (1976).

1(b) Barrow, W.L. and Chu, L.J. "Theory of Electromagnetic Horn" Proc.I.R.E. Vol.27, pp.51-64, January 1939.

2. Chu, L.J. and Barrow, W.L. "Electromagnetic Horn Design" Trans. AIEE Vol.58, pp.333-338, July 1939.

3. Southworth, G.C. and King, A.P. "Metal Horns as Directive Receivers of Ultrashort Waves" Proc. IRE Vol.27 pp.95-102 (1939).

4. Chu, L.J. "Calculation of Radiation Properties of Hollow Pipes and Horns", J.Appl Physics, Vol. II pp.603-610 September 1940.

5. Rust, N.M. "The Phase Correction of horn radiators" Inst. Elec. Eng. Vol.93, Pt.IIIA, pp.50-51, March/ May 1948.

6. Horton, C.W. "On the theory of the radiation patterns of electromagnetic horns of moderate flare angles" Proc. IRE Vol.37 pp.744-749, July 1949.

7. Schorr, M.G. and Beck, F.J. Jr. "Electromagentic field of Conical Horn" J.Applied Physics, Vol.21, pp.795-801, August 1950.

8. King, A.P. "The Radiation Characteristics of Conical Horn Antennas" Proc. IRE Vol.38, pp.249-251 March 1950.

9. Russo, P.M., Rudduck, R.C. and Peters, L. Jr. "A Method for Computing E plane patterns of Horn Antennas" IEEE Trans. Ap. Vol.Ap.13, pp.219-224 March 1965.

10. Yu, J.S., Rudduck, R.C. and Peters L Jr."Comprehensive Analysis for E Plane of horn Antennas by edge diffraction Theory", IEEE Trans. Antennas Prop. Vol. Ap.14, pp.138-149, March 1966.

11. Hamid, M.A.K. "Diffraction by Conical Horn" IEEE Trans Antennas Prop. Vol.Ap.16, pp.520-528 Sept 1968.

12. Narasimhan, M.S., Rao, B.V. "Modes in a Conical Horn New Approach" Proc. Inst. Elec. Eng. Vol.118, pp. 287-292 Feb. 1971.

13. James, J. Epis "Compensated Electromagnetic Horns" Microwave J. Vol.4, pp.84-89, May, 1961.

14. Walton, K.L. and Sundberg, C.V. "Broad band redged horn design" Microwave J. Vol.7, pp.96-101, March 1964.

15. John L. Kerr "Short axial length broad band horn" IEEE Trans Antennas Prop. Vol. Ap.21 pp.710-715.

16. Braun, E.H. "Some data for the design of electromagnetic horns" IEEE Trans. Antennas Prop. Vol.Ap.4, pp.29-31 Jan. 1956.

17. Love, A.W. "The diagonal horn antenna" Microwave J. Vol. V, pp.117-122, March 1962.

18. Seymour B. Cohn, "Flax angle changes in a horn as a means of pattern control" Microwave J. Vol.13 pp41, 42, 44, 46, Oct, 1970.

19. Ching C.H. and Adam N. Wicket "A new multimode rectangular horn antenna generating a circularly polarised elliptical beam" IEEE Trans Antennas Prop. Vol.Ap.22, pp.746-751 Nov. 1974.

20. Simmons A.J. and Kay A.F. "The Scalar feed - A high performance feed for large paraboloid reflectors" IEE Conf. Publ. 21, (1966) pp.213-217.

21. Lawric R.E. and Peters L. "Modifications of horn Antennas for Low side lboes levels" IEEE Trans Antennes Prop. Vol.Ap.14, pp.605-610, Sept. 1966.

22. Clarricoats, P.J.B. "Analysis of Spherical hybrid modes in a corrugated Conical Horn" Elect. Lett. Vol5 pp.189-190, May 1969.

23. Clarricoats, P.J.B. and Saha, P.K. "Radiation Patterns of lens corrected Conical Scalar Horn" Elect. Lett. Vol.5, pp.592-593, Nov. 13, 1969.

24. Clarricoats, P.J.B. and Saha, P.K. "Propagation and radiation behaviour of corrugated feeds Part I and Part II" Proc. Inst. Elec. Eng. Vol. 118, pp.1167-1176 Sept. 1971 and abid pp.1177-1186, Sept. 1971.

25. Jenken M.E. and Lambrechtse, C.W. "Small corrugated conical horn antenna with wide flare angle" Elec. Lett. Vol.5, pp.489-490, Oct. 1969.

26. Narasimhan, M.S. and Rao B.V. "Hybrid modes in corrugated conical horn" Elec. Lett. Vol.6 pp.32-34, Jan.22, 1970.

27. Narasimhan, M.S. "Corrugated conical horns with arbitrary corrugation depth" Radio Electron Eng. Vol. 43 pp.188-192, March 1973.

28. Tsandoulas, G.W. and Fitzgerald, W.D. "Aperture Efficiency enhancement in dielectrically loaded horns" IEEE Trans Antennas Prop. Vol.21, pp.69-74 Jan. 1972.

29. Hamid M.A.K. Jowaij, S.J. and Martens, G.O. "A dielectric loaded circular waveguide antenna" IEEE Trans. Antennas Prop. Vol.Ap.20, pp.96-97 Jan.1972.

30. Toshio Satoh "Dielectric loaded horn antenna" IEEE Trans Antennas Prop. Vol.Ap 20, pp.199-201 March 1972.

31. Bartlett H.E. and Moseley, R.E. "diel guides - Highly efficient low noise antenna feeds" Microwave J. Vol.9 pp.53-58 Dec. 1966.

32. Clarricoats P.J.B. and Salema C.E.R.C. "Antennas employing conical dielectric horns" Proc. Inst. Elec. Eng. Vol. 120 pp.741-749, July 1973.

33. Crawford A.B. Hogg, D.C. and Hunt, L.E. "A horn reflector Antenna for Space Communication" Bell Syst. Tech. J Vol. 40, pp.1095-1116, July 1961.

34. Hines J.N., Tingveli and Turrin, R.H. "The electrical characteristics of the conical horn - reflector antenna" Bellsyst Tech. J. Vol. 42, Pt.2, pp.1187-1211, July 1963.

35. Pao C.S. "Shaping of Primary Patterns of Horn Feed" (1945) Radiation Laboratory Report No.655.

36. Owen A.R.G. and Reynolds L.G. "The Effect of flanges on Radiation Patterns of Small Horns", Journal IEEE (1946) 93 Part III-A. 1523-1533.

37. Butson P.C. and Thompson G.T. "The Effect of flanges on radiation patterns of wave guides and sectoral horns, Proc. IEE (1959), 106 Part B, 422-446.

38. Nair, K.G., Koshy, V.K. and Srivastava, G.P. "A theoretical study of the asymmetric excitation of conducting flanges by a primary aperture antenna and the consequent radiation pattern" Int J. Electronics (1968) Vol.24 No.5, 497-500.

39. Koshy, V.K., Singh, S.B., Nair, K.G. and Srivastava, G.P. "Effect of asymmetry in amplitude of excitation of secondary sources by a primary aperture antenna" Int. J. Electronics (1968) Vol.25 No.3, 289-291.

40. Kraus, J.D. "Corner Reflector Antennas" Proc. IRE 23, 1940, 513-520.

41. Edward E. Harris "An experimental investigation of the corner reflector antennas" Proc. IRE 41, 1953, 645-651.

42. James R. Wait "On the theory of an antennas with an infinite corner reflector", Can J. Physics 32, 1954, 365-371.

43. Cottony H.V. and Wilson A.C. Gain of finite size corner reflector antennas". IRE Trans on Antennas and Propagation AP. 6, 1958, 366-369.

44. Wilson A.C. and Cottony H.V. "Radiation patterns of finite size corner reflector antennas". IRE Trans on Antennas and Propagation". AP 8, 1960, 144-157.

45. Hamid M.A.K. "Diffraction by dielectric loaded horns and corner reflectors" IRE Trans on Antennas and Propagation. AP. 1969 660-662.

46. David Proctor "Graphs simplify corner reflector antenna design.

47. Moullin, E.B. "Radio Aerials" Oxford University Press, London, 1949.

48. Jordan E.C. "Electromagnetic Waves and Radiating Systems" Prentic-Hall of India p.570.

49. Koshy V.K., Nair K.G. and Srivastava G.P. "Analysis of radiation from a flanged aperture antennas" IEEE Trans. Antennas and Propagation Vol. AP 18 pp.407-411 1970.

50. Silver, S. "Microwave Antenna Theory and Design" MIT Radiation Laboratory Series Vol.12, McGraw Hill Book Company, New York 1949 p.199.

51. Montgomery C.G. "Technique of Microwave Measurements" MIT Laboratory Series Vol.11, McGraw-Hill Book Company, New York, 1949, pp.476, 900, 914.

52. Jasik E.A. "Antenna Engineering Hand Book" McGraw-Hill Book Company, New York 1961 pp.1-3.

53. Barlow H.M. and Cullen A.L. "Microwave Measurements" Constable and Company, London 1950, p.347.

54. Wheeler G.J."Indroduction to Microwaves" Prentice-Hall Inc. Eaglewood Cliffs,NJ.

55. Edward A.Wolff "Antenna Analysis" John Wiley and Sons. Inc. U.S.A.

56. Nair, K.G. and Srivastava, G.P. "Beam-shaping of H-plane sectoral horns by metal flanges" J. Inst. Telecommun. Engrs. (India), Vol.13, pp.76-82, February, 1967.